Hydrogeology in the Cordillera Blanca, Peru: significance, processes and implications for regional water resources

By
Michel Baraër
Department of Earth and Planetary Sciences
McGill University, Montreal

April 2012

A thesis submitted to McGill University in partial fulfilment of requirements of the degree of Doctor of Philosophy

Table of content

Abstract

The retreat of the glaciers of Peru's Cordillera Blanca is a potential threat to the human, ecological and economic welfare within the Rio Santa watershed. In a context of increasing stress on regional water resources, the relative contributions of groundwater – a major component of the region's dry-season stream flows - remain poorly characterised and oversimplified in existing hydrological models. By characterising both the variability of the groundwater contribution in space and time, identifying the major relevant hydrogeological processes, and using these data to produce a new mass balance based hydrological model, I investigate to what extent the forecasted loss of volume of the Andean glaciers will affect regional hydrological regimes. The use of hydrochemical, isotopic and hydrological methods shows that groundwater is a major component of the dry-season stream discharge that drains the glacierized valleys of the Cordillera Blanca. This contribution is highly dependent on the preceding two to four years' precipitation. Spatially, it correlates with the watershed glacier cover. Talus slopes are identified as a key component of the groundwater system since they act as buffering units that collect water from areas at higher elevations and release it slowly, allowing connected springs to remain active during the dry season. Integrating the groundwater specific discharge estimated from the groundwater contribution evaluation, the modeling exercise suggests that seven of nine study watersheds have probably crossed a critical transition point and now exhibit a glacier retreat-related decrease in discharge. Once the glaciers completely melt, the annual discharge of the studied watersheds will be lower than present by 2–30% depending on the watershed. The influence of glacier retreat on discharge will be most pronounced during the dry season. At La Balsa, which receives discharge from the entire upper Rio Santa, glacier retreat could lead to a decrease in dry-

season average discharge of 30% compared to present. Glacier-related decreases in discharge are not likely to reverse.

Résumé

Le retrait des glaciers de la Cordillère Blanche au Pérou représente une menace potentielle pour les populations, l'économie et l'écologie de la vallée du Rio Santa. Dans un contexte régional de surexploitation de la ressource en eau, la contribution relative des eaux souterraines, une composante majeure des cours d'eau durant la saison sèche, reste mal comprise et sa modélisation hydrologique est souvent trop simplifiée. J'évalue dans quelle mesure le retrait glaciaire affectera le système hydrologique de la vallée du Rio Santa en caractérisant à la fois la variabilité de la contribution des eaux souterraines dans le temps et dans l'espace, en identifiant les processus hydrogéologiques qui y sont liés, puis en utilisant les données dans un nouveau modèle hydrologique. L'application de méthodes hydrochimiques, isotopiques et hydrologiques montre que les eaux souterraines contribuent de façon importante aux eaux de surface de la saison sèche des vallées partiellement englacées de le Cordillère Blanche. Cette contribution varie d'année en année en fonction des précipitations reçues durant les deux à quatre années précédentes. La variation dans l'espace est fortement dépendante de la couverture glaciaire du bassin. Les dépôts de débris rocheux situés au flanc des parois latérales des vallées glaciaires sont identifiés comme des composantes clefs du système hydrogéologique. Ces éléments, constitués de dépôts para-glaciaires et potentiellement de dépôts glaciaires, agissent comme des zones tampons. Ils collectent les eaux de ruissèlement provenant de plus hautes altitudes et les libèrent avec un délai suffisant pour assurer l'approvisionnement de sources même durant la saison sèche. L'exercice de modélisation, qui intègre les débits spécifiques des eaux souterraines résultant des premières phases de la recherche, suggère que sept des neuf bassins versants étudiés ont probablement passé un point de transition critique et sont maintenant dans une phase de réduction du débit de leur cours d'eau principal due au retrait glaciaire. Lorsque les glaciers auront disparu, le débit annuel de ces cours d'eau se situera, selon le bassin, entre -2 et -30 pourcent de leur niveau actuel. L'influence du retrait glaciaire sur l'hydrologie sera plus prononcée lors de la saison sèche que pour le

reste de l'année. A La Blasa, station située à l'entrée du canyon Del Pato sur le Rio Santa, le retrait glaciaire pourrait générer une diminution du débit de la saison sèche du fleuve d'environ 30% par rapport à son niveau actuel. Ces baisses de débit des rivières dues au retrait glaciaire sont probablement irréversibles.

Acknowledgments

I want to thank Jeffrey McKenzie, my supervisor, for the privilege of being able to do my PhD on the fascinating topic of the influence of climate change on water resources in glacierized watersheds. By joining his collaborative team with its history of work in the Cordillera Blanca since the end of the 1990s, I gained access to well-developed logistical support, a priceless database of field measurements and, most importantly, a stimulating group of great scientists. Collaborating with group leader Bryan Mark was one of the most valuable professional experiences in my life. Our Peruvian colleagues from the *Autoridad Nacional del Agua* (ANA) accomplished a tremendous task in collecting, compiling and interpreting precious field data. I would like to thanks Jesus Gomes in particular for his professional support and his friendship. Part of the field work was made possible thanks to the support of our colleagues from the French *Institut de Recherche pour le Développement* and Thomas Condom in particular. Jeff Bury and Adam French from the University of California Santa Cruz have inspired my work by adding a stimulating human dimension to the hydrological aspects I was studying. Bernhard Lehner, from McGill's Department of Geography, is an active member of my PhD committee. His advice permeates this work.

With his active support and the trust he placed in me, Jeffrey McKenzie was also a fantastic help in making my PhD studies both delightful and fertile. My fellow graduate students from the hydrogeology laboratory of the Earth and Planetary Sciences (EPS) department of McGill University deserve being acknowledged for their support. Among them, Bernado Brixel, Rob Carver, and Stephanie Palmer have provided me with exceptional assistance in my work. I would like to acknowledge the faculty members of the EPS department for their academic input. The personnel that make the department run effectively have been of great help too. I thank Glenna Keaton and Isabelle Richer for their patience in teaching me how to run the analytical equipment. I thank Anne Kosowski, Kristy Thornton and Angela Di Ninno for the excellent job they do in the department.

To my parents and grandparents;

To my wife Marie-Ange and my two wonderful kids Hugo and Marion, for everything and much more.

Contributions of Authors

This thesis is composed, in large part, of three manuscripts for which I am the first author but have written in collaboration with different co-authors. Jeffrey McKenzie, my supervisor, Bryan Mark, a member of my thesis supervisory committee and Jeffrey Bury are co-authors for the three manuscripts. Their general contributions include financing the research, planning the work, challenging the ideas and conclusions and proofreading the documents.

Chapter 2 was published in 2009 in *Advances in Geosciences*[1]. Sara Knox was a co-author for this work. Sara compiled a lot of historical data and performed the GIS based analyses.

Chapter 3 is ready to be submitted to the *Hydrological Processes* journal. Its title is projected to be: Proglacial hydrogeology in the Cordillera Blanca, Peru. Here again, Sara Knox is a co-author, this time with Thomas Condom, Jesus Gomez and Sarah Fortner. Sara's contribution in determining the watersheds' characteristics by using GIS was very important. Thomas Condom participated in most of the field work, making possible some of the sampling and providing expertise in hydrological measurements. Sarah Fortner not only conducted part of the chemical analysis used in the paper but also helped with data interpretation. Finally, Jesus Gomez did part of the sampling and provided logistical support in the field.

Chapter 4 was recently published in the *Journal of Glaciology*[2]. In addition to his general contribution, Bryan Mark wrote sub-chapter 3.5 "Estimation of glacier coverage" and part of sub-chapter 4.1 "Changes in glacierized area". Kyung-In Huh, another co-author, assisted Bryan in estimating glacier cover from GIS datasets. As for chapter 3, Thomas Condom participated in most of the field work and provided expertise and support in hydrological measurements. The co-authors Cesar Portocarrero and Jesus Gomez were involved in field work and logistics.

Their input in treatment of results was of key importance. Under my supervision, Sarah Rathay performed the quality review, and wherever needed and possible, the correction of the original discharge time series.

Published papers included in the present thesis:

Baraer M, McKenzie JM, Mark BG and Palmer S. 2009. Characterizing contributions of glacier melt and groundwater during the dry season in a poorly gauged catchment of the Cordillera Blanca (Peru). *Advances in Geosciences* **22**: 41-49.

Baraer M, Mark BG, McKenzie JM, Condom T, Bury J, Huh K, Portocarrero C, Gomez J and Rathay S. 2012. Glacier recession and water resources in Peru's Cordillera Blanca. *Journal of Glaciology* **58**: 134-150.

1. Introduction / literature review

This introduction provides a general literature review and synthesis of the topic and presents the overall objectives of the thesis. Detailed objectives and corresponding literature reviews for Chapters 2, 3 and 4 are found in each chapter-specific introduction.

1.1 Global glacier retreat and water resources

The loss of ice from retreating glaciers is the most visible change in mountains around the world (Kappenberger, 2007). Observations and measurements of glacier lengths and mass balance describe a general retreat that is expected to have major detrimental impacts on alpine environments globally (Huss *et al.*, 2010). Some of these impacts have already been observed and reported in the literature. Glacier related changes in river discharge seasonality, for example, directly threaten the water quality for millions of people (Kistin *et al.*, 2010). In China, the hydrological consequences of the combined effect of permafrost thaw and glacier retreat have modified downstream ecosystems (Yang *et al.*, 2007). Water supply during the tropical Andean dry season has been shown to be at risk with glacier retreat (Vergara *et al.*, 2007). Studies anticipate an intensification of hydrological impacts related to glacier retreat (Fountain and Tangborn, 1985). Fleming and Clarke (2005) found a strong relation between the watershed glacierization and the flow magnitude. In general, floods are expected to increase during the wet season while increased water scarcity is anticipated during the dry season. This tendency is expected to affect different regions of the world such as the Himalayas (Singh and Bengtsson, 2005), the Alps (Braun *et al.*, 2000; Brown *et al.*, 2010; Uehlinger *et al.*, 2010) and the Andes (Pouyaud *et al.*, 2005).

In addition, impacts of glacier retreat on water resources are predicted to affect long-term trends in stream discharge. In conditions of continuous retreat, glaciers generate a transitory increase in runoff as they lose mass (Mark and McKenzie, 2007). The discharge then reaches a plateau and a subsequent decrease related to the reduction of the ice volume (Mark *et al.*, 2005). This trend will be even more pronounced during the season of low flow: a time of year when the relative contribution of glacier melt water is at its maximum (Nolin *et al.*, 2010; Stahl and Moore, 2006). In addition to annual or dry-season discharge changes, glacier cover reduction is predicted to affect flow variability as well (Collins and Taylor, 1990; Hagg and Braun, 2005).

1.2 Glacial retreat in Peru

Glaciers in South America have experienced a strong generalized retreat and thinning, especially in recent years (Casassa *et al.*, 2007). Observations on glaciers across Ecuador, Peru and Bolivia give a detailed and unequivocal account of rapid shrinkage of the tropical Andean glaciers since the Little Ice Age (Vuille *et al.*, 2008a). In the Cordillera Blanca, the glacier coverage has declined from 800-850 km^2 in 1930 to slightly less than 600 km^2 at the end of the 20^{th} century (Georges, 2004). This fast retreat was confirmed later on by Racoviteanu *et al.* (2008) who calculated a loss of glacial area of 22.4% between 1970 and 2003. Studying changes at 12 glacierized watersheds of the Cordillera Blanca between 1962 and 1997, Mark and Seltzer (2003) report a similar tendency and show that a retreat was measured at all watersheds. Using hydrological records to reconstitute glaciers mass-balances, Kaser *et al.* (2003) concludes that, although the mass balance variations show some differences among the individual catchment basins, the overall trend is uniform.

1.3 The Rio Santa and water resources

The Rio Santa drains a 12 300 km^2 watershed. It flows from Laguna Conococha, a shallow lake at 4000 meters above sea level, down to the Pacific coast. The upper part of the watershed, called Callejón de Huaylas, drains the western slopes of the Cordillera Blanca and the eastern side of the Cordillera Negra. The Cordillera Blanca has the largest glacierized surface area in the tropics, with a total glacial area of around 600 km^2 (Georges, 2004) whereas the Cordillera Negra has no glaciers. The Andean part of the watershed is characterised by strong precipitation seasonality, typical of the outer tropics where more than 80% of precipitation falls between October and April, and the austral winter months of June to August have almost no precipitation.

The Canon del Pato makes a natural boundary between this upper Rio Santa drainage basin and the rest of the watershed. This narrow and deep gorge hosts one of the most important hydropower plants in the country. At higher elevations, the Quechua peasants have used irrigated slope agriculture for centuries which entails a complex system of small channels called *acequias* that are contoured to the slope of the mountains (Condom *et al.*, 2010). These populations already experience climate change-related hydrological impacts as they are affected by the disappearance of many perennial and intermittent springs (Mark *et al.*, 2010). Such hydrological changes are significantly altering water availability in the region and pose critical risks to local populations that are highly dependent on these resources for their livelihoods (Bury *et al.*, 2011).

The Rio Santa valley hosts several middle-sized cities of 20 000 to 120 000 inhabitants, among which is Huaraz, the Ancash province's capital. In its heavily-populated and extremely arid lower reaches, the river's flows are intensively used for large-scale irrigated agriculture and fresh water supplies for major cities (Chevallier *et al.*, 2010a). Measurements I made in the summer of 2011, as part of a different study, suggest that around 80% of current lower Rio Santa flows might be diverted for these purposes.

1.4 Framework

Despite the threat posed by ongoing alpine glacier decline, detailed studies of the future impact of global warming on water resources in potentially affected regions are long overdue (Barnett *et al.*, 2005). This applies for the Cordillera Blanca where attempts to provide accurate predictions of the future of local water resources are scarce and do not always lead to consistent conclusions. Juen *et al*. (2007) and Vuille *et al.* (2008b), for example, suggest that reduced glacier size leads to decreased volume of glacier melt. This decrease is compensated by an increase in direct runoff. Thus, the mean annual total runoff remains almost unchanged, but the seasonality is considerably amplified. On the other hand, other studies suggest that water supply will peak after several decades of continually increasing as a result of net glacier loss, followed by a sudden decrease (Pouyaud *et al.*, 2005). According to Pouyaud, the peak water should occur in 2020 to 2050, depending on the watershed.

One of the difficulties in projecting hydrological changes is the poor understanding and quantification of the groundwater contribution. Although there is extensive research on glacier dynamics in the tropics and modeling gross runoff, there has been very little research focused on the role of groundwater in these systems (Favier *et al.*, 2008; Wagnon *et al.*, 1998). This situation leads to oversimplification in predictive models of the contribution of groundwater to surface water. Modeling glacierized valleys of the Cordillera Blanca, Juen *et al.* (2007) mention, for example, that a variable base flow coefficient was fixed "due to the lack of further information". Kaser *et al.* (2003) assumed no monthly variations in base flow based on simple geomorphologic attributes that are common to the different valleys of the Cordillera Blanca. Pouyaud *et al*. (2005) did not make the distinction between the different sources in non-glacierized areas that contribute to stream flows. Groundwater and surface runoff combined

contribution was simply assumed to be an arbitrarily determined percentage of precipitations.

1.5 Objectives

Based on what was accomplished so far, the major objectives of the thesis were defined as following:

- Estimate the percentage of groundwater contribution to surface water during the dry season across the Cordillera Blanca.
- Evaluate the spatiotemporal variability of this contribution across the Cordillera Blanca.
- Identify the main groundwater sources in the glacierized valleys.
- Understand the principal groundwater recharge and discharge mechanisms.
- Use the findings on groundwater to characterise the impacts of glacier retreat on stream discharge in the Rio Santa watershed.

1.6 Approach

I used natural tracers to characterise the groundwater contribution to surface flows in a context where traditional in-situ hydrologic and hydrogeological methods are difficult to fully deploy due to logistical issues, remote access and vandalism (Mark *et al.*, 2005). Despite the colder temperatures and the shorter rock–water contact times in glacierized catchments, factors which reduce chemical erosion rates, the ionic content of melt water still remain comparable to those in temperate locales with similar specific runoff, thanks to the abundance of freshly comminuted glacial debris (Cooper *et al.*, 2002). The use of these natural tracers has already proven valuable in characterising water flow dynamics in glacierized catchments (Crossman *et al.*, 2011; Roy and Hayashi, 2009b; Ryu *et al*., 2007; Strauch *et al*., 2006; Yang *et al*., 2011). In a reanalysis of samples collected between 1998 and 2007, the first phase of my research, described in chapter two, characterises the groundwater contribution and its variation in time at the scale of

a single glacierized valley of the Cordillera Blanca. It tests and proves the validity of the hydrochemical basin characterisation method (HBCM) I developed to meet the research objective. The use of the HBCM was then extended to four different glacierized valleys spread out in the Cordillera Blanca. Chapter Three describes a double use of natural tracers. Tracers are used for a HBCM based quantification of the groundwater contribution at four different valleys of the Cordillera Blanca, and to characterise groundwater contribution mechanisms and pathways. Finally, specific discharge extrapolated from the groundwater contribution quantification is used in an original water balance-based hydrological model that simulates glacier retreat-related hydrological shifts based on glacier cover and rate of retreat. In chapter four, a comparison of trend analyses conducted on historical discharge time series makes it possible to depict past and future glacier-related changes in stream discharge for the Rio Santa and some of its tributaries.

Context of Chapter 2 within Thesis

Studying the groundwater contribution to surface flows in glacierized valleys of the Cordillera Blanca required adapting traditional hydrochemical/isotopic mixing models to the working environment. In addition to overcoming a limitation in sampling frequency, the HBCM integrated a lake mixing module that had never been used in a similar context. As such, we can see chapter two as a description and an evaluation of the method whose extended use is presented in chapter three. However, because this study makes use of a valuable historical dataset collected at the Querococha watershed since 1998, the chapter 2 contribution is not limited to a method introduction but provides new elements for the understanding of proglacial hydrology in the Cordillera Blanca. Once the method proved reliable, the study quantified the groundwater contribution at different points in the watershed for six different years. This provided the first estimate of the importance of groundwater to the water resources of the Cordillera Blanca in the dry season. This multiyear approach led also to an estimate of the groundwater contribution's variability in time. The use of reconstructed precipitation records made it possible to evaluate the contributing aquifer's storage capacity. These achievements make chapter two a major step toward the completion of the thesis objectives.

2. Characterizing contributions of glacier melt and ground water during the dry season in a poorly gauged catchment of the Cordillera Blanca (Peru)

2.1 Abstract

The retreat of glaciers in the tropics will have a significant impact on water resources. In order to overcome limitations with discontinuous to nonexistent hydrologic measurements in remote mountain watersheds, a hydrochemical and isotopic mass balance model is used to identify and characterize dry-season water origins at the glacier fed Querococha basin located in southern Cordillera Blanca, Peru. Dry-season water samples, collected intermittently between 1998 and 2007, were analyzed for major ions and the stable isotopes of water ($\delta^{18}O$ and $\delta^{2}H$). The hydrochemical and isotopic data are analysed using conservative characteristics of selected tracers and relative contributions are calculated based on pre-identified contributing sources at mixing points sampled across the basin. The results show that during the dry season, groundwater is the largest contributor to basin outflow and that the flux of groundwater is temporally variable. The groundwater contribution significantly correlates (P-value = 0.004 to 0.044) to the antecedent precipitation regime at 3 and 18-36 months. Assuming this indicates a maximum equivalent of 4 years of precipitation accumulation in ground water reserves, the Querococha watershed outflows are potentially vulnerable to multi-year droughts and climate related changes in the precipitation regime. The results show that the use of hydrochemical and isotopic data can contribute to hydrologic studies in remote, data poor regions, and that groundwater contribution to tropical proglacial hydrologic systems is a critical component to dry-season system discharge.

2.2 Introduction

In the tropics, mountain glaciers and seasonal snow pack are an important part of the hydrological cycle as they form the headwaters for hydrologic systems that provide water to some of the most populated areas on earth (Nogues-Bravo *et al.,* 2007). While providing critical hydrologic functionality, glaciers are threatened by ubiquitous recession (Barry, 2006; Kaser *et al.,* 2006; Vuille *et al.*, 2008) that will cause significant hydrologic changes, including a reduction in dry-season water discharge (Barnett *et al.*, 2005), an increase in peak discharges (Mark and Seltzer, 2003), and a general decrease in water resources in Asia, Europe, and the Americas (IPCC, 2007). Despite the threat posed by this ongoing decline, detailed studies of the future impact of global warming on water resources in potentially affected regions are long overdue (Barnett et *al.*, 2005).

Modeling tropical pro-glacial hydrology is important for predicting the future impact of glacial retreat on water resources, but is difficult because of the relatively poor, location specific, understanding of hydrological processes in these remote areas. In addition to glacial melt input, tropical pro-glacial hydrology must include surface and subsurface systems. Although there is extensive research on understanding glacier dynamics in the tropics and modeling gross runoff, there has been very little research focused on the role of groundwater in these systems (Favier *et al.*, 2008; Wagnon et al., 1998). The consequence is that existing proglacial hydrological models frequently oversimplify the input of groundwater to the hydrologic budget (Hood *et al.*, 2006).

One approach to estimate the contribution of groundwater to stream discharge is to use hydrochemical mass balance wherein multiple tracers are used to quantify multi-component mixing (hydrochemistry refers here to dissolved chemical species in water and the stable isotopes, $\delta^{18}O$ and $\delta^{2}H$). This potentially useful approach has not yet been thoroughly applied to pro-glacial systems (Brown *et al.*, 2006), although the chemical weathering of rock, sediment, and soil that deeply

influence the ionic and isotopic composition of surface and ground water applies to those environments. The physical weathering processes that occur at the base of a glacier produce fine fresh particles that are particularly reactive to chemical weathering that should be defined by a specific hydrochemical signature for glacial melt water (Anderson, 2005).

In this study we use a hydrochemical basin characterisation method (HBCM) that quantifies the dry-season relative contribution of glacial melt water and groundwater components to streams across tributaries of the Querococha watershed, a glacierized 64 km^2 large catchment situated in the southern Cordillera Blanca Peru (Figure 2.1). The Rio Santa, which drains the glacierized Cordillera Blanca westward to the Pacific, provides an important water source for hydroelectric power generation and irrigation.

2.3 Study area

The Callejon de Huaylas, Peru, is a 4900 km^2 watershed that captures runoff from the western side of the Cordillera Blanca and the eastern side of the Cordillera Negra (Figure 2.1A). The Rio Santa originates at Laguna Conococha, a shallow lake 4000 meters above sea level (m.a.s.l.) and drains the Callejon de Huaylas down to the Cañon del Pato hydropower plant at 1500 m.a.s.l. The Cordillera Blanca has the largest glacierized surface area in the tropics, with a total glacial area of 631 km^2 (Suarez *et al.*, 2008), whereas the Cordillera Negra has no glaciers. Between 1970 and 1997 the glacial surface area of the Cordillera Blanca has decreased by approximately 15% (Pouyaud *et al.*, 2005), and almost all of these glaciers are predicted to potentially disappear by 2200 in many future climate scenarios (Pouyaud, 2004).

Rio Santa historical discharge records from 1991 to 2000 at La Balsa, a gauging station situated less than 10 km upstream of the hydropower plant has a clear seasonal pattern of discharge. The lowest discharge occurs from July to September

while the peak discharge occurs usually in March and is almost 9 times greater. Variations in discharge closely follow precipitation seasonality, typical of the outer tropics where more than 80% of precipitation falls between October and May, and the austral winter months of June to September have essentially zero precipitation. In the Rio Santa watershed glacial melt provides 10 to 20% of the total annual discharge, and may exceed 40% in the dry season (Mark *et al.*, 2005). The average annual average air temperature is less variable than the daily temperature range, as is typical of the tropics. In contrast with mid-latitudes, the absence of any major thermal seasonality in the tropics causes glacier ablation throughout the year (Kaser *et al., 1999*). The year round ice melt that occurs in the relatively steady ablation area provides melt water some stability in its hydrochemical signature that makes tropical glacier-fed watersheds of particular interest for hydrochemical basin characterisation. In addition, by limiting the seasonality of the snow cover extent, the relative thermal steadiness marginalises its effects.

The Querococha valley (Figure 2.1B) is situated between 4000 and 5150 meters above sea level (m.a.s.l.). The Querococha Lake, with an area of 1.4 km^2, marks its outlet. The two main streams within the watershed drain directly into the lake, one from the Yanamarey and G2 glaciers and the other from a non-glacierized valley. The basin contains steep sided flat-bottomed valleys filled with Quaternary sediments. As of 2005, the Yanamarey glacier has an area of 0.89 km^2 and is situated between 4650 and 5150 m.a.s.l. The G2 glacier is slightly larger with a total surface area of 1.1 km^2, and is situated between 4800 and 5150 m.a.s.l. (Racoviteanu, 2005). Combined, the glaciers cover 3% of the total catchment area. The Querococha basin is mainly composed of the sedimentary, highly weathered, Chicama formation. It includes also a limited plutonic intrusion present around the south and west boundaries (Love *et al.*, 2004).

2.4 Methodology

For tracers that are conservative at the basin scale, it is assumed that the mass at a given point within a sub-basin is derived entirely from source components, which in the dry-season tropical proglacial setting are assumed to be glacial melt water, groundwater and up-gradient nested streams. The hydrochemical basin characterisation method (HBCM) uses a multi-component mass balance approach to identify the relative or absolute contributions of these source components at a given point. HBCM geospatial coverage is based on dividing the watershed into nested interconnected sub-basins. Nested areas are used to compile component contributions for the total watershed. HBCM requires a minimum of *n-1* tracers to determine the relative contribution of *n* end-members at a mixing point.

Where instantaneous mixing can be assumed, a mass balance is applied to each selected conservative natural tracer *j*, assuming a well mixed system, with the following equation:

$$C_{tot_j} = \frac{\sum_{i=1}^{n} (C_{i_j} . Q_i) + \varepsilon_j}{Q_{tot}} \qquad (2.1)$$

C_{tot_j} and C_{i_j} represent the relative concentration or proportion of a tracer *j* at mixing point and at one of the *n* identified potential end members *i,* respectively; Q_{tot} and Q_i correspond to the total discharge at the mixing point and the proportional contribution of the tracer *i* and ε_j ; which ideally tends to zero, corresponds to the accumulation of inaccuracies, uncertainties, errors, and approximations that can occur during the sampling, handling, and analysis for the tracer *j*.

The HBCM solves for the unknown $\frac{Q_i}{Q_{tot}}$ by minimizing the cumulative residual error $\sum_{j=1}^{m} \varepsilon_j$ while solving the water balance within a 0.5% tolerance. The water balance is:

$$\sum_{i=1}^{n} Q_i = Q_{tot} \qquad (2.2)$$

In cases where mixing occurs in large water bodies such as the Querococha Lake, instantaneous mixing cannot be assumed, and a retention factor must be included. For lakes the mass balance equation (2.1) is modified to include a time component:

$$\int_{t=1}^{d} C_{out_{j\,t}} . V_{out_t} . dt + \Delta S_j = \varepsilon_j + \sum_{i=1}^{n} \left(\int_{t=1}^{d} C_{ij_t} . V_{i\,t} . dt \right) \qquad (2.3)$$

where t is time expressed in days and d is the number of days between two sampling events; V_{out_t} is the daily volume of water passing through the lake outlet between the 2 sampling events; V_{i_t} is the volume of water supplied by an end member i; and $C_{out_{jt}}$ and $C_{i_{jt}}$ are the daily concentration or value of the tracer j at the basin outlet and of an end member i respectively. ΔS_j is the change in mass of tracer j in the lake over the considered time period:

$$\Delta S_j = \left(C_{out\,j_1} - C_{out\,j_d} \right) V_{mix} \qquad (2.4)$$

At any time, the average value of a tracer j in the lake is assumed to be the same as the concentration at the outlet $C_{out_{jt}}$. V_{mix} *represents* a conceptual homogeneous volume of lake water (less than or equal to the total volume of the lake) that would be fully mixed during the time between the two sampling events. It is assumed that

the lowest V_{mix} occurs during the dry season and the highest V_{mix} occurs during intense precipitation periods; therefore V_{mix} is a function of measured precipitation. $C_{i_{jt}}$ the concentration of the tracer j for the end member i at any t time of the period from 1 to d is considered equal to the average value of $C_{i_{j1}}$ and $C_{i_{jd}}$. The same rule applies to V_{i_t} and V_{out_t}. For a given time T, $C_{out_{jT}}$ is therefore computed as follows:

$$\begin{cases} \int_{t=1}^{T} C_{out\,j_t}.V_{out\,t}.dt = \int_{t=1}^{T-1} C_{out\,j_t}.V_{out\,t}.dt + V_{out_T}.C_{out\,j_T} & (2.5) \\ C_{out\,j_t} = \dfrac{\sum_{i=1}^{n}(C_{i\,j_t}.V_{i_t}) + C_{out\,j_{(t-1)}}.V_{mix} - C_{out\,j_t}.V_{out_t}}{V_{mix}} & (2.6) \end{cases}$$

The water balance, Equation (2.2), is also modified to incorporate the lake module:

$$\sum_{i=1}^{n}(V_{i_t}) + P_t = Q_{out\,t} - E_t \qquad (2.7)$$

where P_t and E_t correspond to the daily volume of precipitation and evaporation to and from the lake respectively. Evaporation is calculated based on a different evaluation made on the nearby Titicaca Lake (Delclaux *et al.*, 2007). The lake module of HBCM requires sampling at two different times so that volumes flowing in and leaving the lake have a significant impact on its water concentrations. In this study, a 10 and 50 day sampling interval was used to assess residence time without being affected by seasonal changes. $\delta^{18}O$ and $\delta^{2}H$ are not considered as acceptable tracers for the lake component due to evaporitic isotopic fractionation and spatial/temporal variability (Gonfiantini *et al.*, 2001).

The ability of HBCM to accurately simulate watershed hydrology is validated using an inverse mass balance equation (2.1) as proposed by Christophersen et al.

(1990). The principle of that validation step is that back-calculated concentrations based on a multi tracer mass balance calculation should match the measured values of any tracer taken individually.

Among the most critical conditions for HBCM application are the conservative behaviour of tracers within the study area and its ability to identify the end-members uniquely and distinctly (Soulsby *et al.,* 2003). For the HBCM, a set of criterion are used to select applicable ions or isotopes. These are:

- The tracer must have a consistently conservative behaviour. For the HBCM, non-conservative behaviour is defined as a tracer, as measured at a mixing point within the watershed, having a value outside the range defined by the end-members.
- The measured tracer value at the mixing point and a minimum of one end member must be above the detection limit of the analytical methods.
- There should be a minimum 20% difference between extremes in end-member tracer values.

Compliance of the three requirements is evaluated. Tracers that demonstrate compliance to the 3 requirements are used for HBCM application.

The Querococha watershed is divided into 5 sub-basins (Q1, Q2-1, Q2-2, Q2-3, and Q3 (Figure 2.1B)) defined using SRTM DEM data, with areas calculated using ArcGIS. The GLIMS glaciers database (Racoviteanu, 2005) was used to define the 2005 glacial coverage. The primary geospatial characteristics of the Querococha watershed and delineated sub-basins are summarized in Table 2.1.

The HBCM was applied to hydrochemical data sets from the Querococha watershed using a synoptic sampling approach whereby water samples are taken from a wide variety of sources in a very short time span (Mark and Seltzer, 2003; Mark *et al*., 2005; Mark and McKenzie, 2007). Synoptic sampling captures the instantaneous end members and mixtures chemical and isotopic signatures of

tracers that are time dependant. This is the case for examples of the stable isotopes of water. Oxygen 18 and deuterium undergo fractionation on different occasions generating variations in samples isotopic signatures and making them improper for use in conditions different than instantaneous mixing. The buffering effects of natural reservoirs such as aquifers and proglacial lakes allows temporal signatures to remain valid long enough to be used at all the different studied mixing points of the basin, with the exception of the Querococha Lake. Spatially, it is assumed that the hydrochemical composition of end-members is homogeneous throughout the watershed as the bedrock geology is nearly uniform in the study area (a more detailed description of the geological context is given at chapter 3). The hydrochemical composition of the lowest measured discharge from the non-glacierized sub-basin (Q1) is assumed to be representative of the basin wide groundwater. Samples taken of the Yanamarey glacier melt (Yan) are used to represent both the Yanamarey and G2 glaciers melt waters. Annual samplings are detailed at Table 2.2.

For each sample collected, electrical conductivity, pH, and temperature are measured directly in the field. Samples for laboratory analysis are filtered onsite and stored in completely filled HDPE 30 or 60 ml bottles and stored at 4^{o}C whenever possible. Major anions (F^-, Cl^-, Br^-, NO_2^-, NO_3^-, SO_4^{2-}) are measured by ion chromatography and major cations (Fe^{2+} & Fe^{3+}, Ca^{2+}, Mg^+, K^+, Na^+, Sr^{2+}) and silica (S_iO_2) are measured using either ion chromatography, atomic absorption/emission, or direct current plasma spectroscopy. The stable isotopes of oxygen and hydrogen ($\delta^{18}O$ and δ^2H) are measured by mass spectrometry at Syracuse University and The Ohio State University (Finnigan MAT Delta Plus coupled to a HDO water equilibrator) Stable isotopes results are reported using the δ-notation reported relative to the Vienna-Standard Mean Ocean Water (VSMOW) standard, with an accuracy of ±0.1‰ for $\delta^{18}O$ and ±1‰ for δ^2H.

Bi-carbonate concentration is calculated as the difference in the solution charge balance. The sum of anions and sum of cations are calculated as the sum of the

respective milliequivalent values. TDS is the sum of all ions multiplied by a 0.8 correction factor.

The geospatial location of the mixing points is used to assess the groundwater contribution variations both temporally and spatially by relating the calculated dry-season groundwater relative contribution to the percent glacierized area of different sub-basin using a simple dilution model:

$$Gl_{\%} = \frac{\frac{q_{gw}}{q_{gl}}(100 - A_{gl})}{(A_{gl} + \frac{q_{gw}}{q_{gl}}(100 - A_{gl}))} \qquad (2.8)$$

where A_{gl} and $Gl_{\%}$ represent the percentage of glacierized surface for the sub-basin whose mixing point defines the outlet, and the rate of groundwater contribution projected at this point respectively, and q_{gw} and q_{gl} correspond to the groundwater and melt water specific discharge. Melt water specific discharge is defined as the volume of melt water divided by the glacier area.

The HBCM and dilution model results are compared for dry-season years with adequate data using a non-linear regression analysis, specifically 1998, 1999, 2006, and 2007. A strong correlation between the dilution model and the HBCM results suggests that the relative groundwater contribution is broadly distributed across the sub-basins whereas a weak correlation would suggest that groundwater input is spatially dependent.

The q_{gw}/q_{gl} ratio, calculated by fitting the dilution model to the HBCM results, is an indicator of the relative importance of ground water input to the basin discharge; a dry season characterised by a high q_{gw}/q_{gl} ratio indicates a high input of ground water to the total system discharge. In this study, the q_{gw}/q_{gl} ratio is used as a metric of groundwater contribution to the dry-season Querococha basin discharge.

Finally the ratios computed at the modeling stage are compared to normalised precipitation records from onsite rain gauges to evaluate what influence the past precipitation amounts have on the relative dry-season contribution of ground water at the basin scale. The historical precipitation record spans 1981-1999 for the Yanamarey meteorological station (09°39'26"S; 77°16'20"W) data and 2001-2007 for the new Yanamarey station (09°39'33"S; 77°16'17"W). The 1982-1999 time-series is complete from September 1981 to August 1994 but is missing 54% of monthly data from September 1994 to July 1999. The missing data are reconstructed from the Querococha meteorological station 11 km away (09°43'43"S; 77°19'49"W) using a linear transform function. The 2001-2007 time series is missing 60% of the monthly totals data. The missing data are reconstructed using the average of two nearby totalizing rain gauges, YP1 (09°39'20"S; 77°16'34"W) and YP2 (09°39'24"S; 77°16'49"W). Computed q_{gw}/q_{gl} ratios from the 1998, 1999, 2006, and 2007 dry seasons, are compared to normalized monthly antecedent precipitations for periods of 1 to 60 months using a Pearson correlation test ($\alpha = 0.05$).

2.5 Results and discussion

The nine tracers that meet the usability criterion for HBCM are conductivity, bicarbonate, magnesium, sum of anions, sulphate, TDS, hydrogen ion, and the two stable isotopes of water ratios. Figure 2.2, a box plot of relative concentration for individual variables, shows that the selected variables provide end-members with a unique and distinct signature that can be used to differentiate end-members contribution in mixing equations. Results show that the high sulphate concentrations (> 50 ppm on average) in the glacial melt provide a signature that is exclusive to the melt water. The oxidation of the pyrite present in the Jurassic Chicama formation that underlies most of the Querococha basin is the likely origin of these anomalously high sulphate values (Mark *et al.,* 2005). High sulphate concentrations also affect the conductivity, TDS, and sum of anions, thereby enhancing hydrochemical differences between end members. The acidic pH of the

melt water may be due to the formation of sulphuric acid from the dissolution of this pyrite or other potential sulphides.

The back-calculation HBCM validation was conducted on sulphate, the tracer with the largest concentration range between the end members. Figure 2.3 compares sulphate concentrations back-calculated from HBCM results with the measured concentrations at all mixing points of the Q2 sub-basin. The coefficient of determination (R^2) resulting from that comparison is 0.96. Considering that back calculated concentrations originates from two consecutive uses of the same mass balance equation and that intermediate results were based on three to five different tracers, we can consider this determination coefficient as an indicator of very good HBCM performance.

The HBCM was used for all of the mixing points within the partially glacierized Q2 sub-basin for the dry seasons of sampled years to determine the relative contribution of melt water and groundwater to surface water (Table 2.3). The median relative contribution of groundwater at the Q2 mixing point is 59% of the total discharge, indicating that groundwater is the dominant end member in more than half of the studied dry seasons. This confirms that groundwater is a major dry-season contributor to streams in this glacier fed tropical basin. The largest calculated Q2 groundwater contribution was 74% in 2007 and the minimum contribution was 18% in 1998. The resulting 56% range of relative groundwater contribution over the studied period indicates a high degree of inter-annual variability. With such high variability and dominant overall contribution, groundwater appears to be as important as melt water in contributing dry-season stream flow at the Q2 point. Modeling the pro-glacial hydrology for this catchment would therefore require incorporating realistic groundwater contribution processes. Geospatial variation in relative end member contribution is calculated for the 2006 and 2007 dry seasons, the only years with sufficient sample coverage (Figure 2.4). The HBCM results show that the two glacierized sub-basins, Q2-2 and Q2-3, both have similar relative groundwater contributions during the dry season. This is

potentially related to the common geomorphologic characteristics these two sub-basins exhibit. They both have comparable basin sizes, glacier orientation and elevation range and show a slight difference only in the percentage of glacierized area (Table 2.1). The results show also that, at the Q2-1 non glacierized catchment, groundwater contributes to almost half of the total outflow of Q2-2 and Q2-3. As three sub-basins present an important groundwater contribution, it can be concluded that groundwater input does not only occur in particular sub-catchment of the Q2 basins only but is distributed throughout them all.

How similar the sub-basins are in generating groundwater is studied by using the mixing model (Equation 2.8). The non-linear regression analysis between percentage of glacierized area of a sub-basin and its relative ground water contribution provides first an indication of how well the model fits with the HBCM findings. Results from the analysis for the years 1998, 1999, 2006 and 2007 made using the Q2, Q3 and Yan Pampa down as distributed watersheds are presented in Table 2.4. The model fit is evaluated through the coefficient of determination (R^2) that ranges from 0.97 to 1.00 indicating a close relationship between the HBCM calculated groundwater contributions and the dilution model and that there is not a dominant relationship between sub-catchment geographic position and the pattern of groundwater contribution to stream flow. What happens within the sub-basin is not discerned by HBCM. Localised disparities in groundwater contribution like surface water contribution to ground water spots (i.e. a losing stream reach) may exist but would require a finer HBCM spatial resolution to be identified.

The regression analysis provides also yearly computed values of the model parameter q_{gw}/q_{gl}. Over the four studied years, this ratio varies from 0.02 to 0.13. These values translate specific contributions of melt water q_{gl}, defined as melt water discharge divided by glaciated area, that are 8 to 50 times greater than that of groundwater. Normalized q_{gw}/q_{gl} ratios show that relative groundwater contributions are lower in 1998 and 1999 than in 2006 and 2007. By definition,

this lower relative contribution of groundwater in 1998-1999 maybe due to a q_{gw} being lower than in 2006-2007, a higher q_{gl} or a combination of both. The Yanamarey glacier mass balance presented in Bury et al. (2009) for the 1999-2008 period shows that the glacier absolute contribution was higher in 2006-2007 than in 1999, suggesting that the low 1998-1999 relative groundwater contribution was a consequence of a low q_{gw}. Antecedent precipitation normalized to the 1982-2007 monthly average, presented in Table 2.5, suggests that low groundwater yields may be related to the lack of precipitation that occurred months and/or years ahead of July 1998. This relation is confirmed by the correlation study conducted on the normalized q_{gw}/q_{gl} ratios and the antecedent precipitation, which are expressed both as statistically representative correlation coefficient, r_{xy}, and the P-value (Table 2.5). Of the 10 considered normalized precipitation periods, four present a significant ($\alpha = 0.05$) correlation with the normalized q_{gw}/q_{gl} ratio. These periods are the antecedent 3, 18, 24 and 36 months. This result suggests that the dry-season relative groundwater contribution is influenced both by a short and recent period (3 months before dry season) as well as by a long and older period (from 18 to 36 months prior studied dry season) of antecedent precipitations. The different contributing periods suggests the existence of both short and longer groundwater pathways from surface infiltration to stream discharge. At antecedent periods greater than 48 months there is very little precipitation influence, suggesting that the maximum volume of water being stored into the groundwater system at once is equivalent to around four years of average precipitations.

2.6 Conclusions

By combining limited physical hydrology data with hydrochemical data through the HBCM analysis, it is possible to estimate source contributions to a glaciated watershed in the tropics and to make initial connections between climate and hydrology. While the HBCM was only used for the Quererococha basin and sub-basins within, it is easily adaptable to other tropical or subtropical proglacial valleys where the impact of glacial retreat on water resource needs to be assessed.

It provides a method of delineating source contributions without a major investment in infrastructure for hydrologic measurements. Querococha, our pilot watershed, is now better instrumented and has more historical data than most glaciated watershed in the tropics. Actual instrumentation, that includes both upstream and downstream gauging stations, is planned to further refine HBCM results, for example by increasing the temporal resolution and to identify end members at the year scale.

The HBCM results show considerable temporal variability in volumetric groundwater contributions. Of the studied dry seasons, groundwater is a dominant contributor to the Querococha surface water. The analysis of antecedent precipitation patterns before each dry season indicates that groundwater follows both a fast (three months) and a slow (three years) flow systems. This may reflect local and intermediate flow systems or other hydrogeological complexities that are not the focus of the HBCM. Further research is required to assess the groundwater processes that control this system.

The present study demonstrates that modeling pro-glacial catchments such as Querococha or other comparable basins requires incorporating adequate groundwater contributions and mechanisms. With a relative contribution that varies from 18 to 74% for a basin that, like the entire Cordillera Blanca, is 7% glaciated, pro-glacial groundwater contributions are a key component of the dry-season local hydrogeological system and possibly of the entire Cordillera Blanca. Neglecting this groundwater component in proglacial hydrology modeling would therefore lead to incomplete and inaccurate projections at annual and climatically appropriate time scales.

Both of the glaciers in the Querococha basin are rapidly retreating and will disappear in the coming decades. Assuming a complete loss of Querococha glaciers while maintaining current precipitation regime (*Painter,* 2007), the dry-season discharge would be decreased by almost half of what was observed in

1998, 1999, and 2004-2007. This decrease in the melt water contributions could lead to increased discharge inter-annual variability. A multi-year drought, in addition to the absence of glacial melt inputs, would cause, with possibly a one and half year delay, an even more significant drop in watershed discharge.

2.7 Acknowledgements

The authors would like to thank Marcos Zapata and Jesus Gomez, ANA, Peru for providing data and logistical support, the Ice Core Group and Ping-Nan Lin and the Byrd Polar Research Center, The Ohio State University, for stable isotope analysis. Financial support from McGill University, Geochemistry and Geodynamics Research Center (GEOTOP) of Quebec, Natural Science and Engineering Research Council (NSERC) of Canada, and The Ohio State University.

2.8 Tables

Table 2.1. Geospatial characteristics of the Querococha watershed and sub-basins.

Sub-basin	Glacier	% glacierized	Total Area (km2)	Contribution from	Contribution to	Sampling spots
Q1	-	-	20.02	-	Q3	Q1
Q2-1	-	-	10.48	Q2-2 & Q2-3	Q3	Q2
Q2-2	Yanamarey	9.9	9.02	-	Q2-1	PD & Yan
Q2-3	G2	13.4	8.25	-	Q2-1	YOG
Q2 tot	Yan. & G2	7.2	27.75	-	Q3	
Q3	-	-	16.09	Q1 & Q2	Quero.	Q3
Quero.	Yan. & G2	3.1	63.86	-	-	all

Table 2.2. Description of dry-season yearly samplings performed at the Querococha basin between 1998 and 2007. Blanks indicate no data available.

Mixing Point	**1998**	**1999**	**2004**	**2005**	**2006**	**2007**	Total
Q3	2	2	1	1	1	2	9
Q1	2	2	1	1	1	2	9
Q2	2	2	1	1	1	2	9
YOG			1	1	1	1	4
PD					1	3	4
Yan	2	2	4	1	1	2	12
Total	8	8	8	5	6	12	47

Table 2.3. Prediction of relative ground water contribution (%) during the dry season at the Querococha watershed outlet, Q2, and PD mixing points. Empty cells indicate insufficient data.

	A_{gl} (%)	1998	1999	2004	2005	2006	2007	Average	Median
Outlet	3.1	42	68				79		
Q2	7.2	18	52	71	46	65	74	**54**	**59**
PD	9.9					49	46		

Table 2.4. Dilution model (Equation 2.8) results for groundwater contributions to Quererocha discharge for the 1998, 1999, 2006 and 2007 dry seasons. q_{gw}/q_{gl} represents the ratio of groundwater and meltwater specific discharges. Normalized q_{gw}/q_{gl} is the q_{gw}/q_{gl} ratio minus the average q_{gw}/q_{gl} value from 1998, 1999, 2006 and 2007 dry seasons. R^2_{model} is the coefficient of determination between the dilution model results and the relative groundwater contribution results, calculated with HBCM, as a function of the basin glacierized surfaces.

Parameter	**1998**	**1999**	**2006**	**2007**	**Average**
$\mathbf{q_{gw}/q_{gl}}$	0.02	0.08	0.12	0.13	**0.1**
Normalised $\mathbf{q_{gw}/q_{gl}}$	-0.08	-0.03	0.02	0.03	
$\mathbf{R^2}$ model.	0.99	1.00	0.99	0.97	

Table 2.5. Precipitation / groundwater relative contribution correlation results to Querococha discharge for the 1998, 1999, 2006, and 2007 dry seasons. Normalized precipitation, $P_{m,}$ is the antecedent precipitation, normalized to the 1982-2007 monthly average, for *m* months prior to the month of July. Normalized precipitation is expressed in mm. r_{xy} is the correlation coefficient for the q_{gw}/q_{gl} ratios and the normalized precipitation. Only the statistically representative r_{xy} are presented.

P_m	1998	1999	2006	2007	P-value	r_{xy} *
P_1	-12	39	52	-12	0.667	
P_2	-53	85	11	16	0.573	
P_3	-130	9	114	162	**0.004**	**0.996**
P_6	-380	408	213	23	0.427	
P_{12}	-560	89	129	165	0.083	
P_{18}	-576	-291	63	378	**0.044**	**0.956**
P_{24}	-679	-470	197	294	**0.041**	**0.959**
P_{36}	-992	-589	403	362	**0.030**	**0.970**
P_{48}	-1307	-903	780	568	0.058	
P_{60}	-815	-1218	896	946	0.182	

**significant for alpha = 0.05*

2.9 Figures

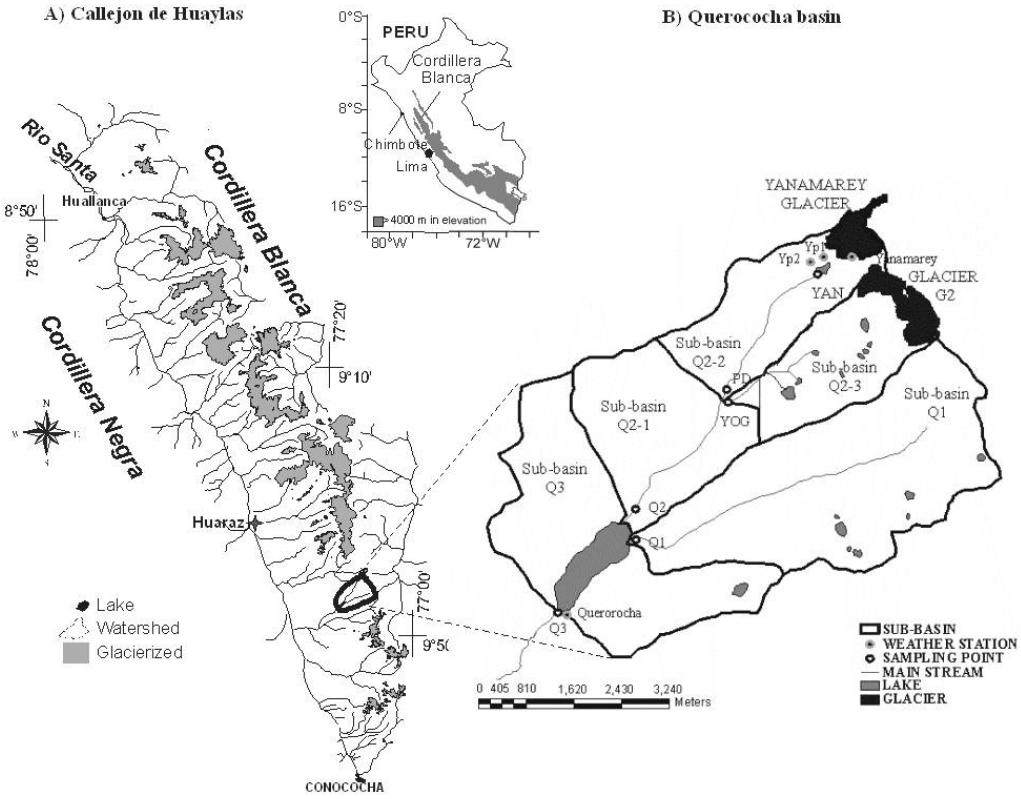

Figure 2.1. Map of study area. A) Callejon de Huaylas map; B) Querococha basin map. Sub-basins are delineated for using the HBCM.

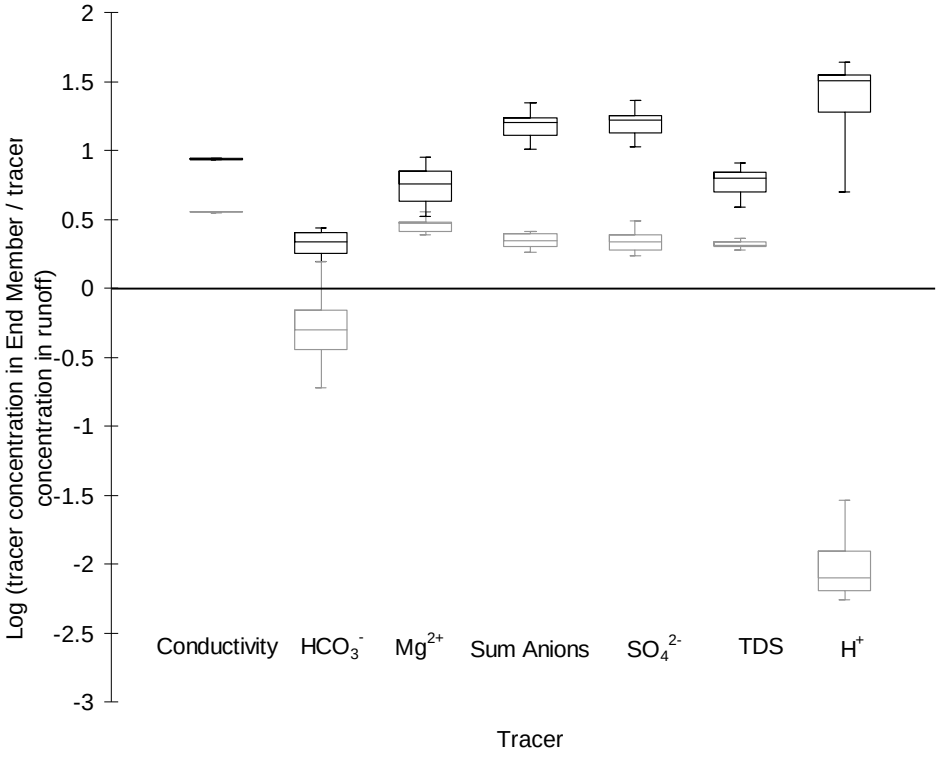

Figure 2.2. End member hydrochemical signature as related to tracer selection. Boxplots represent the log of the tracer's concentration, normalized to its runoff concentration for melt water (dark line) and groundwater (grey line). Relative measures are computed by dividing individual values by the average tracer measure in runoff.

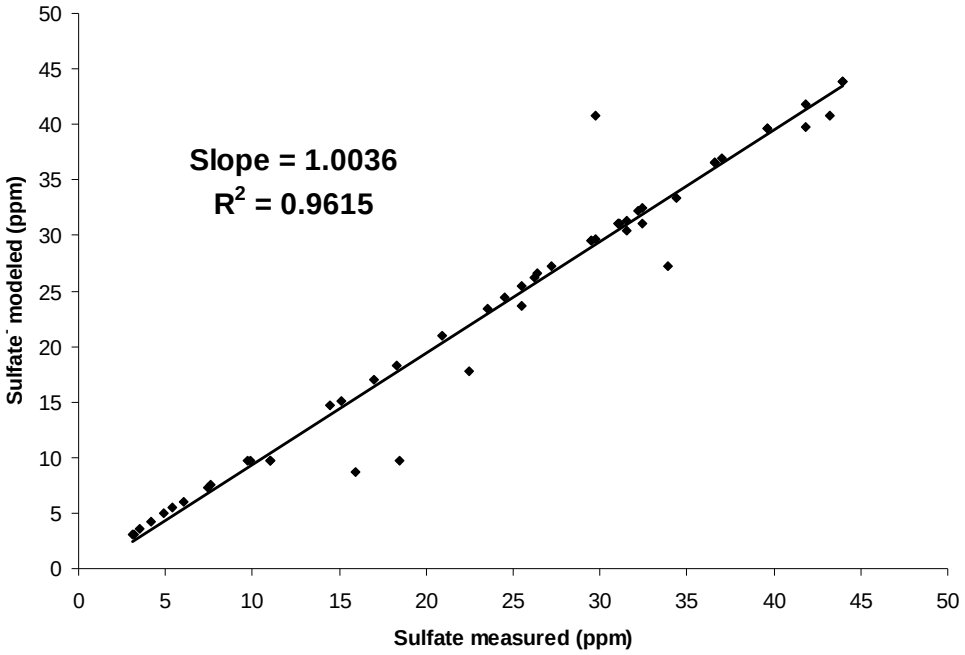

Figure 2.3. Comparison between measured and calculated sulphate concentrations at all mixing points on the Q2 sub-basin.

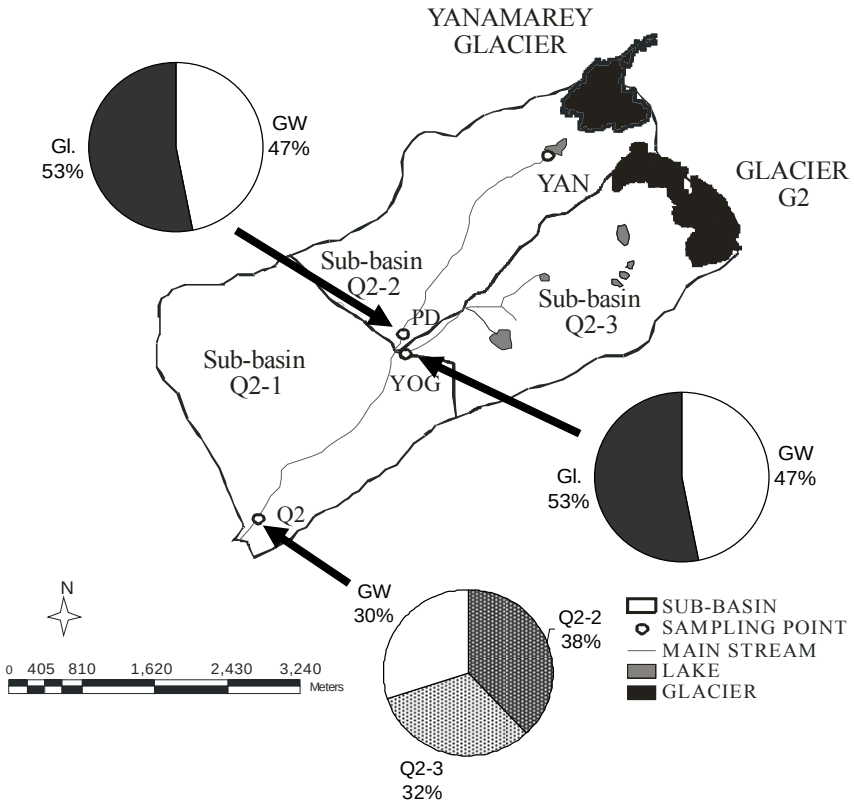

Figure 2.4. 2006-2007 dry-seasons end members and tributaries relative contribution to surface flows of the Q2 basin. Each pie-chart related to the sub-basin map represents the average contributions at the pointed mixing point. Groundwater is represented in white and melt water in black. For the 2006-2007 dry season the overall Q2 relative contribution is 30% from glacial melt and 70% from groundwater.

Context of Chapter Three within Thesis

In 2008, our objective to further characterise the groundwater contribution to the entire Cordillera Blanca led to intense sampling at four different sub-watersheds of the Rio Santa, representative of the different lithologies and glacier cover found in the region. This synoptic sampling aimed to collect, in very limited time, stream water, melt water and groundwater at different areas in each watershed. Since the findings that emerged from this intense 2008 work were less precise than desired, we increased the sampling density in 2009 and, due to logistical constraints, applied it to the Quilcayhuanca watershed only. Chapter three is based wholly on these two campaigns. It details the way hydrochemical, isotopic and hydrological measurements were used to work toward three different objectives of the thesis:

- Evaluate the spatial variability of the groundwater contribution to streams across the Cordillera Blanca.
- Identify the main groundwater flow at the glacierized valleys.
- Understand the principal hydrogeological recharge and discharge mechanisms.

In meeting these objectives, chapter 3 represents a key element of the present thesis.

3. Proglacial Hydrogeology in the Cordillera Blanca, Peru

3.1 Abstract

The rapid retreat of the glaciers of the Cordillera Blanca is having a noticeable impact on the water resources for the local population who depend upon them. While groundwater is a critical hydrologic component that sustains dry-season steam flows, its contribution and characteristics remain poorly understood. In this study, we use the hydrochemical and isotopic signatures of potential hydrologic sources and surface waters to characterise the proglacial hydrogeology in four glacially fed watersheds within the Cordillera Blanca, Peru. Water samples from streams, glacial melt and groundwater were collected in 2008 and 2009 and analysed for major ions and the stable isotopes of water ($\delta^{18}O$ and $\delta^{2}H$). Multivariate variance analysis was used to select the hydrochemical and isotopic characteristics of the water samples that depend primarily on the origin of the water. We applied the Hydrochemical Basin Characterisation Method (HBCM), a multi-component spatial mixing model, to quantify the contribution of different water sources to the four watershed outflows. The HBCM results show that groundwater is a major component of the dry-season discharge and that groundwater specific discharge is greater than 0.26 mm d^{-1} for all of the valleys studied. The results are used to develop a conceptual hydrological model for the proglacial hydrogeology of Cordillera Blanca valleys. Talus and avalanche cones are identified as key components of the studied valleys hydrogeology. The talus deposits collect direct precipitation and runoff from higher elevations and release significant water volumes with a residence time long enough to remain active throughout the dry season.

3.2 Introduction

Over the last century the world's tropical glaciers have been retreating raising concerns about downstream water supplies (Mark and Seltzer, 2003). In Peru, the western side of the Cordillera Blanca is drained by the Rio Santa, which exhibits a dry season decline in flow related to glacier retreat (Baraer *et al.*, 2012). Such hydrological changes significantly alter the availability of water in the region and pose critical risks to the local population who are highly dependent on these resources for their livelihoods (Bury *et al.*, 2011). In addition to the consequences of the general decrease in regional water resources, households are also affected by the disappearance of many of the perennial and intermittent springs that provide a nearby safe access to the resource (Mark *et al.*, 2010).

During the dry season when rainfall is low or absent, natural hydrologic storage systems release water accumulated during the rainy seasons. Within proglacial valleys, glaciers represent the most studied water storage system (Bradley *et al.*, 2006; Chevallier *et al.*, 2004; Coudrain *et al.*, 2005; Juen *et al.*, 2007; Mark and Seltzer, 2003; Pouyaud *et al.*, 2005), whereas groundwater systems, despite their importance, are poorly understood (Mark and McKenzie, 2007). Baraer *et al.* (2009b) using a hydrochemical mixing model, found that on the scale of a single glaciated watershed (7% glacierised) in the Cordillera Blanca, groundwater was the largest contributor to the catchment outflow during the dry season and that the flux of groundwater was temporally variable. In addition, they found that the groundwater storage capacity of a watershed was sufficient to sustain dry-season flows for a period of two to four years (Baraer *et al.*, 2009b). However, many aspects of the groundwater system, such as spatial variability and the processes controlling groundwater flow, remain unquantified in the Cordillera Blanca. In the present study, we further investigate the hydrogeological system using hydrochemical and isotopic parameters. The use of natural tracers has already proven valuable in characterising hydraulic dynamics in glacierised catchments (Crossman *et al.*, 2011; Roy and Hayashi, 2009b; Ryu *et al.*, 2007; Strauch *et al.*,

2006; Yang *et al.*, 2011) and is a powerful research tool where conventional in situ hydrological and hydrogeological methods are difficult to deploy (Mark *et al.*, 2005).

The hydrochemical composition of natural water is strongly influenced by the porous substrate through which it flows (Sidle, 1998). Weathering processes that generate hydrochemical signatures can be physical, biological, or chemical and are characterised by a reaction type (e.g., dissolution) and reaction time. Rock/soil contact time usually has a positive correlation with increased total solute concentration in water. Chemical weathering rates usually increase if the rate of physical, or mechanical weathering increases (Langmuir, 1997). Cations exchange processes also play an important role in controlling the chemical composition of water in addition to dissolution processes (Yamanaka *et al.*, 2005). These temperature dependent mechanisms make watershed geomorphic parameters (e.g., rock/soil characteristics or relief), climate, vegetation and residence time important environmental factors that influence the chemistry of meteoric water flowing through a watershed (Drever, 2005).

Unlike hydrochemical characteristics, the isotopic composition of oxygen and hydrogen in groundwater does not change significantly with water-rock interactions at low temperature. Isotopic precipitation compositions in the Andes are primarily dependent on the elevation gradient, the seasonality of precipitation and the inter-annual variability (Gonfiantini *et al.*, 2001). In the tropical Andes, the seasonal pattern of precipitation $\delta^{18}O$ isotopic values is in phase with the precipitation volume and variations in the "amount effect" (Risi *et al.*, 2008; Vimeux *et al.*, 2005). It is characterised by a period of isotopically depleted precipitation between January and April, followed by a period of comparatively isotopically enriched precipitation between August and November (Gonfiantini *et al.*, 2001; Mark and Seltzer, 2003). As a consequence of the amount effect, the yearly average meteoric $\delta^{18}O$ isotopic value is closer to the depleted level than the enriched one. In alpine environments, at watersheds where spatial variations in

yearly average meteoric $\delta^{18}O$ isotopic values are shown to be elevation gradient driven, the groundwater samples $\delta^{18}O$ isotopic signatures can be used to identify the origins and pathways of the groundwater recharge (Barbieri *et al.*, 2005; Jeelani *et al.*, 2010; Kohfahl *et al.*, 2008; McKenzie *et al.*, 2001).

The present study examines the regional dry-season groundwater characteristics of four different glacierised valleys across the Cordillera Blanca, using water samples collected in 2008 and 2009. Hydrochemical and isotopic signatures of the samples are used to quantify the groundwater contribution to watershed flows by using a distributed mixing model. In addition, these signatures are used to identify the main flow paths of contributing groundwater sources and to evaluate the recharge areas elevations. The results of the study are used to develop a conceptual model that depicts the main proglacial hydrogeological processes of the glacierised valleys of the Cordillera Blanca.

3.3 Study Site

The Callejon de Huaylas, Peru, is a 4900 km^2 watershed that captures runoff from the western side of the Cordillera Blanca (Figure 3.1) and the eastern side of the Cordillera Negra. The Cordillera Blanca has the largest glaciated surface area in the tropics (Suarez *et al.*, 2008), whereas the Cordillera Negra is glacier free. The glacial coverage of the Cordillera Blanca declined from 800–850 km^2 in 1930, to slightly less than 600 km^2 by the end of the 20^{th} century (Georges, 2004). Almost all of these glaciers are predicted to disappear by 2200 in most future climate scenarios (Pouyaud, 2004). The region is characterised by strong seasonal precipitation typical of the outer tropics, where more than 80% of precipitation falls between October and April and the austral winter months of June to August have almost no precipitation. In the Callejon de Huaylas, glacial melt provides 10 to 20% of the total annual river discharge and may exceed 40% in the dry season (Mark *et al.*, 2005). Typical of the tropics, the daily temperature range is much larger than seasonal changes in daily mean temperature. Unlike glaciers in the mid

to high latitudes, this absence of thermal seasonality in the tropics permits glacier ablation continually throughout the year (Kaser and Georges, 1999).

Geologically, the Cordillera Blanca is approximately 10 million years old and sits on the magmatic Andean arc caused by the subduction of the Nazca plate under the South America plate. Exhumed by the NW-SE trending Cordillera Blanca Detachment Fault, the bedrock of most of the western side of the Cordillera Blanca is 80 to 90% granodiorite (with high silicate content), the remainder being isolated areas of tonalite and diorite (McNulty *et al.*, 1998). The Jurassic sedimentary Chicama formation that mainly comprises the eastern side of the Cordillera Blanca (Petford and Atherton, 1992) is composed of weathered shale, argillite, and sandstone, and characterised in some areas by extensive pyrite (Fortner *et al.*, 2011).This type of formation allows cations exchange processes that modify the chemical composition of the water that flows through it (Cerling *et al.*, 1989). The geology at the southwest headwaters of the Rio Santa basin is dominated by the volcanic ignimbrite Calipuy formation, comprising sequences of terrestrial andesite, dacite and rhyolite (Myers, 1975).

Over the past 2 million years, the Andes have undergone several glacial cycles (Menzies, 2002), with the last glacial maximum estimated at being between 14,000 and 38,000 years ago (Rodbell, 1993; Smith *et al.*, 2005). Sequences of glacial advance and retreat, together with paraglacial sidewall mass wasting episodes, have produced unique depositional systems (Ballantyne, 2002; Goldthwait and Matsch, 1989) made of differentiated layers of landslide deposits and glacial, glaciolacustrine, glaciofluvial, eolian, and/or alluvial sediments. Hydrogeologically, these systems can be seen as a network of areas with distinct hydraulic conductivity and storage capacity (Van de Griend *et al.*, 1986). For example, deposits of glaciolacustrine origin are often poor aquifers (Parriaux and Nicoud, 1993), while coarse grained proglacial deposits often have high porosity and permeability (Knutsson, 2008; Meriano and Eyles, 2003; Robinson *et al.*, 2008).

The glaciated valleys of the Cordillera Blanca are characterised by pampas, landforms defined as high altitude low-gradient valley-bottom areas, likely formed by paludification of moraine dammed lakes. They are characterised by organic rich unconsolidated material that builds on glacial deposits (Mark and McKenzie, 2007). However, their hydrogeological functionality is not well understood.

We selected the Llanganuco, Quilcayhuanca, Yanamarey, and Pumapampa watersheds (Figure 3.1) for their representativeness of the numerous proglacial valleys of the Cordillera Blanca that drain into the Rio Santa. With a combined area of 250 km^2, they are located across the geographical extent of the mountain range. At the extremes, Llanganuco is situated in the northern half of the Cordillera Blanca where the valleys are deeply incised and the valley walls near vertical and Pumapampa is situated at the southern end of the range with a gentler topography and a smaller elevation gradient between the valley bottom and the watershed divide.

The selected study watersheds provide a wide range of glacierised areas, geological characteristics, and pampa coverage (Table 3.1). Evaluated using the 2005 Global Land Ice Measurements from Space (GLIMS) database (Racoviteanu, 2005), the glacierised area is greatest in Llanganuco (41.5%) and decreases towards the southern valleys with Pumapampa having the lowest glaciated area (2.1%). The geological characteristics of the four studied watersheds were extracted from geological maps (Selveradjou *et al.*, 2005). Llanganuco has the largest plutonic formation coverage, followed by; Quilcayhuanca, Yanamarey and Pumapampa. The geology of Yanamarey and Quilcayhuanca is dominated by metasedimentary rocks, whilst Pumapampa primarily comprises the volcanic ignimbrite Calipuy. Pampa area was estimated using the Advanced Spaceborne Thermal Emission and Reflection Radiometer (ASTER) satellite imagery derived Digital Elevation Model (DEM) with a 30 m cell size. Pampa was defined as a valley bottom region with a slope less than or equal to 10°, with a minimum

elevation greater than 3500 m above sea level. Pampa coverage for the studied watersheds ranges from 1.2% in Llanganuco, to 11.6% in Pumapampa.

3.4 Method

3.4.1 General considerations

Characterisation of the hydrogeology of the Cordillera Blanca valleys required identifying and classifying potential water sources that feed the main stream (stream that flows from the highest identified water source down to the valley outlet). The regional seasonality in precipitation limits the major types of water sources during the dry season to glacial melt water and groundwater. For the purpose of this study, we considered that any sub-watershed with a glacierised area of more than 45% to be a source of melt water (MELT). This threshold is justified by the fact that the specific discharge of glaciers in the dry season is much higher than that of non-glacierised lands (Baraer *et al.*, 2009a). Groundwater origins were divided into three categories: pampa (GWP), spring (GWS) and other (GW).

Pampas are found throughout the Cordillera Blanca (Mark and McKenzie, 2007). They share similar attributes with paramos, the natural grasslands of the northern Andes that are of critical importance for regional water resources (Buytaert *et al.*, 2006; Girard, 2005). Like paramos, pampas are located at high elevations in the Andes; they are treeless with a top layer made of organic matter. These common characteristics make pampas potential hydrogeological features that can store groundwater for release during the dry season. Pampa groundwater (GWP) samples were taken from shallow wells made using a hand auger. The auger holes were two to three metres long and showed a common sequence of 15 to 20 cm of organic soils followed by 25 to 60 cm of organic rich clay. Below this were various layers of clay, silt, gravel and sand. At some sites, larger material such as clasts and boulders were also found at depth. From the auger holes, the water table was found to be generally situated between one and two metres below the land

surface. Samples pumped from shallow aquifers outside of the pampas were classified as being from other origins (GW).

A large number of springs (GWS) were observed during site visits. On the first five kilometres from the outlet of the Quilcayhuanca watershed, we counted 59 springs at the valley floor, leading to a density of around 44 springs per km^2. Most of these springs were situated at the lateral slopes deposits at the valley bottom. This type of spring has been shown to play a key hydrological role in base flows of alpine environments (Langston *et al.*, 2011; McClymont *et al.*, 2011; Muir *et al.*, 2011; Roy and Hayashi, 2009a), including the tropical valley of the Zongo glacier in Bolivia (Caballero *et al.*, 2002), which makes them of specific interest for this study.

We considered two surface water categories: water sampled from the main streams was identified as a mixture of different sources (MIX), while water that originated from the smaller tributaries was identified as being from other valleys (VAL). Tributaries from non-glacierised catchments were considered to originate from groundwater. Samples were collected in 2008 and 2009 using a synoptic sampling approach whereby water samples are taken from a wide variety of sources in a very short time span (Mark and Seltzer, 2003). The 2008 sampling campaign covered the four study watersheds extensively (Figure 3.1), whereas the 2009 sampling campaign focused mainly on the Quilcayhuanca watershed with a greater sample density than in 2008 (Figure 3.2). MELT samples were taken from proglacial streams or lakes situated downstream of the glacier tongue. GW and GWP samples were pumped from shallow aquifers. GWS samples were taken at the spring mouths with the exception of Yanamarey, where it was collected at the outlet of a spring fed non-glacierised valley situated next to the studied watershed. Cumulative precipitation samples, used to establish the local meteoric water line, were taken on a monthly basis in 2008 and 2009 at the office of the Autoridad Nacional del Agua in Huaraz. Due to equipment failure in 2009, we were not able to pump water out of the ground at any watershed except Yanamarey.

Samples collected for hydrochemical analysis were filtered and acidified onsite, kept in completely filled HDPE 30 or 60 ml bottles and stored at 4 °C whenever possible. Sampling for isotopic analysis followed a similar protocol with the exception that no onsite filtration and acidification was performed. Major cations (Fe^{2+}, Fe^{3+}, Ca^{2+}, Mg^{2+}, K^{+}, Na^{+}) as well as the stable isotopes of oxygen and hydrogen ($\delta^{18}O$ and $\delta^{2}H$) were measured at The Ohio State University using a Dionex DX500 ion chromatography system and a Finnigan MAT Delta plus mass spectrometer coupled to a HDO water equilibrator, respectively. Major anions (F^{-}, Cl^{-}, Br^{-}, SO_4^{2-}) were measured using a Dionex DX500 ion chromatography system at McGill University. Bicarbonate concentrations were calculated as the residual from the charge balance equation.

3.4.2 Quantifying the dry-season groundwater contribution to individual watersheds

Quantification of the dry-season groundwater contribution to the outflow of the studied watersheds was based on samples taken during the 2008 dry season at individual watersheds. We used the hydrochemical basin characterisation method (HBCM) that estimates the relative contribution of different water sources at different mixing points of the watershed, using a multi-component mass balance approach (Baraer *et al.*, 2009a).

Watersheds were divided into nested interconnected sub-basins based on the location of the mixing points (Figure 3.1), making those points both outlet of a sub-watershed and contributors to the subsequent downstream sub-watershed. Nested watershed areas were calculated using ARC HYDRO (Maidment, 2002) with 1:100,000 digitized contour lines. For each mixing point, HBCM computed the total residuals for a set of mass balance equations applied to selected tracers. From 10,000 to 100,000 possible combinations of the water sources relative contributions were tested. The 20 lowest of the total residues were used to determine a range of relative contributions for each source of water (See Baraer *et*

al., 2009 for complete methodological details). All potential sources of water were identified and tested for each sub-watershed separately.

Tracers were selected from hydrochemical and isotopic analytic data. Selected tracers exhibited conservative behaviour (absence of sign of unaccounted gain or loss at the sub-watershed scale), were above the analytical detection limits and differentiated between the potential water sources. Tracers were normalised to the samples average to provide equal weight in mass balance equations.

Using HBCM, we estimated relative discharge and converted it to absolute discharge using stream discharge measurements made onsite using the cross-sectional averaging technique (Mark and Seltzer, 2003). Stream water velocity was measured with a mechanical flow meter (Model FP101, Global Waters Inc.). The measurement method we used was well adapted to the logistical constrain that characterise the study area, but has an associated error of 40% and a tendency for overestimation (Shrestha and Simonovic, 2010).

Tributaries from glacierised catchments with a glacierised area less than 45% were considered being from an unknown origin. Their contribution was not accounted for in the watershed water budget. As a consequence, the compiled contributions of groundwater and melt water refer to virtual watersheds that differ slightly from the true ones. The virtual watershed area was defined as the true watershed area minus the tributaries of drainage areas of unknown origin. The names of the virtual watersheds are appended with an '*' and their characteristics are presented in Table 3.2.

3.4.3 Identifying indicators of water origin

In order to characterise the flow of groundwater in the glaciated valleys of the Cordillera Blanca, the four studied watersheds were considered together. Firstly, we analysed the hydrochemical signatures of different water sources looking for elements, or groups of elements, that depended significantly on the different types

of water sources, independent of the studied watershed of origin. These "indicators of water origin" were then used to identify the most important sources of water for the valleys.

Identification of these indicators of water origin was done using a multivariate variance analysis (ANOVA). Each water source sampled during the 2008 dry season was identified by two attributes: the water source category (process) and the watershed from which the sample was collected (site). Tracers that were significantly process dependant with no significant site influence were considered as indicators of water origin. To minimise the influence of water residence time (e.g. mineral dissolution into groundwater) the ANOVA test was performed on relative concentrations as opposed to the absolute concentrations. The use of the indicators of water origin to characterise sampled waters was verified by using hierarchical clustering. For each watershed, clustering was realised by cross comparing dissimilarities (named distances) between water sources samples. Distances were calculated by summing the normalised absolute differences in indicator concentrations. Clustering results were represented using a dendrogram.

3.4.4 Identification of contributing water sources

For conservative tracers, the position on a mixing diagram of a mixture relative to the location of the source it comes from is dictated by the conservation of mass law. For example, in a case of a mixture made of just two sources, the mixture plots on a line that relates the sources. We used that property in the context of our research to identify which groundwater types were major contributors to watershed outflows. As glaciers make the headwater of the main streams, we expected to observe mixing points plotting away from the melt water spots towards contributing groundwater points and/or, towards tributary points. Where only one groundwater type contributes significantly to watershed outflows, all mixing points and tributaries are situated on a single line that has the melt water and the contributing groundwater points at its extremities. Assuming this was the case at the different watersheds, we defined mixing lines as being the MIX plus VAL

samples regression line, of which we computed the regression prediction with 95% confidence intervals. Verification of the single mixing line assumption was made by calculating the mixing lines correlation coefficient (R^2) and its associated p-value. Where the regression p-value was lower than 0.05, the assumption of single dominating groundwater type was accepted. Groundwater samples that were outside of the prediction 95% confidence intervals were considered as not appreciably contributing to the main stream flows. Samples of water sources that plotted within the regression confidence interval and were situated at the other extremity of the mixing line compared with the MELT samples were considered as major contributors. Repeating this analysis for different watersheds and several tracers minimized the risk of misclassification of random origins.

3.4.5 Evaluating spring recharge elevation

We assessed spring recharge elevation by using the relation between $\delta^{18}O$ in precipitation and elevation (Gonfiantini *et al.*, 2001). We verified that conditions were met for such assessment by verifying that no major post precipitation fractionation had occurred (Gat, 2010). We compared water stable isotopes values of all 2008 and 2009 source type water samples with precipitation from Huaraz. The validation of the absence of post precipitation fractionation hypothesis for the studied system required that no significant deviation of a water source from the precipitation samples based local meteoric water line was observed.

Consecutively, we plotted the 2008 samples $\delta^{18}O$ values against their "representative elevation" that we defined as the mean elevation of the water source recharge area. For MELT samples, because the melt occurs predominantly at the glacier ablation area, which is above the sampling point and because the glacier ice flow feeds the ablation area with ice and snow from higher elevations, we used the glacier median elevation as the representative elevation. For the GWP samples, we used the sampling location elevation as the representative elevation as in similar environments shallow groundwater $\delta^{18}O$ values have been shown to be a good proxy for mean elevation (McKenzie *et al.*, 2010). Using these two source

types we quantified the relation that exists between $\delta^{18}O$ values and elevation using a linear regression.

The GWS representative elevation was unknown for all watersheds except Yanamarey. To evaluate the GWS samples recharge area, we arbitrarily fixed their representative elevation at the spring outlet. The recharge area was then estimated by graphically evaluating where the GWS points were situated on the GWP-MELT regression line.

Because the Yanamarey GWS sampling point drains an entire glacier-free valley, it was possible to estimate its recharge area based on hypsometric data. This specificity was used to test the spring recharge area elevation estimation method.

We applied the same method on all source types sampled in 2008 from the four different studied watersheds. We performed a linear regression on the GWS points and compared the resulting line to the MELT-GWP line using an ANOVA test.

3.4.6 Spring characterisation

The 2009 sampling campaign had a higher density in the coverage of springs than in 2008. Of the 11 sampled springs, 9 were situated at the bottom of lateral talus and landslides. The two others, QGWS7 and QGWS4, were situated approximately half-way between the valley wall and the river bed. As in artesian springs, QGWS7 water rose up to the pampa surface from a vertical hole that was estimated to be deeper than one and a half metres. The QGWS4 spring was situated at the bottom of a deposit that extends across the valley floor and is likely to be the remains of an end moraine, or an old avalanche cone.

The samples hydrochemical signatures were examined using a hierarchical clustering analysis, which is a similar method to the one described above for the 2008 samples. In addition to the MELT and GWS samples, five other samples of known origin were included in the analysis as a reference. Two samples, QVAL3

and QVAL7, originated from non-glacierised sub-watersheds and three others; QVAL 1, QVAL5 and QMIX3, were at least partly made of melt water. Finally, the spring recharge relative elevation was studied using a δ-diagram.

3.5 Results

3.5.1 Quantifying the groundwater contribution to dry-season outflow of individual watersheds

The subdivision of the four watersheds into cells is presented in Figure 3.3. Ranging from three cells in Yanamarey to seven in Llanganuco, the number of cells was mainly a function of the basin complexity and the sampling density. For all cells except one in Llanganuco, HBCM was able to provide estimations of the contribution of groundwater with an average uncertainty of three percent. The uncertainty was noticeably higher at Llanganuco and Pumapampa, than in Yanamarey and Quilcayhuanca, indicating differences in the adequacy of the sampling plan and/or, a lower contrast in hydrochemical signatures between the different source water types. Because of the very similar hydrochemical signatures of LMELT5 and LMIX3, the most downstream cell of Llanganuco was not characterised by HBCM. Confirming observations made by Baraer *et al*., (2009a) the results (Figure 3.3) do not reveal any obvious relationship between the relative contribution of groundwater and HBCM cells position.

As Quilcayhuanca is the watershed where the most stream discharge measurements were performed in 2008, the evaluation of the HBCM performance in estimating ungauged stream discharge was performed using this dataset. The HBCM relative discharge results were converted into absolute discharge by using the lowest gauging point of the watershed as reference. The evaluation was done by graphically comparing the measured discharge to HBCM estimate. As the discharge measurement method had an associated error of 40% (Shrestha and Simonovic, 2010), measurements were represented with an error bar of +/- 20% (Figure 3.4). The plot shows a very high correlation (R^2=0.99) between the

measured and the HBCM estimated discharges with a very high statistical significance (p-value < 10^{-6}).The equation of the regression line shows a tendency for a systematic overestimation of the measured discharge, confirming the findings of Shrestha and Simonovic (2010). This HBCM performance verification shows that the method was suitable for the purpose of this study and that the degree of uncertainly it carries is compatible with the objective we had to evaluate to what extend the groundwater contributes to the dry-season discharge at different glacierised valleys of the Cordillera Blanca.

The compilation of the HBCM cell results at the watershed level required discounting any tributaries with an undetermined groundwater contribution. Therefore, 6 of the 41sampling points were consequently excluded from the virtual watershed characterisation: 3 at Quilcayhuanca*, 2 at Pumapampa* and 1 at Llanganuco* (Table 3.2). The virtual Yanamarey* area remained unchanged compared with the true Yanamarey and the virtual Llanganuco* area lost only 5% of the true Llanganuco area. Pumapampa* was the most truncated virtual watershed with only 50% of the true watershed area retained.

At Yanamarey* and Pumapampa*, the groundwater contribution was larger than that of melt water. The opposite situation occurred at Llanganuco* and an overlap in the prediction ranges made such a comparison inconclusive for Quilcayhuanca*. The average specific groundwater discharge for the virtual watersheds varied from 0.36 mm/d at Quilcayhuanca*, to 0.80 mm/d at Pumapampa*. The estimate from Pumapampa* had the highest uncertainty (+/- 0.22 mm/d). We observed that none of the virtual watersheds had a minimum groundwater specific discharge less than 0.26 mm/d.

To understand the variability of groundwater contribution at the scale of the Cordillera Blanca, the relative groundwater contribution of each virtual watershed was plotted against the percentage of its glacierised area (Figure 3.5). The

relationship that exists between these two parameters was assessed with a nonlinear regression using a simple dilution model (Baraer *et al.*, 2009a):

$$GW = (a(100 - A_{gl}))/((A_{gl} + a(100 - A_{gl})) \qquad (3.1)$$

where *GW* represents the percentage of groundwater contribution, A_{gl} represents the percentage of glacierised area and *a* is a constant. The regression used the four virtual watershed points plus the two boundary points that are areas 0% and 100% glacierised. Despite the low number of points, the results show a good overall agreement between the average virtual watershed points and the dilution model (Figure 3.5; R^2=0.98). Regression prediction intervals suggest that the groundwater should have contributed to the 2008 dry-season discharge in watersheds where the glacierised area was less than 50% of the total area and that the contribution of groundwater should have been higher than melt water for all watersheds with areas less than 8% glacierised (lowest grey area at Figure 3.5).

3.5.2 Regional indicators of water origin

Multivariate variance analysis identified which factors control the variation of an ion's relative concentration from one source type to another (Table 3.3). Of the 13 tested relative concentrations, 4 showed variations being significantly (α=0.05) dependent on source type (*Process*) and were used as indicators of water origin: sulphates, carbonates, iron and the sum of calcium and magnesium. Three other tracers were more influenced by the type of water source than by the sampling site, but at a lower significance (α=0.1). Only one of the relative ion concentrations, fluorine, was significantly site dependant.

Results from the hierarchical cluster analysis confirm the conclusions of the multivariate variance analysis by showing the ability of the four indicators of water origin to differentiate between different water sources (Figure 3.6). With the exception of the GW samples, all other types of water sources cluster for each site. The differentiation between the MELT samples and the different groundwater

sources is unambiguous. GW samples clusters both with GWS (Quilcayhuanca) and with GWP (Yanamarey). This indicates that the GW samples are not homogenous and that a more detailed analysis is need to clarify their characteristics.

3.5.3 Identification of contributing water sources

We plotted the concentration of ions against the sum of cations, or the sum of anions for each identified indicator of water origin and for each watershed (Figure 3.7). In order to improve the interpretation of the results, one sample (QVAL4) has not been reported on the graphs. Possibly as a result of intense pyrite oxidation (Fortner *et al.*, 2011), this sample had hydrochemical characteristics far outside the range of the other samples. QVAL4 TDS, sulphate and magnesium concentrations were between four and seven times those of the second most concentrated samples. Thus, exclusion was made taking into account that this sample was hydrochemically atypical and that the tributary from which it was sampled had an insignificant discharge on the watershed scale.

The absence of iron ions in the stream samples of Llanganuco did not permit mixing line characterisation. For all the other tracers, we observed a well-defined and significant regression line (p-value < 0.05). However, while all the MELT samples systematically plot within the 95% prediction confidence interval of the mixing line, none of the GWP samples do, suggesting that the GWP type did not significantly contribute to the watershed discharge at Llanganuco.

At Quilcayhuanca, the mixing lines are statistically (p-value < 0.05) characterised for all tracers. Of the two GWP samples pumped out of the watershed, one is systematically excluded from the 95% prediction confidence interval of the regression line and the other one is at the limit of the confidence interval (Figure 3.7). Quilcayhuanca mixing diagrams also show that for all tracers, GWS and MELT samples are within the 95% prediction confidence interval of the mixing line and that all MIX and VAL samples plot between these two water sources.

Unlike Quilcayhuanca, Yanamarey presents only one well-defined mixing line: the sum of calcium and magnesium. The low number of mixing or tributary samples used for the regression may explain the three weak correlations. The calcium and magnesium diagram (Figure 3.7) shows an almost perfect alignment of the GWS, MIX and MELT samples with GW and GWP plotting away from the 95% prediction confidence interval. Diagrams of sulphates and bi-carbonates show an alignment of the MELT, GWS and MIX samples (red line on the Figure 3.7, Yanamarey / sulphate graph). If we calculate the regression parameters using these categories instead of only the MIX samples, the R^2 becomes 0.91 with a p-value of 0.001. This confirms the strong influence of the MELT and GWS water sources on stream water composition. The GWP and GW samples distinctly plot away from this line, suggesting that these sources did not contribute significantly to the stream water. As with Llanganuco, the absence of iron in the MIX, GWP and MELT samples makes the interpretation the Yanamarey iron mixing diagram difficult.

The Pumapampa mixing diagrams show a more complex situation than at the other watersheds. The plot of MELT sample outside the 95% prediction confidence interval of the calcium plus magnesium mixing line, suggests that the binary mixing model does not apply to this watershed. Instead, mixing diagrams suggest the presence of a ternary mixing. The sulphate and bi-carbonate diagrams show three possible water sources; one MELT and the two GWS samples, forming a triangle (in red on the Pumapampa, sulphates graph; Figure 3.7) within which all of the mixing points plot. Such a ternary mixing can be seen as two successive binary mixings. First, the melt water would mix with a PGWS2-like groundwater and then the stream water would mix with PGWS1-like groundwater. This hypothesis is supported by the fact that the two points that plot between PMELT1 and PGWS2 are the two most upstream MIX points of the watershed and that the two that plot between the first mixing line and the PGWS1 are the two most downstream. This hypothesis would explain why the MELT sample and one GWS

sample plot outside the 95% prediction confidence interval of the calcium plus magnesium mixing line. The Pumapampa iron mixing diagram does not provide any specific mixing information due to the absence of iron in most of tested samples.

Overall, Figure 3.7 is valuable for the evaluation of the contribution of different water source types to the stream flows of the watersheds. With MELT samples forming one of the mixing line ends almost each time the line is well defined (p-value < 0.05), the mixing diagrams consistently represent what is observed at the headwater of the watersheds. Plotting most of the time at the other extremity of the mixing line, the GWS samples are likely representing the major groundwater contributor to the dry-season watershed discharge. Except for one occasion, wherever the mixing line is well defined (p-value < 0.05) the GWP samples systematically plot outside the 95% prediction confidence intervals of the mixing regression. This shows a very limited influence of the GWS samples on the stream water concentration of the studied tracers. This makes GWP an improbable major contributor to the stream discharge on the watershed scale. The situation with GW samples is more ambiguous; at Yanamarey, GW samples do not appear to be a major influence for the stream water chemistry, while for Quilcayhuanca the situation is inconclusive. This further suggests that GW samples may not make a unique cluster and that a more in-depth analysis is required to better categorise them.

3.5.4 Evaluating the elevation of spring recharge

The δ-diagram of all samples taken in 2008 and 2009 does not show any significant deviation of the water sources from the local meteoric line made by the precipitation samples (Figure 3.8). The 95% confidence intervals of the melt samples, the different groundwater samples and the precipitation samples clearly overlap. Figure 3.8 shows that the post precipitation fractionation effects on the sample's isotopic values are minimal, suggesting that conditions are met for using $\delta^{2}H$ and $\delta^{18}O$ values as proxies for water source recharge areas mean elevation.

The test we conducted with the Yanamarey samples shows that the GWS samples plot below the GWP/MELT line, rejecting the assumption that the recharge area is at the same elevation as the sampling point (Figure 3.9). Calculated using the GWP-MELT line slope, the evaluated recharge mean elevation is situated more than 500 metres above the sampling point, at 4530 metres above sea level (m.a.s.l.) in 2008 and 4570 m.a.s.l. in 2009. These elevations are very close to the median elevation of the YGWS1 drainage area, calculated using the sub-watershed hypsometric profile, which is at 4550 m.a.s.l..

These results suggest that the method we tested provides results that are accurate enough for the purpose of this study. It should be noted that the method as applied here, compares samples taken within a relatively short time interval. Comparing samples taken from different years could affect the accuracy of the method.

Extended across the four studied watersheds, the successfully tested method shows that the four GWS points are all situated below the MELT-GWP regression line (Figure 3.10). The GWS regression line lies outside the 95% confidence interval of the MELT-GWP regression. An ANOVA test performed with the two groups of samples confirms this result. With a p-value of 0.035, the hypothesis of similarity of both regression lines is rejected. This means that the spring recharge area is situated at significantly higher elevations than the sampling points. The distance between the two lines suggests that the difference in elevation between the spring sampled outlet and the mean elevation of the recharge area is greater than 500 metres. This places the recharge area at a much higher elevation than the height of the valley side deposits from which most of the springs originate.

3.5.5 Spring characterisation

Quilcayhuanca samples taken during the 2009 dry season were studied using a hierarchical cluster analysis (Figure 3.11). As confirmed by the position on the diagram of the VAL and MELT samples used as reference, the figure distinguishes well between a melt water cluster (red lines) and a precipitation water cluster (blue lines). The dendrogram shows a strict separation between these two clusters as the minimum normalised distance between both (5.5) represents more than twice the maximum distance between sub-clusters (2.3 at QGWS5). None of the samples taken in glacierised catchments (QVAL1, QVAL5 and QMIX3) plot into the precipitation cluster or opposite.

From the results we observe a geospatial proximity influence on clustering. For example, QGWS11 and QGWS10, which form the cluster of lowest normalised distance, are also the closest springs that were sampled. A similar situation occurs with QGWS8 and QGWS9, two nearby springs that cluster, presenting the second lowest normalised distance cluster. Such similarities in hydrochemical characteristics are possibly due to springs being different outlets of a communal aquifer. The physical proximity is not the only factor that affects springs hydrochemical proprieties. Clusters formed by springs that are distant from each other, such as QGWS3 and QGWS6, show that most of the springs of the valley share some hydrochemical characteristics that make them distinct from other tested water sources, confirming at a larger scale, what was observed from the 2008 samples. The QGWS7 and QGWS4 samples that originated from springs not situated at the bottom valley lateral deposits do not form a specific cluster, but group with the other precipitation fed springs instead. QGWS7 is the only artesian spring that was found during the dry season 2009 sampling campaign. It forms a cluster with the two nearby springs GWS8 and GWS9. This makes the QGWS7 sample part of the GWS group that is clearly distinguished from the water pumped in pampa shallow aquifers (GWP) for the 2008 samples. The QGWS7 water would therefore not originate from the Pampa shallow aquifer, but from the lateral

deposits. The relative position of the springs in the valley (Figure 3.2) supports the assumption that water circulates underneath the valley floor, from the valley side to the middle of the pampa and is confined by the lower permeable glaciolacustrine pampa material. QGWS4 was also not sampled from a lateral deposit, but instead flowed out of frontal deposits. The QGWS4 position in the middle of the precipitation cluster, does not distinguish it from the springs that flow from lateral deposits.

With the exception of the QGWS2 sample, all GWS samples are part of the precipitation cluster. The QGWS2 sample belongs to the melt water cluster that groups all the MELT samples, as well as the glacier fed tributaries samples that were used as reference. Together with QVAL1 they form the cluster of lowest normalised distance within the melt water cluster. This strong relationship shows that QGWS2 is, at least partially fed with melt water.

The plot of δ^2H versus $\delta^{18}O$ (Figure 3.12) provides additional information about the springs. QGWS2 has the samples lowest $\delta^{18}O$ and δ^2H values, even lower than the MELT samples, confirming that spring as individual. A DEM analysis shows that the peaks above QGWS2 are 5400 m.a.s.l., more than 250 metres above the median elevation of the glaciers of the Quilcayhuanca valley (Table 3.1). If we consider the influence of elevation on samples δ^2H and $\delta^{18}O$ values that were verified based on the 2008 samples, the QGWS2 position on the δ-diagram relative to MELT implies the spring being fed by water that originates from the highest part of the surrounding peaks. Field observation revealed the presence of small glacial remains or dead ice (less than 100 metres long) on the summits above the springs. Melt water from this ice, at least partly feeding QGWS2, is the scenario that best explains the spring water hydrochemical and isotopic characteristics. More generally, the geospatial proximity influence observed on the cluster analysis is observed with the δ-diagram as well. QGWS10 and QGWS11 have very similar δ^2H and $\delta^{18}O$ values. The same observation is true for QGWS8 and QGWS9. The sampled artesian spring QGWS7, has slightly lower δ^2H and $\delta^{18}O$

values than the other two other springs that it was grouped with in the cluster analysis. This difference indicates that the average elevation of the recharge area of the artesian spring is slightly higher than the other two springs.

3.6 Discussion

The quantitative evaluation of groundwater contribution to the hydrologic systems shows that significant groundwater volumes are observed in the four studied watersheds. Despite the differences in their attributes (location, geology, glacial cover, etc.) all of the studied valleys appear to capture precipitation at a certain time of the year and to store it in a hydrogeological system that releases it year-round. Important differences exist in the relative contribution of groundwater between the watersheds, but these differences are partly explained by disparities in glacierised area. On the scale of the Cordillera Blanca, we estimate that for watersheds that are less than 50% glacierised, groundwater should be a significant contributor to the surface flow during the dry season. Furthermore, the results suggest that there are water source types (e.g., melt water, groundwater) that are shared by the Cordillera Blanca valleys, and that they can be distinguished from one another using particular hydrochemical / isotopic characteristics.

Samples collected from springs and pumped from shallow pampa aquifers have distinct characteristics. The pampa's groundwater appears to have very little influence on stream water hydrochemical characteristics, showing that these aquifers are more likely a minor component of the net flux of water to the main valley streams. In contrast, aquifers that feed the springs contribute significantly to the overall basin discharge. Most of the springs were sampled at the bottom of talus deposits made of moraines and/or, paraglacial deposits. These springs are fed by precipitation that flows down from elevations significantly higher than the location of the springs. This makes the lateral deposits of the valleys an important feature for groundwater processes. This agrees with comparable studies conducted in other alpine environments (McClymont *et al.*, 2011; Roy and Hayashi, 2009b).

Precipitation-fed springs that flow out of the lateral deposits are the most numerous we observed, but a few exceptions have been found. One of the springs we sampled flowed from lateral deposits, but is at least partly, melt water fed. One artesian spring was sampled in 2009, which had hydrochemical characteristics close to those of the nearby lateral springs, suggesting related origins, or even a shared aquifer. Following a different pathway to the nearby lateral springs, the artesian spring water flows from the talus bottom deposit underneath the pampa floor then, over-pressurised, the water escapes through a hole in the pampa top layer. Hydrochemical and isotopic characteristics of the groundwater pumped from non pampa shallow aquifers, exhibit inconsistent hydrological proprieties. The binary diagrams indicate that they do not represent major surface water contributors. However, additional samples would help to further interpret these specific results.

Using these results, we propose a conceptual groundwater model for a generic Cordillera Blanca proglacial valley during the dry season (Figure 3.13). It presents the valley side deposits as key hydrogeological features of the system. The top layer of the pampas is considered as having a low permeability and being an area of low contribution to the surface water. Lateral deposit recharge is of three origins: direct precipitation falling at the deposit surface, recent precipitation that flows from areas of higher elevations and melt water from glaciers or dead ice. Water flows out of these deposits either through springs that are situated at the interface between lateral deposits and the surface of the pampas, or from artesian springs flowing through the pampa surface. This second outlet implies a transfer of water between the lateral deposits and the ground deposits. Water that transits through the lateral deposits has a retention time long enough to maintain lateral springs throughout the dry season. Since a long retention time is unlikely to occur in the coarse deposits observed at the talus surfaces, we propose two hypotheses to explain this situation. The first hypothesis is that the presence of different types of deposits, such as remains from lateral moraines buffers part of the water collected

at the talus surface. The other hypothesis is the existence of a fracture flow in the bedrock underneath the lateral deposits. However, further studies are needed to test these hypotheses.

3.7 Conclusion

Hydrochemical and isotopic signatures of different water source types were used to study the hydrogeological characteristics of four different glaciated valleys of the Cordillera Blanca, Peru. The methods we tested were shown to be specifically adapted for pro-glacial systems. However, they are potentially transferable to other watersheds assuming the necessary tracer characteristics exist. The methods showed particular merit in remote regions where intensive and expensive physical hydrology methods are not practical.

Our results provide new perspectives on the regional proglacial hydrology. Among the different findings, three appear to be of particular interest for both general alpine hydrology and for Peruvian water resources:

- Groundwater is a major hydrologic contributor during the dry season in the glacierised watersheds of the Cordillera Blanca, Peru. For 2008, we estimated that watersheds that were less than 8% glacierised had more groundwater discharge than glacial melt water.
- In the pro-glacial valleys, talus deposits are an important component of the hydrogeological system. They both collect water running off from higher elevations and release it at lower elevations. They also can act as preferential pathways for groundwater to flow into unconsolidated aquifers within the valley-bottom floor.
- Most of the springs are recharged by precipitation, but at least one spring fed by melt water was identified. There is a possibility that this type of spring will become ephemeral when the small amount of ice providing melt water is gone.

Using our hydrochemical analysis as a guide, we have proposed a conceptual hydrologic model. We consider this model as being a preliminary schematic description of the hydrogeological system of the glacierised watersheds of the Cordillera Blanca. This conceptual model aims to be a starting point for further discussion. The model leaves several questions unanswered, such as what are the processes by which water that is captured by the talus is retained long enough to produce perennial springs? The talus surface, being mainly made of porous paraglacial deposits should in theory rapidly release the captured water, unless fracture flows or layers of other deposits are involved.

3.8 Acknowledgements

We are grateful for the funding provided by the National Science Foundation (BCS-0752175), the Geochemistry and Geodynamics Research Center (GEOTOP) of Quebec, the Natural Science and Engineering Research Council (NSERC) of Canada, McGill University, and The Ohio State University's Climate, Water and Carbon Program.

3.10 Tables

Table 3.1. Geospatial characteristics of the study watersheds. Glacierised area and median elevation were calculated using the 2005 GLIM database (Racoviteanu, 2005). Pampa area was derived using ASTER derived DEM with 30 m cell size. The bedrock type was estimated from geological maps (Selveradjou et al., 2005).

Basin	Basin area (km^2)	Glaciated area (km^2)	Glaciated area (%)	Glacier median elevation (m)	Pampa area (%)	Bedrock type (%)		
						Plutonic	Volcanic	Sedimentary
Llanganuco	63.76	26.46	41.5	5231	1.2	50	0	50
Quilcayhua	87.66	17.98	20.5	5139	4.1	15	0	85
Yanamarey	26.93	1.69	6.3	4946	9.4	5	0	95
Pumapamp	56.14	1.15	2.1	5128	11.6	0	65	35

Table 3.2. Main characteristics and contribution estimations for virtual watersheds. “GW” is groundwater and “MELT” is glacier melt water.

Virtual Watershed	Area (km^2)	Area (% of watershed)	Glaciated area (km^2)	Compilation of HBCM estimations				**GW specific discharge (mm/d)**
				GW max (m^3/s)	GW min (m^3/s)	MELT max (m^3/s)	MELT min (m^3/s)	
Llanganuco*	60.2	95	26.38	0.55	0.49	1.56	1.50	0.75 +/-0.04
Quilcayhuanca	71.5	82	12.36	0.38	0.22	0.37	0.37	0.36 +/- 0.1
Yanamarey*	26.9	100	1.69	0.2	0.19	0.06	0.05	0.63 +/-0.02
Pumapampa*	28	50	1.01	0.33	0.19	0.10	0.07	0.80 +/-0.22

Table 3.3. Multivariate variance analysis results for 2008 MELT, GW, GWS and GWP samples, all sites. *Process* represents the different sources of water and *Site* the sampled watershed.

	Process		*Site*	
Tracer	*F factor*	*P*	*F factor*	*P*
$SO_4^{2-}/\Sigma A^-$	9.41	**0.0008**	0.39	0.7652
$HCO_3^-/\Sigma A^-$	10.78	**0.0004**	0.33	0.8008
$F^-/\Sigma A^-$	0.68	0.5776	8.00	**0.0018**
$Cl^-/\Sigma A^-$	0.49	0.6952	0.71	0.5611
$Ca^{2+}/\Sigma C^+$	2.22	0.1256	0.84	0.4930
$Mg^{2+}/\Sigma C^+$	1.57	0.2358	2.03	0.1504
$Na^+/\Sigma C^+$	0.87	0.4759	0.81	0.5082
$K^+/\Sigma C^+$	2.55	0.0923	0.46	0.7150
$Fe^{2+,3+}/\Sigma C^+$	3.60	**0.0368**	1.32	0.3038
$(Ca^{2+}+Mg^{2+})/\Sigma C^+$	3.68	**0.0346**	1.22	0.3346
$(Na^+ + K^+)/\Sigma C^+$	0.84	0.4905	0.65	0.5961
$SO_4^{2-}/(Na^+ + K^+)$	2.70	0.0806	1.48	0.2573
$SO_4^{2-}/(Ca^{2+}+Mg^{2+})$	2.78	0.0750	1.28	0.3151

3.11

Figures

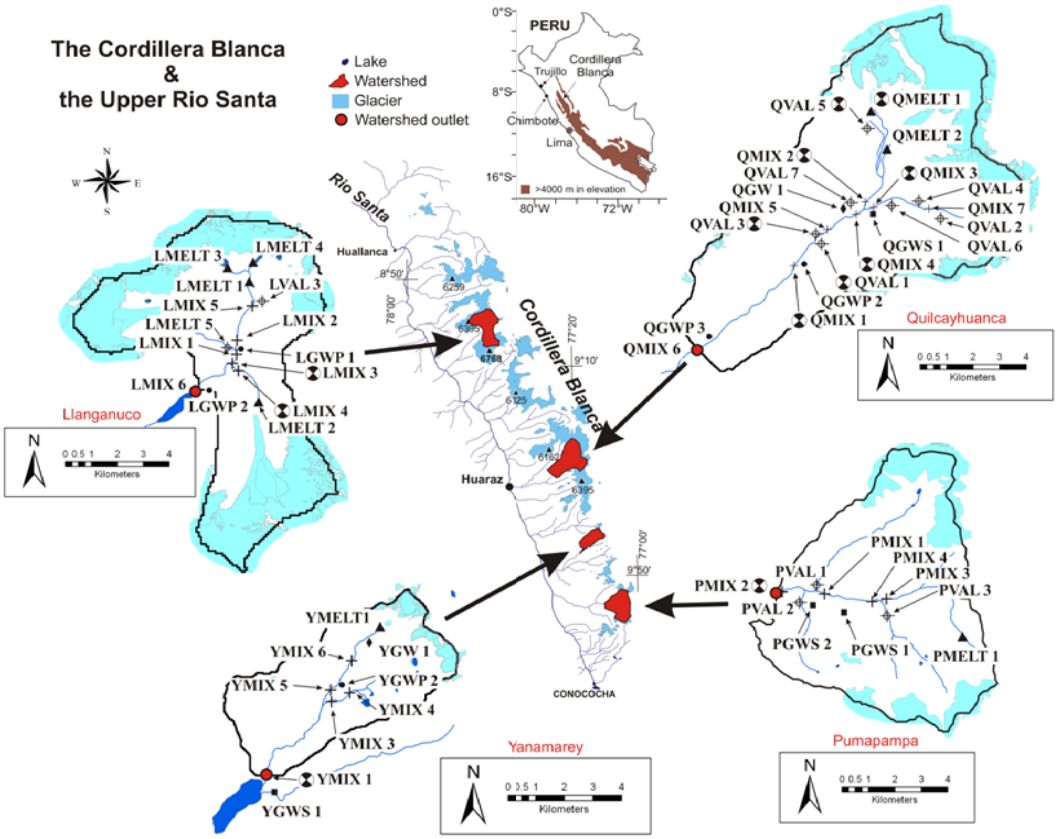

Figure 3.1. The Cordillera Blanca and the upper Rio Santa watershed. Samples taken at least once in 2008 are identified on the detailed maps of the studied watersheds. Identification numbers are structured as follow: XYYY#, where X represents the site, YYY the sample type, and # the sequence number of a sample. The following acronyms (symbols) are used to describe the sample type: MIX (+) represents samples from the main stream, VAL (⊕) defines samples from main stream tributaries, MELT (▲) represents melt water, GWS (■) are used for spring water, GWP (●) identifies water pumped from a shallow pampa aquifer, and GW (♦) are used for water pumped from a shallow aquifer outside pampa areas. Gauging locations are marked with "⊗".

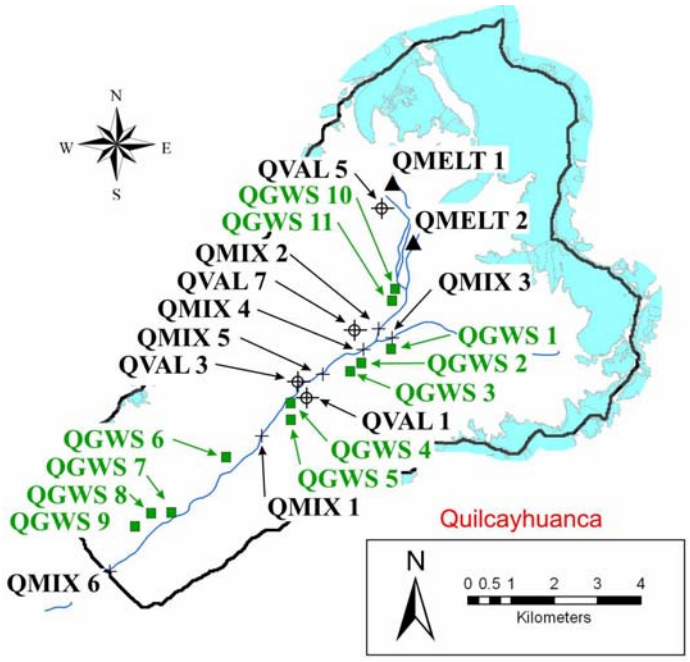

Figure 3.2. 2009 Quilcayhuanca Sampling. Acronyms and sample identification methods are the same as at Figure 3.1. Labels in green represent groundwater.

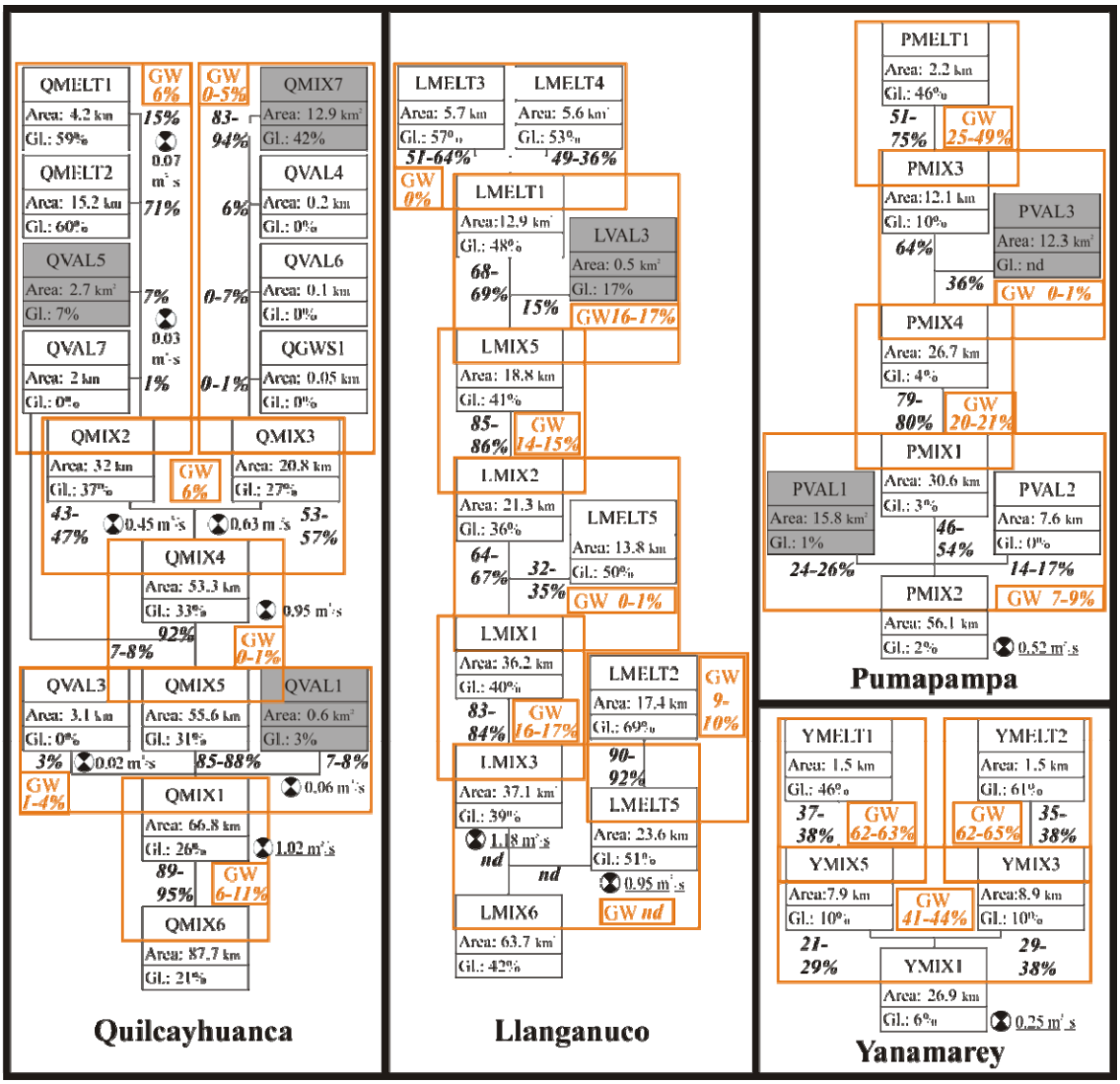

Figure 3.3. HBCM results for 2008. MELT, MIX and VAL samples are represented by thin black line contoured boxes that include the total area and the percentage of glacierised area of their drainage area. Greyed boxes represent drainage areas not accounted for in virtual watersheds data compilation. Each HBCM cell is delimited in orange, it presents in bold characters, the HBCM estimated relative discharge (in %) for each water source. Groundwater contribution is indicated in orange in each cell. The ⧓ symbol is used wherever discharge measurements were made and measurements results are expressed in cubic metres per second. "*nd*" stands for non-determined.

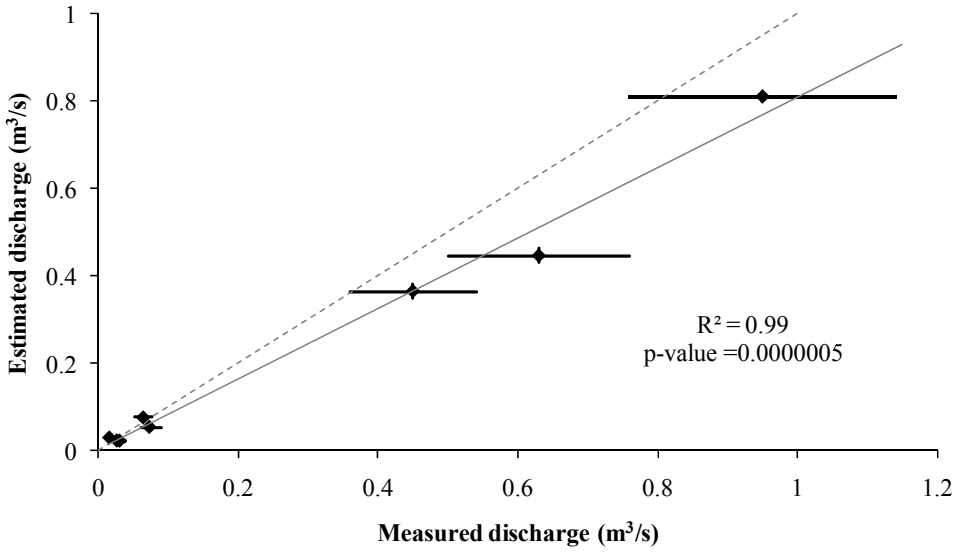

Figure 3.4. HBCM estimated discharge as a function of the measured discharge (black symbols). Discharge measurement uncertainty (+/- 20%) is represented by horizontal lines. The grey solid line represents the linear regression between measured and estimated values and the grey dashed line is the 1:1 line.

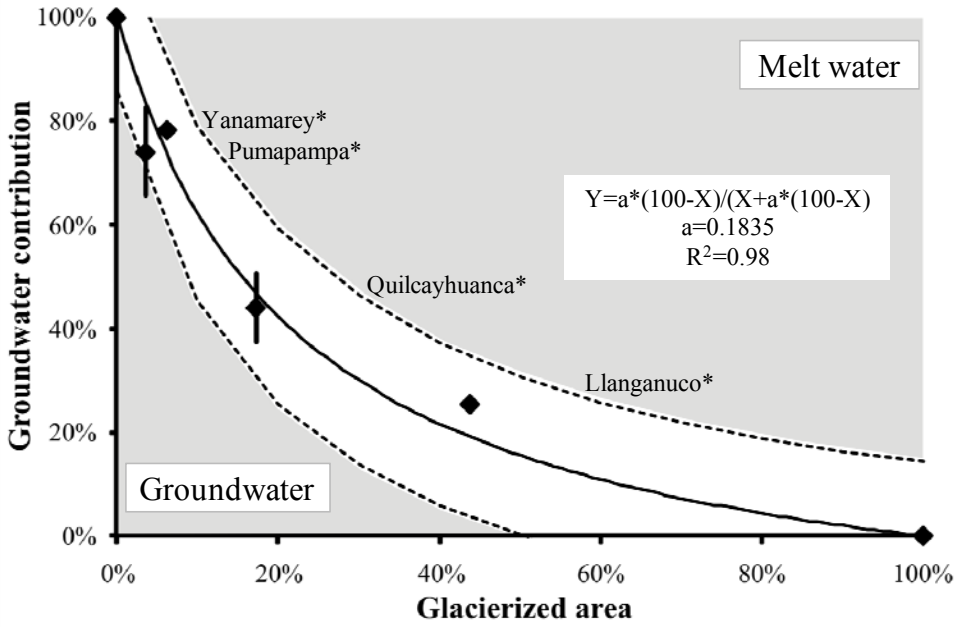

Figure 3.5. HBCM estimated relative groundwater contributions to virtual watershed discharge as a function of the relative glacierised area (black diamond). HBCM errors are shown as thick black lines. The best fit for the dilution model (equation inset on graph) is represented by the thin black line. Dashed lines delimit the regression prediction 95% confidence interval that can be interpreted as the groundwater and melt water† (labelled on the diagram) minimum contributions for a given glacierised area for the dry season, 2008.

† The melt water minimum contribution is calculated as: 100% - groundwater contribution

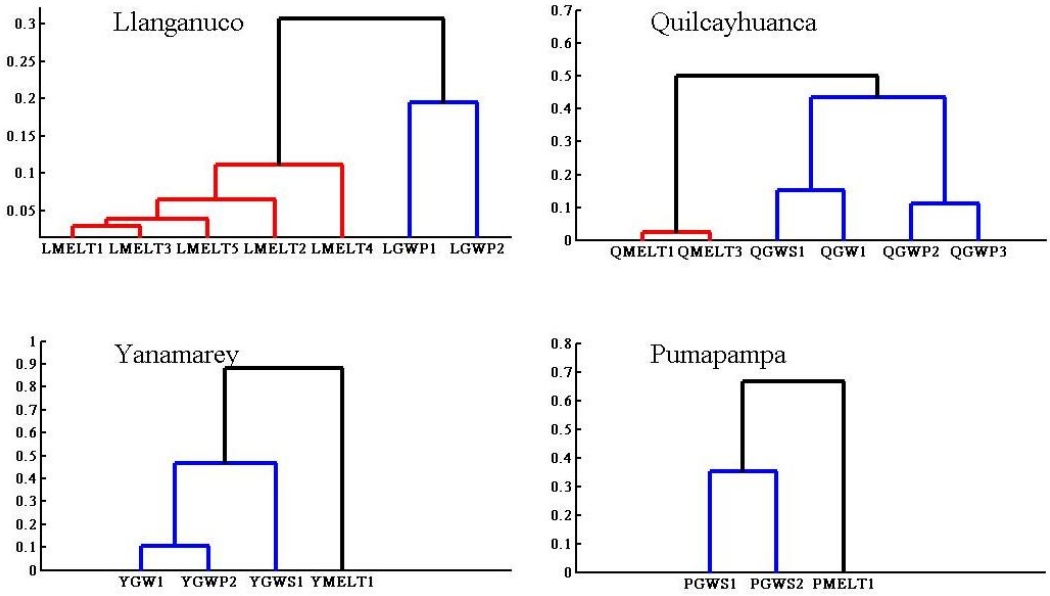

Figure 3.6. Verification of the effectiveness of indicators of water sources for the 2008 samples. The dendrograms represent watersheds hierarchical clustering. The Y axes are normalised distances (dimensionless). The red and blue lines identify melt water and groundwater clusters.

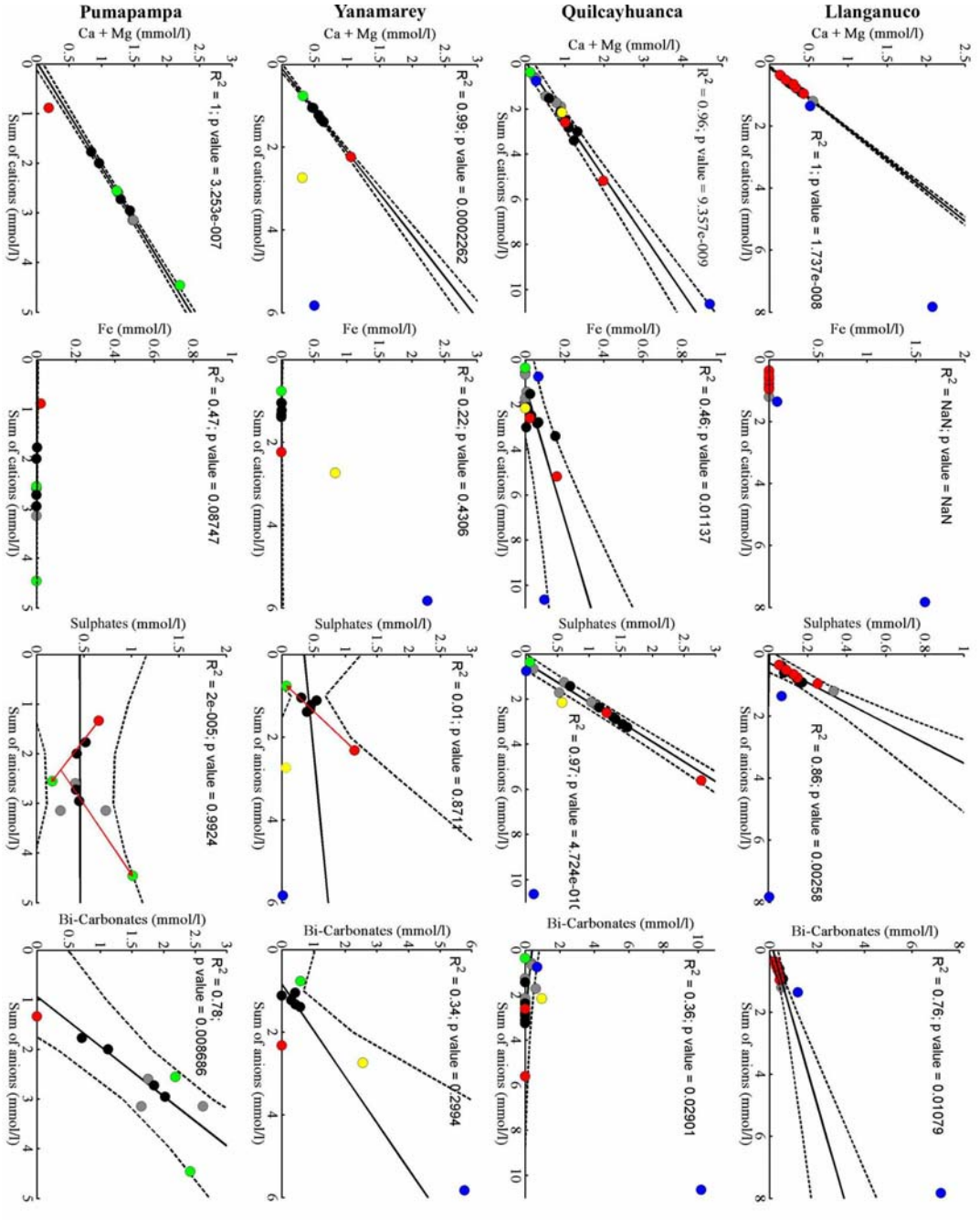

Figure 3.7. Watershed mixing diagrams for the four indicators of water origin. MELT samples are in red, GWP in blue, GWS in green, GW in yellow, MIX in black and VAL in grey. Solid lines represent the mixing lines defined by the linear

regression of the MIX and VAL samples, while the dashed lines delineate the regression 95% prediction confidence interval.

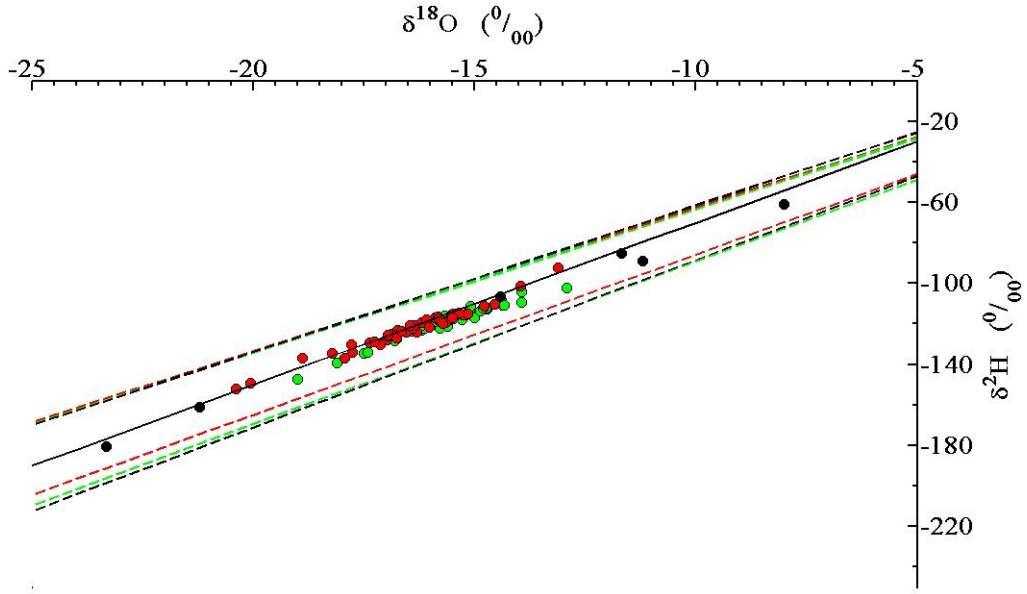

Figure 3.8. *δ*-diagram ($\delta^{18}O$ and $\delta^{2}H$ in ‰ VSMOW) for all samples taken in 2008 and 2009 from the Llanganuco, Quilcayhuanca, Yanamarey and Pumapampa watersheds. MELT samples are in red and groundwater (GW, GWP and GWS) are in green. Black circles represent precipitation samples taken in Huaraz during the same period. Dashed lines indicate the 95% confidence interval for the respective sample type linear regression (colour coded). The global meteoric water line is given as reference (solid black line).

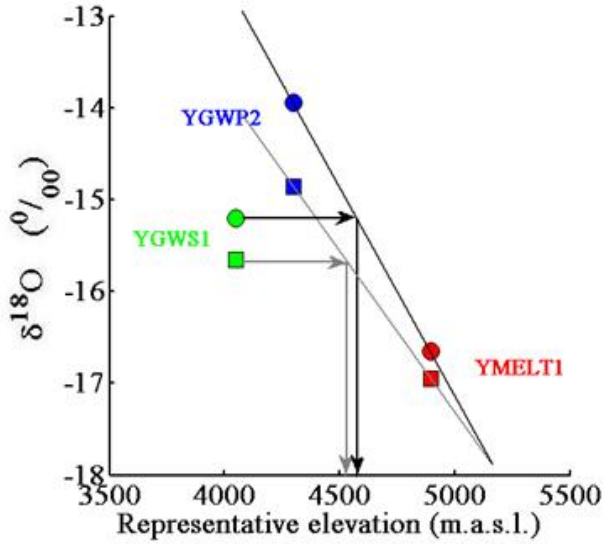

Figure 3.9. Verification of the relationship between $\delta^{18}O$ (‰ VSMOW) and samples representative elevation. Squares represent 2008 values and circles 2009 values. Drainage area median elevation is 4550 m.a.s.l..

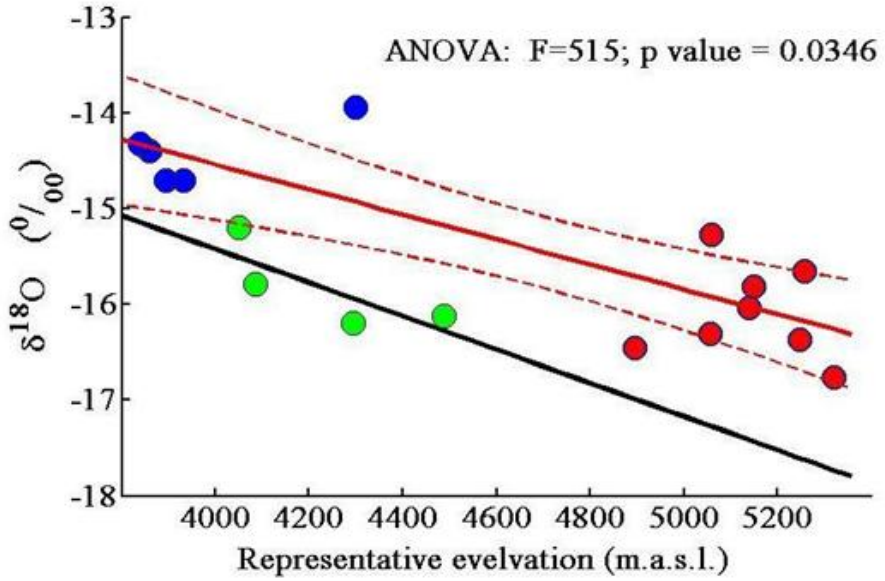

Figure 3.10. $\delta^{18}O$ (‰ VSMOW) versus representative sample elevation. GWP and MELT samples are plotted in red and blue, respectively. GWS samples are plotted in green. The red full line represents the regression line for the MELT and GWP samples and the dashed line delimits the 95% confidence interval of the linear regression. The black line shows the GWS regression result. The ANOVA F statistic and p values characterise the similarity hypothesis test for the two different lines. The distance between the two lines suggests that the difference in elevation between the spring sampled outlet and the average elevation of the recharge area, is greater than 500 metres.

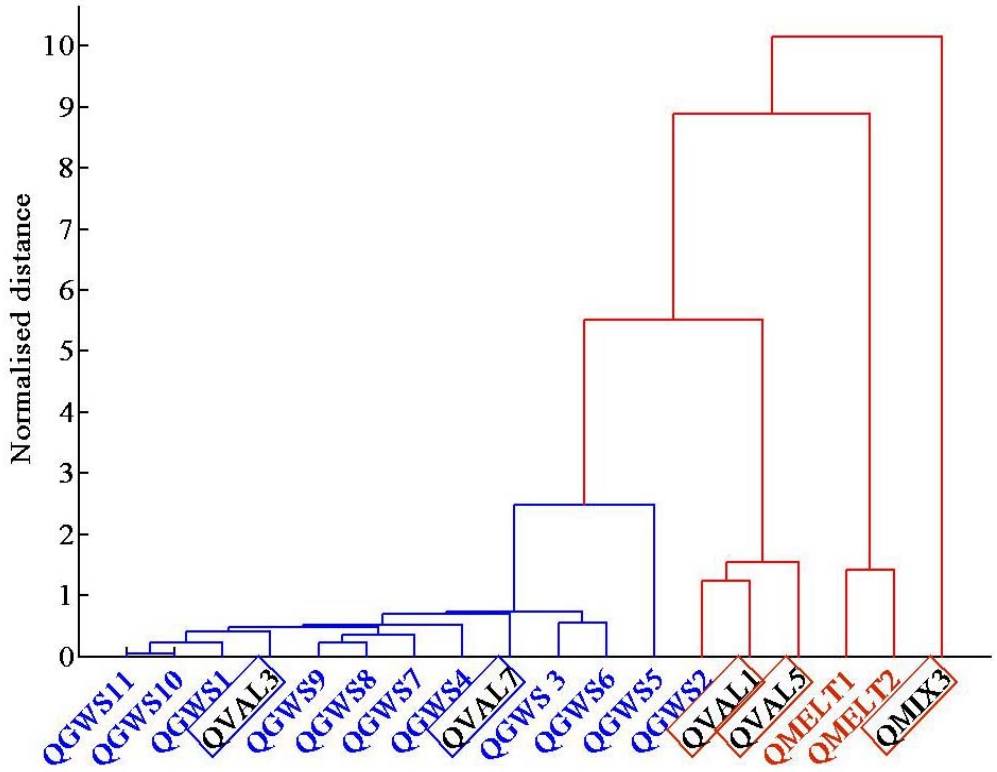

Figure 3.11. Dendrogram of the Quilcayhuanca samples taken during the 2009 summer. Blue lines characterise the precipitation cluster and the red ones represent the melt water cluster. Samples names written in black are stream or tributary samples used as reference. Slope slope

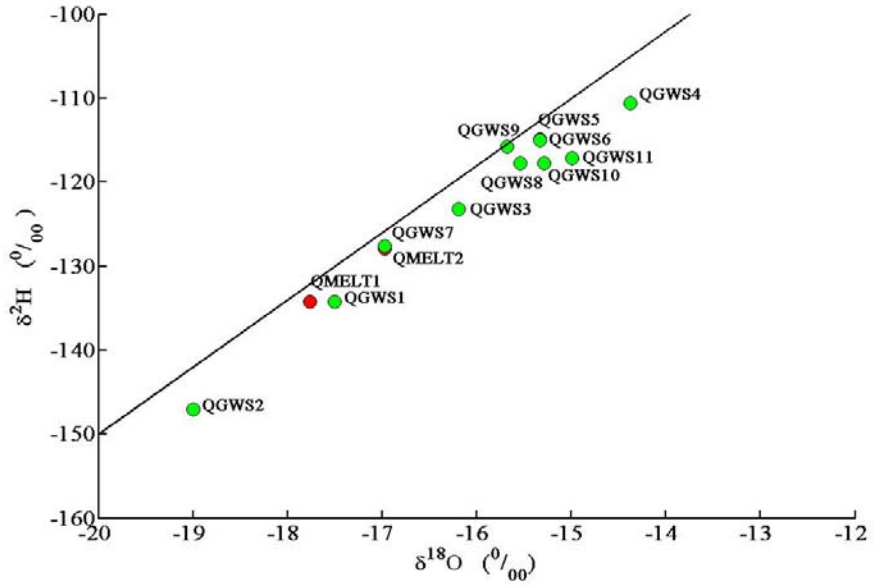

Figure 3.12. *δ*–diagram ($\delta^{18}O$ and $\delta^{2}H$ in ‰ VSMOW) for all water sources samples taken in 2009 in Quilcayhuanca. MELT samples are in red, GWS in green. The global meteoric water line is given as reference (black line).

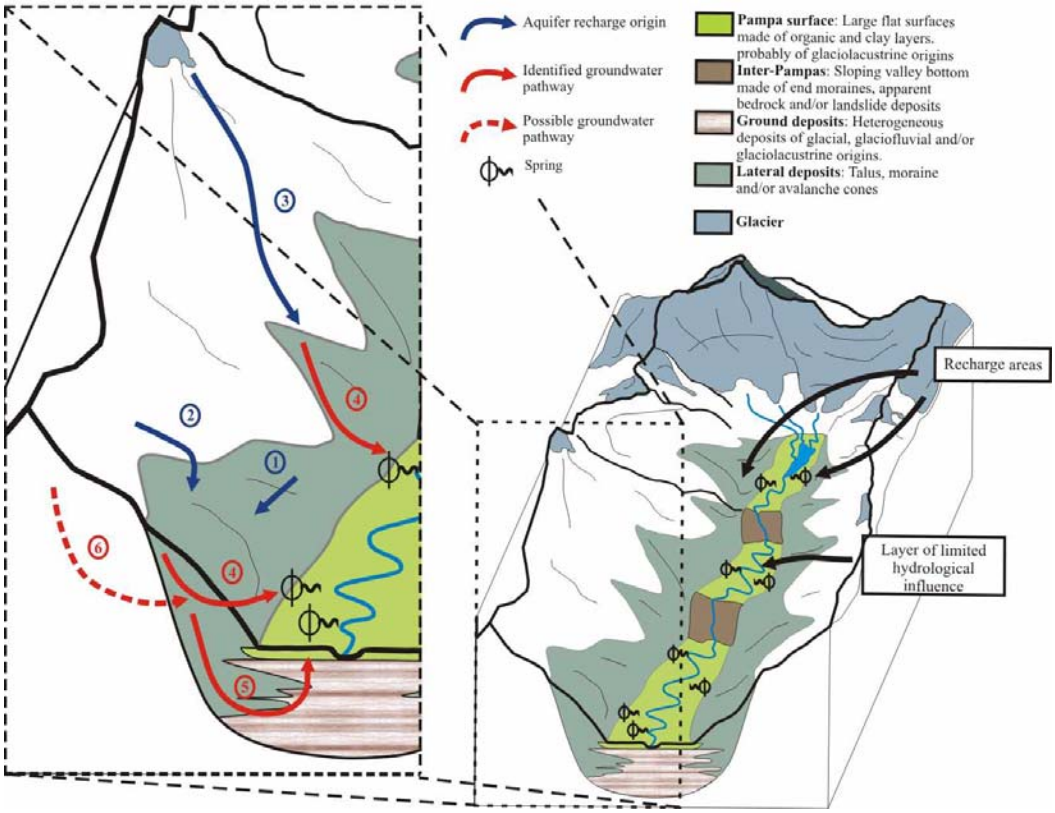

Figure 3.13. Conceptual model of the dry-season hydrological pathways and processes for the glacierised valleys of the Cordillera Blanca. Recharge and pathway numbers are: (1) direct recharge from precipitation, (2) surface runoff from overlying surfaces, (3) recharge from melt water, (4) flow through the talus slopes, (5) flow through the talus and interconnected glacial deposits, and (6) possible fracture flow through bedrock.

Context of Chapter Four within Thesis

The groundwater characteristics depicted in the two previous chapters were used to simulate the impact of glacier retreat on stream discharge for different watersheds of the Cordillera Blanca. The model I designed for this purpose integrated the groundwater specific discharge obtained from chapters two and three into a drainage basin-wide water balance equation. Unlike what has been done so far, the model does not simulate the glacier melt from climatic or energy exchange but uses the glacial retreat observations as an input. This made it possible to situate each studied watershed in a retreat sequence phase and therefore characterise the impacts of glacier retreat on stream discharge in the entire Rio Santa watershed. In addition, the hydrological model I designed showed being a potential tool for assessing glacier retreat related evolution of water resources at other glacierized watersheds of the world. The chapter complements chapters two and three by meeting the final objective of the thesis.

4. Glacier recession and water resources in Peru's Cordillera Blanca

4.1 Abstract

The tropical glaciers of the Cordillera Blanca, Peru, are rapidly retreating, resulting in complex impacts on the hydrology of the upper Rio Santa watershed. The effect of this retreat on water resources is evaluated by analyzing historical and recent time series of daily discharge at nine measurement points. Using the Mann-Kendall non-parametric statistical test, the significance of trends in three hydrograph parameters was studied. Results are interpreted by using synthetic time series generated from a hydrologic model that calculates hydrographs based on glacier retreat sequences. The results suggest that seven of the nine study watersheds have probably crossed a critical transition point, and now exhibit decreasing dry-season discharge. Our results suggest also that once the glaciers completely melt, annual discharge will be lower than present by 2% to 30 % depending of the watershed. The retreat influence on discharge will be more pronounced during the dry season than at other periods of the year. At La Balsa, which measures discharge from the upper Rio Santa, the glacier retreat could lead to a decrease in dry-season average discharge of 30%.

4.2 Introduction

In a context of a resource under pressure, the retreat of mountain glaciers in response to ongoing climate change is expected to have a major impact on alpine environments globally (Huss *et al.*, 2010). Many studies predict detrimental societal, ecological and economic impacts due to glacier retreat-related hydrological changes (Braun *et al.*, 2000; Brown *et al.*, 2010; Hannah *et al.*, 2007; Jansson *et al.*, 2003; Kistin *et al.*, 2010; Uehlinger *et al.*, 2010; Vergara *et al.*, 2007). In the Cordillera Blanca, Peru, coupled natural-human studies have shown

that, in the context of an increasing regional population, the vulnerability of Andean society is tied directly to water availability (Bury *et al.*, 2011; Mark *et al.*, 2010). However, evaluating the influence of melt water runoff on large river basin flows in different environments remains a major scientific challenge (Kaser *et al.*, 2010; Milner *et al.*, 2009). This challenge is often amplified by logistical difficulties in gathering long-term, reliable measurements like those faced in high-elevation tropical environments (Hofer *et al.*, 2010).

In conditions of continuous retreat, glaciers generate a transitory increase in runoff as they lose mass (Mark and McKenzie, 2007). This increase is limited in time as the amount of frozen water that is stored in the glaciers decreases (Mark *et al.*, 2005). As a consequence, the reduction in ice volume will yield a significant increase in annual runoff for only a few decades, followed by a decrease in runoff (Huss *et al.*, 2008). This trend will be even more pronounced during the season of low flow, a period of the year when the relative contribution of glacier melt water is at its maximum (Nolin *et al.*, 2010; Stahl and Moore, 2006). Year-to-year variability of runoff from a glacierized mountain basin is moderated by the interaction of temperature and precipitation (Collins and Taylor, 1990). This buffering effect is greatest in basins that have moderate glacier cover while variation in runoff is greatest in heavily glacierized and unglacierized watersheds. For example, Hagg and Braun (2005) suggest that the minimum year-to-year variations are found where the percentage of glacierized area is between 20 and 50%.

Glaciers, which are vulnerable to predicted future warming, buffer stream discharge from highly seasonal precipitation (Bradley *et al.*, 2006; Vuille *et al.*, 2008a). Kaser et al (2003) describe the response of Cordillera Blanca glaciers to recent climatic fluctuations in a comprehensive analysis of glacier mass balances based on discharge and precipitation data. The use of historical hydrologic observations for predictive modeling has not always lead to consistent conclusions about the future contribution of glacial melt water to stream flow. For example,

Juen et al. (2007) and Vuille et al. (2008b) showed that reduced glacier size leads to decreased volume of glacier melt. This decrease is compensated by an increase in direct runoff. Thus, the mean annual total runoff remains almost unchanged but the seasonality is considerably amplified. On the other hand, other studies suggest that water supply will peak after several decades of continually increasing as a result of net glacier loss, followed by a sudden decrease (Pouyaud *et al.*, 2005).

In this context, accurate predictions of both societal adaptive capacity and water resource availability require sustained measurements and more quantitative assessments of glacier retreat impacts at the watershed scale.

The objective of the present study is to evaluate the influence of recent and ongoing glacier recession on the hydrological regime for different watersheds of the Cordillera Blanca. In particular, it aims to evaluate the impact of glacial retreat on changes to historical trends in watershed discharge characteristics. To reach these objectives we apply the Mann-Kendall method in analyzing trends in daily average historical discharge records from nine glacierized watersheds. We present a new water-balance model that synthesizes hydrographs for different basin parameters and glacier retreat scenarios. This model, validated to trends in the historical field data, allows us to refine the theoretical curves of glacier retreat influence on hydrological regimes and to anticipate how these regimes will continue to change in the future.

4.3 Study Site

The upper Rio Santa watershed in northern Peru captures runoff from the Cordillera Negra to the west, with a dry climate and no glaciers (Mark and McKenzie, 2007; Suarez *et al.*, 2008) and the Cordillera Blanca to the east, which receives more precipitation and is Earth's most glacierized tropical mountain range. The glacier coverage of the Cordillera Blanca has declined from 800-850 km^2 in 1930 to slightly less than 600 km^2 at the end of the 20^{th} century (Georges,

2004). The majority of glaciers terminate in watersheds that are drained by the Rio Santa to the Pacific Ocean (Figure 4.1). In the Rio Santa, melt water provides 10 to 20% of the total annual discharge, and may exceed 40% in the dry season (Mark and Seltzer, 2003). The region has a strong precipitation seasonality, which is typical of the outer tropics where more than 80% of precipitation falls between October and May, and the austral winter receives almost no precipitation. In addition, the average annual air temperature is less variable than daily temperature. Glacial ablation occurs continually through the year, although sublimation reduces the melt rate during the dry season to some extent. Accumulation, on the other hand, occurs mainly during the wet season, and only on the higher elevation portions of the glaciers (Kaser *et al.*, 2003).

The Cañon del Pato 50 MW hydroelectric generation plant located at Huallanca on the Rio Santa defines the outflow of a 5,000 km^2 watershed that captures runoff from the majority of the glacierized valleys of the Cordillera Blanca. Starting when the dam was put into operation, the watershed's stream flow has been carefully monitored. As a result, many of the glacierized Santa tributaries were equipped with stream stage and precipitation gauges starting in the 1950s. Regrettably, the long-standing gauge network fell into disrepair at the end of the 20^{th} century in the midst of reforms that privatized hydroelectric generation (Carey, 2010). By the beginning of the 21^{st} century, only three of the stream stage stations - La Balsa (situated just upstream of the power plant), Paron and Llanganuco - remained in operation or had been reactivated after an interruption of several years.

4.4 Methodology

4.4.1 Data acquisition and screening

In 2008, Ohio State University, McGill University, the French Institut de Recherche pour le Developpement (IRD) and the Peruvian glaciology unit of the Autoridad Nacional del Agua (ANA) launched a joint project to improve the

stream gauging station network throughout the Cordillera Blanca. Of a total of 13 stations put into operation in 2008 and 2009, five were at historical network measurement points (Figure 4.1): Chancos, La Recreta, Pachacoto, Querococha and Miraflores (not used in this study).

The stations that are presented in this study are equipped with two Solinst 3001 Levelogger series pressure transducers. One transducer is placed into the water at a depth that ensures constant immersion and a second transducer is placed above the maximum water level to measure atmospheric pressure. The water level is calculated by subtracting the atmospheric pressure from the total pressure measured by the submerged transducer. Both sensors record the pressure at synchronous 15-minute intervals and, for the purpose of this study, records are averaged to daily values. Water levels are converted to discharges using standard hydrological techniques (Dingman, 2002).

In addition to the new discharge data, we analyzed the original historical discharge dataset which begins in 1952 and includes times series for 17 stations. A quality control analysis of the time series was used to prevent interpretation errors. Suspect drops, peaks or plateaus disqualified portions of a station's record. Missing data and interruptions in records were evaluated for possible interpolation in order to avoid the losses of valuable data which arise from the outright rejection of years with gaps. At the same time, the following rules were developed to prevent filling data gaps inappropriately: (1) gaps of less than seven days were systematically filled using linear interpolation between the two points delimiting the gap, (2) for gaps greater than seven days, a decision was made case by case, with linear or polynomial interpolation applied where there was no risk of corrupting the time series, (3) years that had remaining gaps were systematically rejected, and (4) time series for which more than 12 years were rejected were not considered for the study. Of the 17 stations, only nine were found suitable for the trend analysis based on these criteria. About 6,000 (less than 5%) of the 132,000 daily discharge values are derived from interpolation (Table 4.1). A total of 66

years of data were rejected due to potentially insufficient data quality. Despite the efforts and major discarding made during the data screening, it remains possible that the interpolation could affect the quality of the datasets. This risk, characteristic of historical data research, has to be considered when interpreting the study results though by following our strict criterion these problems should be minimized.

In the historical dataset, Paron represents a special case. Beginning in the mid-1980s after several years of civil engineering work, the level of Lake Paron was regulated by a drainage tunnel. So, even though the discharge at the lake outlet continued to be monitored, making use of these records for the purpose of the present study was inappropriate.

Precipitation records originally included times series for 36 measurement points, with the oldest starting in the late 1940s and the most recent ending in the early 2000s. Pouyaud et al. (2003) made a detailed analysis of this dataset. As the original data quality differs from location to location, they selected a group of seven measurement points for which they have performed a critical review and a homogenization of measurements that lead to reconstituted time series for 1954 to 1999 (Pouyaud *et al.*, 2005). In the present study, we make use of these seven time series (Paron, Llanganuco, Chancos, Huaraz, Querococha, Pachacoto and La Recreta) to study precipitation trends for the Cordillera Blanca region (Figure 4.1).

4.4.2 Trend analysis

The impact of glacier retreat on medium to large watersheds includes changes in annual discharge, dry-season discharge and flow variability (e.g. Barnett *et al.*, 2005; Braun *et al.*, 2000; Collins, 2008; Hagg and Braun, 2005; Jansson *et al.*, 2003; Moore *et al.*, 2009; Stahl and Moore, 2006). Therefore, when there is sustained glacier retreat it should be possible to quantify the influence of glacier retreat on watershed hydrology by identifying trends in these discharge characteristics.

In the present study three discharge characteristics were used to quantify change in: (1) the mean annual discharge (Q), (2) the dry-season discharge, and (3) the yearly coefficient of variation in daily discharge (Cv). As the timing of the dry season may vary slightly from one year to another, we used two values for dry-season discharge: the dry-season average (Q_d) and the lowest, ten consecutive day average for a given year (Q_{min}). Q_d is computed by averaging daily discharge from July and August, the lowest discharge months at La Balsa.

The Mann-Kendall test (Mann, 1945), a non-parametric distribution-free method, is used to identify significant trends in Q, Q_d, Q_{min} and Cv time series and to differentiate between significant evolution of annual parameters and random variations. This test is used in numerous hydrological studies (e.g. Hirsch and Slack, 1984; Kundzewicz *et al.*, 2005; Marengo, 1995; Xu *et al.*, 2010), and is justified by its high efficiency even with non-normal, incomplete time series (Yue and Pilon, 2004). The sign of the standard normal statistic (e.g. Xu *et al.*, 2010) indicates the slope of the trend. A positive slope denotes an increase with time, whereas a negative slope indicates a decrease. The tested significance levels (α) are 0.001, 0.01, 0.05 and 0.1.

Mann-Kendall tests were performed on all historical time series that were found acceptable through the quality control described above. The new discharge measurements were considered in the trend analysis where the number of years between the end of the historical record and the station rehabilitation time was considered as not susceptible to bias the trend analysis. As a consequence, for datasets that present more than 50% of years with missing data over the 1989-2009 period, the recent measurements are given for information only and are not integrated into the historical time series used for the trend analysis. This criterion, although not 100% selective, was used to ensure the trend analysis quality while keeping time series as long as possible. If significant bias were to still arise from these minor temporal gaps, it would be detected at the model validation stage (below).

Mann-Kendall tests were applied at two levels. At the first level the overall time series trend was evaluated by considering the complete period of the accepted records. For stations that had a change in the trend, a linear trend characterization would misrepresent the true rate of parameter change with time. Therefore trends on subsets of the complete time series segments were analyzed. Possible minima or maxima in the complete time series were identified where the derivative of the quadratic regression equation (for the different parameters of interest) was zero. A second level of Mann-Kendall linear trend analysis was then applied to sub-periods corresponding to the time before and after the year of trend change. The same procedure is applied to yearly precipitation amounts.

4.4.3 Trend interpretation model

We relate detected measured trends to changes in glacial hydrological influence by the use of a simple model of water-balance. This model generates synthetic hydrographs from the watershed area, the glacierized surfaces, and the annual rate of loss in ice area. The glacierized coverage of a watershed is a critical parameter that generates disparities among basins in hydrological response to glacial retreat (Alford and Armstrong, 2010; Birsan *et al.*, 2005; Koboltschnig and Schoner, 2010; Lambrecht and Mayer, 2009; Viviroli *et al.*, 2010). However, just the percentage of glacier area is often insufficient to describe glacial influence on stream discharge for a given watershed. The melt component of basin discharge is primarily dependent on the energy balance of snow and ice with different characteristics such as hypsometry, orientation, or density (Ohmura, 2001). These factors vary from basin to basin, creating differences in hydrological response to glacier retreat. We here account for these variations by using the annual rate of ice area loss, γ.

The following water balance equation is used with yearly average values for studied watersheds:

$$Q = \Delta S + PP + GW_{in} - GW_{out} - ET \quad (4.1)$$

where Q is the stream's outflow, ΔS is the change in water storage over the same period, PP is the yearly volume of precipitation entering the watershed, ET is basin-wide evapotranspiration and GW_{in} and GW_{out} are the groundwater fluxes entering and leaving the watersheds respectively. Considering that all watersheds studied are situated in mountainous environments, we hypothesize that the net watershed groundwater exchange, GW_{in}-GW_{out}, is very small compared to the other components of the water balance and can be ignored. The evapotranspiration term includes evaporation from rivers and lakes (ET_{rl}), evaporation from bare soil, vegetative surfaces (ET_{ngl}) and sublimation from ice and snow surfaces (Sub) (adapted from Dingman, 2002). Substituting, Equation (4.1) is then:

$$Q = \Delta S + PP - ET_{ri} - ET_{ngi} - Sub \quad (4.2)$$

For time series that are several decades long, we consider that the change of water storage is only dependent on glacier volume changes, with other storage variations balancing over decadal time periods. ΔS is therefore assumed to be equivalent to the annual change in glacier volume expressed in water equivalent. To account for the amount of sublimated volume as a factor, the PP term is split into precipitation that falls on a glacierized area and that which reaches the ground in non-glacierized areas:

$$Q = (\Delta V_{gl} + pp.A_{gl}).d_{melt} + (A_T - A_{gl}).(pp - et_{ngl}) - ET_{ri} \quad (4.3)$$

where ΔV_{gl} is the inter-annual change in glacier volume expressed in water equivalent, pp and et_{ngl} are the average volume of precipitation rate and the non-glacierized volume of evapotranspiration rate per unit area respectively, d_{melt} represents the fraction of annually ablated ice (or snow or firn) that is not lost by

sublimation and A_{gl} and A_T represent the glacierized areas and total watershed areas respectively.

To simplify Equation (4.3), we introduce β, a factor that relates V_{gl} to the glacierized area $A_{gl.}$ Assuming β is constant over time, we can consider:

$$\beta = \frac{\Delta V_{gl}}{\Delta A_{gl}^{\,2}} = \frac{V_{gl_0}}{A_{gl_0}^{\,2}} \qquad (4.4)$$

where V_{gl_0} and A_{gl_0} are the initial ice volume and glacier area respectively. The annual rate of ice area loss, γ, is the inter-annual change in glacial area ΔA_{gl} divided by the glacial area, A_{gl}, of the previous year. In a time series context, applying simple algebra to this definition for a given year, n, makes it possible to relate γ_n to $\Delta(A_{gl_n}^{\,2})$ and the glacierized area, A_{gl_n} to the initial glacier cover A_{gl_0} as follows:

$$\begin{cases} \Delta(A_{gl_n}^{\,2}) = ((1-\gamma_n)^2 - 1).A_{gl_{n-1}}^{\,2} \\ A_{gl_n} = A_{gl_0}.\prod_{t=2}^{n}[(1-\gamma_t)] \end{cases} \qquad (4.5)$$

Combining Equations (4.3), (4.4), and (4.5) leads to the following expression of the annual discharge for a given year, n:

$$Q_n = d_{melt}\left(\beta.A_{gl_0}^{\,2}.\prod_{t=1}^{n-1}(1-\gamma_t)^2.((1-\gamma_n)^2-1) + pp_n.A_{gl_0}.\prod_{t=2}^{n}(1-\gamma_t)\right) + [(pp]_n - et_{ngl}).\left(A_T - A_{gl}\right.$$

With Equation (4.6) it is possible to estimate the annual average discharge using data on precipitation and glacial retreat, as well as the watershed and initial glacierized surfaces. This assumes that the evapotranspiration terms, ET_{rl} and

ET_{ngl}, and the sublimation factor, $(1\text{-}d_{melt})$, do not vary significantly during the study period.

When focusing on the dry season, a distinction is made between fast flow and slow flow for the non-glacierized area of the watershed. Fast flow is defined here as the portion of precipitation that reaches the watershed outlet within a few days of falling, and assumes no loss due to evapotranspiration. Slow flow is defined as water that is released from the watershed over a time span longer than a few days, and is assumed to be mainly groundwater based. Considering that the Cordillera Blanca receives almost no precipitation between June and September, it is assumed that the fast-flow component for the dry season is negligible. The dry-season slow-flow discharge, q_{ngl}, accounts for the water released from groundwater minus the specific evapotranspiration, ET_{ngl}, from non-glacierized areas.

Focusing on the dry season requires accounting for the seasonality of the glacier melt rates. During the dry season, the specific humidity is low, and the vertical water vapour pressure gradient over the glacier surface is generally positive downward, making conditions favourable for sublimation to occur and decreasing the amount of energy available for total ablation (Winkler *et al.*, 2009). We introduce α, defined as the fraction of annual ablation that occurs during July and August, and use d'_{melt} instead of d_{melt} to adapt Equation (4.6) for dry-season discharge:

$$Q_{d_n} = \alpha . d'_{melt} . \left(\beta . A_{gi_0} . \prod_{t=1}^{n-1} (1-\gamma_t) . ((1-\gamma_n) - 1) + pp_n . A_{gi_0} . \prod_{t=1}^{n} (1-\gamma_t) \right) + q_{ngl} . \left(A_T - A_{gi_0} . \prod_{t=1}^{n} (1 -$$

Again it is possible to estimate the average discharge of the dry season using precipitation and the rate of glacial retreat time series, as well as the watershed and

initial glacierized surfaces. This assumes that ET_{rl}, q_{ngl}, and the sublimation factor, $(1-d_{melt})$, do not vary significantly over the study period.

The yearly coefficient of variation of discharge, Cv, is:

$$Cv = \frac{\sigma}{Q} = \frac{\sqrt{\sigma^2_{Q_{melt}} + \sigma^2_{Q_{slow}} + \sigma^2_{Q_{fast}} + \Sigma_{cov}}}{(Q_{melt} + Q_{slow} + Q_{fast})} \quad (4.8)$$

where Q_{melt}, Q_{slow}, Q_{fast} are the melt, slow-flow and fast-flow components of the yearly average discharge respectively, σ_{Qmelt}, σ_{Qslow} and $\sigma_{Qfast,}$ are the melt, slow-flow and fast-flow standard deviations and Σ_{cov} describes the sum of flow types pairs covariance. If we consider the individual coefficient of variation for the three flow components as being constant over the years, the equation is:

$$Cv = \frac{\sqrt{(Cv_{melt} \cdot Q_{melt})^2 + (Cv_{slow} \cdot Q_{slow})^2 + (Cv_{fast} \cdot Q_{fast})^2 + \Sigma_{cov}}}{Q} \quad (4.9)$$

Based on Equations (4.6), (4.7) and (4.9), the model generates annual average discharge, dry-season discharge and discharge coefficient of variation for periods greater than ten years. Due to the diverse assumptions made in the model design, it is expected that the trends in modeled parameters, as well as the final (for $A_{gl} = 0$) versus initial discharge ratios, will be most accurately reproduced.

4.4.4 Assessing influence of precipitation on discharge trends

Equations (4.1) to (4.6) indicate it is possible to estimate the annual average discharge using only precipitation and glacial retreat data if we assume that the evaporation and sublimation related terms do not vary significantly during the study period. This means that characterising the impact of glacier retreat on discharge first requires characterizing the influence of precipitation.

A correlation study between the seven precipitation time series at Paron, Llanganuco, Chancos, Huaraz, Querococha, Pachacoto and La Recreta (Pouyaud

et al., 2005) is used to assess the spatial homogeneity of precipitation across the region. A trend analysis (described earlier) is also performed on each time series, and the results of both analyses are used to further explore the regional variability and possible regional patterns of yearly precipitation values. We then statistically compare discharge parameters from all studied watersheds to regional precipitation records. When a "minimal coefficient of determination" ($R^2 \geq 0.2$ and p-value ≤ 0.1) is not obtained between Q, Q_d, Q_{min} or Cv and the yearly amount of precipitation of the closest measurement points, it is considered that discharge variability cannot be explained by precipitation changes. For all cases where a minimal correlation is detected, a new trend analysis is performed with the precipitation time series using the same time periods as the corresponding discharge parameter. In cases where significant trends of similar sign (i.e. positive or negative) are detected both in precipitation records and in discharge parameter values, the discharge parameter trend is excluded from the result interpretation.

In addition, to avoid identifying trends related to temporary climatic phenomena that could arise from shortening time series, the discharge dataset are screened for generalized common patterns in measurements. If such a case is detected, corresponding datasets are similarly excluded.

4.4.5 Estimation of glacier coverage

The published data on glacierized areas by watershed that we considered in the present study cover different time periods: (1) 1963-1970 and 1997 (Mark and Seltzer, 2003), (2) 1990-1991 (Kaser *et al.*, 2003), (3) 1930, 1970 and 1990 (Georges, 2004), and (4) 1948, 1962 and 1973 (for the Yanamarey glacier only) (Hastenrath and Ames, 1995). Combining these published data required occasional adjustments to ensure consistent definitions of watershed areas. There are only minor differences in watershed areas between the two first studies, so that the calculation of watershed glacial cover was considered comparable for publications one and two. However, the extensive dataset in Georges (2004) features a format

that presents glacierized areas by mountain group, rather than by watershed. To accurately compare formats, we first evaluated the proportion of glaciers in the mountain groups of publication (3) that drain into the watersheds of publications (1) and (2), and weighted the published glacierized areas accordingly to derive watershed-based glacier coverage for the same years 1930, 1970 and 1990. The same procedure was applied for the computation of the Querococha watershed glacierized area with publication (4). Overlaps between studies were used to fine-tune the weighted average factors.

ASTER satellite imagery was used for recent estimates of glacier area. Despite the lower resolution of ASTER imagery compared to other sources, it has provided an important multi-temporal data product to map glacier changes as part of the Global Land Ice Measurement from Space (GLIMS) project, and the Cordillera Blanca has been featured as a specific case example of the GLIMS application (Racoviteanu *et al.*, 2008; Raup *et al.*, 2008). We selected images from 2001-2003 and 2009-2010 that spanned the entire mountain range. This necessitated compilations of multiple images to obtain cloud-free coverage. For each time period, we computed the amount of glacierized coverage by digitizing glacier boundaries with GIS software. The lower termini were used to evaluate changes in area. Delimiting edges between individual glaciers at the upper regions of watersheds is inherently uncertain given the steep terrain, uniform surface reflectance, and limited image resolution. But because our objective was to compute relative changes in glacierized area aggregated by watershed, we did not need to distinguish between individual glaciers. We did not apply ASTER resolution (15 m panchromatic) to define individual glaciers, but rather the changes in total glacier coverage between periods. We calculated the watershed areas using 1:100,000 digitized contour lines and lakes and rivers from Instituto Geographico National, Peru. The glacierized area of each watershed was calculated based on the method and recommendations formulated by Racoviteanu *et al.* (2009).

The resulting glacier coverage data were used to compute the annual rate of ice loss, γ, for each studied watershed. Linear extrapolations were used between the discrete years of published or estimated glacierized areas to estimate the annual values required for the model. The glacier coverage data are used to generate synthetic datasets for model calibration and were limited to the years matching those used for the discharge data trend analysis.

4.4.6 Model parameterization and validation

The initial parameterization of the model was based on published parameter values (Table 4.2). When directly applicable parameters were not available, specific parameters were developed to estimate them such as the factor β that relates the watershed glacierized area, A_{gl}, to its volume V_{gl} (see Equation (4.4)). We use the glacier volume-area power relationship (Bahr, 1997; Bahr *et al.*, 1997) to determine the relationship between the volume of a single glacier and its surface area in the Cordillera Blanca. As tropical glaciers are generally thinner than alpine glaciers due to their relatively high inclination (Kaser and Ostmaston, 2002), the scaling factor of the power equation is computed based on published local volumes and areas. We use published glacier volumes or mass balances for glaciers situated in the tropical Andes in Bolivia (Rabatel *et al.*, 2006; Ramirez *et al.*, 2001; Soruco *et al.*, 2009) and in Peru (Ames and Hastenrath, 1996; Hastenrath and Ames, 1995). Using the scaling exponent of 1.375 suggested by Bahr (1997), the best non-linear regression result ($R^2 = 0.94$; Root Mean Square Error = 0.008 km) was obtained with a scaling factor of 0.04088 (Figure 4.2).

While valid for individual glaciers, the resulting power relationship is not directly applicable to the model which requires watershed glacierized area. For watersheds with an area of less than one square kilometre, the ice-volume estimation would remain valid; but it would be overestimated for larger glacierized areas that are usually a combination of several individual glaciers. To establish a relation between individual glaciers and watershed glacierized area thicknesses we use a simplified version (using three bins) of the area-frequency distribution of the 485

glaciers of the Cordillera Blanca that was established by Racoviteanu et al. (2008). We calculate the initial watershed glacierized volumes V_{gl_0}, as follows:

$$V_{gl_0} = \beta . A_{gl_0}{}^{\delta} = \sum_{i=1}^{8} n_i . V_{u_i} \quad (4.10)$$

where i is the repartition bin number, n_i is the number of glaciers for bin i, V_{ui} is the corresponding glacier volume area of the bin compiled from Racoviteanu et al. (2008). The β factor is determined from a watershed's initial conditions using Equation (4.10) and remains constant during the simulation. The relation between V_{gl_0} and A_{gl_0} that results from the Equation (4.10) is plotted on Figure 4.2.

The initial values of other parameters and the sources used to estimate them are given in Table 4.2. A limited number of initial parameters (Table 4.2) were adjusted to obtain the best possible fit between projected and measured variables at the study watersheds. The model's ability to reproduce trends was assessed by comparing model output to the Mann-Kendall results of the measured discharge data. Evaluating the model's ability to situate the final (Q_{end}) versus the initial (Q_0) discharges ratio was not achievable directly as none of the observed discharge time series covers the complete disappearance of the glaciers. Therefore, we used the stream's yearly discharge in the last year of the time series (Q_n) instead of Q_{end}. The error associated with Q_n/Q_0 ratio estimation is therefore considered greater than those related to Q_{end}/Q_0.

4.4.7 Model sensitivity to glacier retreat scenarios

Once calibrated, the model is used for a sensitivity analysis to determine how the key model parameters affect the simulated trend of discharge-related parameters under different scenarios of glacier retreat. Annual precipitation is kept constant across the entire simulation period, based on results of the precipitation trend analysis shown below.

A "median" scenario is defined, based on a quasi-exponential increase of γ_n and on studied watershed characteristics. Sensitivity analysis is done by comparing this median simulation (scenario a) with five "variant" scenario outputs (b to f, Table

4.3), each differing from the median scenario in one parameter only. Because of the numerous ways in which γ_n can vary with n, two variants of the γ_n function are tested: scenario "e" has a continuous glacial retreat scenario (linear) while scenario "f" involves more complexity (an oscillating function with periodic negative recession phases and a positive average in the period studied). Simulations are run until the glacier area approaches zero and the yearly average discharge stabilizes.

The median scenario is also used to explore the notion of phases of glacier retreat as a function of watershed parameters, a useful prognostic used in other studies (e.g. Collins, 2008; Milner *et al.*, 2009; Moore *et al.*, 2009). Four different phases are defined on the basis of significant trend changes that occur in model outputs while the glacier coverage decreases. This classification is subsequently used to categorize the nine different studied watersheds.

4.4.8 Potential future hydrologic impacts of glacier retreat

To determine how glacier retreat will affect future hydrological regimes, the model is run in a "rapid retreat simulation" with a hypothetical extreme rate of glacier retreat. The rapid retreat initial conditions are comparable to those of our study watersheds in 2009 as opposed to decades ago. The "median" retreat scenario (scenario a, Table 4.3) is used as a starting point and more than 2000 Q_o values are calculated based on combinations of percentage of initial glacierized area cover A_{gl0} and annual rate of ice area loss, γ_0. A_{gl0} ranges from 0.1% to 50%, γ_0 from 0 to 0.04, and watershed area was constant at 200 km^2. For each of the initial condition combinations, the annual rate of ice area loss, γ, is increased by one percent of glacier area per year until the glacier is completely melted, which is almost 50 times faster than the average γ increase observed at the nine studied watersheds between 1930 and 2009. This hypothetical retreat would generate a melt water release and a subsequent discharge increase for at least the first simulation year regardless of the initial condition. The magnitude and duration of this simulated increase reflects the capacity of glaciers to further increase the watershed flows. To evaluate this capacity $\int Q^+$, a dimensionless parameter that represents how much

the perturbed discharge Q_i exceeds initial discharge Q_0 is used, and is computed as follows:

$$\int Q^{+} = \sum \frac{(Q_i - Q_0)}{Q_0} \text{ for years } i \text{ where } Q_i > Q_0 \qquad (4.11)$$

Simultaneously, the impact on the watershed annual discharge of a glacier completely melting is evaluated by computing Q_{end}/Q_0, the final versus initial mean annual discharges ratio. This ratio provides a direct indication of how much the annual discharge will decrease once the glacier disappears compared with that calculated based on initial conditions.

In addition to annual discharges, the rapid retreat simulations are used to compute $\int Q^{+}$ and Q_{end}/Q_0 for dry-season discharge. We estimate of the $\int Q^{+}$ and Q_{end}/Q_0 values for the studied watershed by comparing watershed A_{gl} and γ values calculated for 2009 with the rapid retreat simulation results. This method of interpretation of simulated results makes it possible to qualitatively describe potential future hydrologic impacts of glacier retreat on the studied watersheds.

4.5 Results and discussion

4.5.1 Changes in glacierized area

The studied watersheds have a wide range of percent glacierized area (Table 4.4). With 39% in 2009, Paron is the most highly glacierized watershed while La Recreta is the least glacierized with 1% the same year. The percent glacierized area within every watershed decreases from 1930 to 2009. This is confirmed by the γ_{period} values (the annual rate of ice area loss from 1930 to 2009; Table 4.4) which are all positive for the period studied. The La Balsa watershed, which drains the entire upper Rio Santa, has an average of 0.61% area loss per year which is the median for the nine studied watersheds. The Llanganuco and Querococha

watersheds exhibit the fastest glacial area reduction and have an average loss of 1 and 1.1 % respectively. Los Cedros has the lowest γ_{period} with an average percent loss of 0.38 % per year. Except for Colcas, Los Cedros and Paron, there is a clear acceleration in glacierized area reduction across the studied watersheds over the past two decades. The average γ values for the period of 1990-2009 was double that for the period of 1930-2009 at Chancos, La Recreta, Pachacoto, and Querococha, indicating a probable exponential rate of depletion. La Balsa figures confirm this acceleration. The 1990-2009 annual percentage of glacier area loss reaches 0.81, which is roughly 30 % greater than what was measured during the 1930-2009 period.

The recession rate results provide an internally consistent comparison of changes over time. Our protocol to generate γ time series invokes a level of uncertainty, estimated at around five percent based upon our inclusion of historical estimates of glacierized areas from different sources and comprising different interpretations of glacier areas by different methods (Table 4.4). Despite these unavoidable limitations, the generated γ time series was considered to be adequate for the purpose of this study because the model simulations generated from these time series are used to compute trend analyses only and the results obtained from these simulations are compared to observed discharges for model validation.

4.5.2 Trends in discharge parameters

The dry-season average discharge time series are used to illustrate how the studied watersheds evolve hydrologically over time (Figure 4.3). Overall, the data show a dominant decrease in dry-season average discharge during the studied period. An increase in dry-season average is observed with the Paron dataset, a particularity that could be related to the length of the study period for this watershed. No trend is detected in the Llanganuco dry season throughout the entire study period. There is a decrease in dry-season stream discharge between the 1950s and 1990s for the

seven other watersheds. This regionally dominant pattern is also observed in the La Balsa time series which has lost more than 10% of its average dry-season discharge in little more than half a century. This decrease cannot be attributed fully to the change in glacial cover as other factors, such as changes in land use, agricultural practices or population density, also might have affected regional river discharge regimes. However, high elevation watersheds like Querococha or Pachacoto, where there is low human impact, also present an overall dry-season discharge decrease, suggesting that the change in glacial cover explains, at least partly, the observed dry-season discharge decrease at La Balsa. Four of the watersheds feature a local maximum in polynomial regression curves and four a minimum. No maximum or minimum is detected at Llanganuco. The timing of minima or maxima in polynomial regression curves vary from 1958 for Paron to 1994 for La Balsa. These differences in curve profiles suggest that it is unlikely that trends related to short inter-annual climatic phenomenon would be detected by the Mann-Kendall test.

For Mann-Kendall tests with significance values of 0.1 or lower, the random origin of trends can be excluded, allowing further refinement of the trend analyses (Table 4.5). With the exception of Paron, all significant discharge trends indicate a decrease in discharge throughout the total period and/or during the second sub-period. On no occasion were contradicting indications observed between Q, Q_d and Q_{min}. At Chancos, Los Cedros, and Querococha, the decrease in discharge was preceded by an increase in at least one of the three discharge parameters. This phase ended much earlier (around 1962) at Los Cedros than at the two others locations (1980 and 1975, respectively). On five occasions, Cv presented significant trends. At La Balsa and La Recreta, the results indicate an increase in variability with time, either for the full period of record or at least for one of the sub-periods. The only watersheds where significant decreases in yearly discharge variability were detected are Paron (across the full time series) and Colcas (in the first sub-period). The results show that an increase in discharge is systematically associated with a decrease in variability and vice versa.

For the precipitation records, the trend analysis shows a more heterogeneous situation. Of the seven time series we studied, three exhibit a negative trend and four a positive trend during the 1954-1999 period. Chancos and Huaraz both have positive, statistically significant trends. The same disparity is observed for trends analysed using sub-periods: three (one significant) of the seven time series show a negative trend during the first sub-period and two (one significant) on the second sub-period. Years of minimum or maximum values differ widely between measurement locations. These results suggest the absence of a clear region-wide trend in precipitation over the studied period. This spatial disparity is confirmed by the correlation study performed on the seven precipitation data sets (Table 4.6). Significant coefficients of determinations vary from only 0.09 between Paron and Chancos, to 0.54 between Pachacoto and La Recreta. Most of the R^2 values are around 0.3, corresponding to a low level of linear correlation. These results are in line with previously published studies that describe unclear trends in regional precipitation data or in projections (Chevallier *et al.*, 2010; Urrutia and Vuille, 2009). Vuille et al. (2008a) also describe the lack of a clear trend in precipitation for the Cordillera Blanca area. They report a difference in tendency between regions situated south (a possible decrease) and north (a possible increase) of about 11ºS. Situated between 8º38'S and 10º02'S, the Cordillera Blanca lies near the boundary of these two regions. Therefore, since using a single precipitation time series to represent a regional tendency is not possible, time series from the three nearest measurement points are used for comparison to each watershed's discharge parameters.

4.5.3 Precipitation influence on discharge trends

Results of the correlation study between precipitation records and discharge parameters are reported in Table 4.7. First, we note that the degree of influence (number and magnitude of detected "minimal correlations") vary from watershed to watershed. Broadly, the watersheds that present the lowest relative glacierized

areas (Table 4.4) have discharge parameters more correlated to annual precipitation. The degree of influence of precipitation on discharge parameter variation also differs from parameter to parameter. With only one exception (Q_d at La Recreta), Q_d and Q_{min} do not correlate or correlate weakly with the precipitation. Correlation with Q and Cv is more established but still weak as less than 50% of the calculated R^2 values do not reach the minimal correlation level and 75% of those that do are below 0.5. As a general pattern the influence of precipitation on discharge parameter variations is small,(Table 4.7), and mainly affects the less glacierized watersheds. Based on this correlation study, trends in all studied discharge parameters at Colcas and Paron are considered to be free of the influence of precipitation while at the other watersheds only Q_d and Q_{min} are independent of precipitation (Q_{min} only at La Recreta).

The lack of a regional trend in yearly precipitation amounts, as well as the weak level of correlation that exists between discharge parameters and yearly precipitation, makes it difficult to justify using a precipitation trend to force the model. We therefore fix watershed-specific yearly precipitation values in all model simulations.

4.5.4 Model validation

Modeled discharge trends were compared with measured discharge trends by counting how often a significant trend detected in measured discharge was reproduced by the model. The results in Table 4.8 are reported as the percentage of times that both trends were similar for both linear and quadratic regressions. Of the 37 significant trends detected using the Mann-Kendall test, 36 were correctly reproduced by the model for an overall match value of 97%. Despite the uncertainty related to the glacierized area evaluation and the hydro-climatic datasets, the model reproduced the trend of the four different parameters used in the study very satisfactorily. The model performance in estimating the Q_{end}/Q_0 ratios is poorer than in reproducing trends but its mean absolute error, less than 0.17, is acceptable for the purpose of the study. Evaluating the Q_n/Q_0 ratios

correctly is not explicitly required as the simpler Q_{end}/Q_0 ratio only is used. This validation step did not highlight any deviation that would characterize bias in dataset related to gaps in the historical data. This supports the assumption made earlier that these gaps did not generate miss estimation of the trends.

4.5.5 Model simulations

To test the model sensitivity, six synthetic sets of time series were generated. The median scenario (Figure 4.4a) visually conforms to the expected hydrologic progression (see Methodology references). While the glacier area is continually decreasing, both the annual average discharge and the dry-season discharge experience a period of increase followed by a period of decrease and then a period of stabilization below the initial levels. The ending dry-season discharge is approximately 50% lower than at the beginning, while the ending annual average discharge declines by no more than 10% of its initial level. The maximum dry-season discharge occurs approximately 10 years before the maximum annual average discharge. The period of increasing discharge is shorter than the decreasing and stabilization periods combined. In contrast to what was observed for average discharge, the coefficient of variation first decreased slightly for more than 50 years and then increased rapidly until it stabilized at a value that is ~50% higher.

When the same simulation is run with a higher initial glacierized area (Figure 4.4b), we see an important change in the amplitude of the output parameters' variation. The variation tempo remains similar to that obtained by using scenario a, but all of the minimums are lower and the maximum is higher with scenario b. This is visually evident in the case of the coefficient of variation whose final value is approximately 150% that of scenario a. The difference in scenario c (Figure 4.4c) is less pronounced. Although a change in amplitude is observed, it is minor if we consider that the watershed area is five times that of scenario a. Starting with an initial annual glacier area loss of 0.5% instead of 0 (Figure 4.4d) leads to a much greater difference. None of the discharge values show a period of increase,

while the coefficient of variation increases continuously. End values are different than those achieved with scenario a as mean annual and dry-season discharges end lower, while the coefficient of variation is higher.

Changing the annual rate of glacier area loss to a linear function (Figure 4.4e) does not affect the end values. For this case the rate of change is affected, with maximum discharge values (minimum for *Cv*) occurring earlier than in scenario a. These extreme values are of slightly higher amplitude as well. Similarly, the last tested scenario (Figure 4.4f) preserves the end values computed with scenarios a, c and e but amplifies the intermediate fluctuation. The amplification, which is caused by an extreme glacier area loss applied to the first 30 years of the simulation, is the largest observed among the six datasets. The strong model response to the first γ_n increase wave is not replicated in the second and third waves. Peaks in the discharge average and coefficient of variation are of low amplitude in the second wave and not detectable in the third one.

Overall, the sensitivity analysis shows that the watershed area has the least effect on the simulations. It supports the hypothesis that not only is A_{gl_0} critical to determining how glaciers influence a watershed's hydrology, but also that γ, the rate of glacier area loss, is critical. Regardless of scenario, the complete disappearance of glaciers always led to a decrease in annual discharge, an even greater decrease in dry-season discharge and an increase in variability. The sequence of a single increase followed by a decrease in discharge is for continuous retreat scenarios. With a fluctuating glacier area (scenario f), local minima and maxima are simulated but the hydrological response decreases and approaches zero as the glacier area decreases.

We used the "median" scenario, which is based on a quasi-exponential increase of γ_n and on the studied watersheds' characteristics, to depict typical hydrological impact phases (Figure 4.5). The evolution of hydrological parameters under the "median" glacier retreat scenario enables us to distinguish four impact phases.

Phase one, the early stages of deglaciation, is characterised by a smooth increase in dry-season and yearly average discharge due to a smooth initial deglaciation and ends when the coefficient of variation reaches its minimum. In phase two the increase in annual average discharge slows until it reaches its maximum while the dry-season discharge increases and then declines and the coefficient of variation begins to increase. Phase three starts from the maximum average annual discharge and covers the pronounced decline in discharges and the corresponding increase in the coefficient of variation. Phase four includes the end of the glacier influence on outflows when changes in discharges are progressively less pronounced, asymptotically reaching a non-glacierized basin state.

This sequence of four phases is based on a continuously increasing rate of ice area loss. As observed in the sensitivity analysis, deviations from this path may change the phase sequence. However, the probability of this occurring decreases as we move away from highly glacierized conditions. Returning to a phase two from a late phase three or a phase four would necessitate either extremely high rates of deglaciation or a new long-term glacial expansion. The likelihood of this happening is not supported by recent climate change projections (Urrutia and Vuille, 2009).

Each watershed is interpreted individually by comparing the significant trends in measured discharge to the definition of the impact phase (Table 4.9). This interpretation applies to the final year of observations used in the trend analysis. Significant trends in discharge parameters that show possible influence from precipitation data (three in total) are excluded from the phase allocation exercise (described above in the "Possible precipitation influence" section). Results from the phase determination suggest that seven of the nine studied watersheds are in impact phase three. One watershed, La Recreta, shows characteristics of phase four and another, Paron, is still in phase one at the end of the studied discharge time series. With an overall linear regression-based decrease in dry-season discharge, La Balsa exhibits watershed characteristics of phase three. A transition

from phase two possibly occurred around 1970, the year in which the increase in *Cv* becomes significant based on the quadratic regression-based analysis, although this possibility is not confirmed by other parameters. The fact that, on the second sub-period, an increase in *Cv* is measured in parallel to the dry-season discharge reduction is an indication that glacial factors are at least partially the cause for the measured decrease in discharge.

None of the 38 measured significant trends used in this study contradicted each other in phase allocation, confirming the model's ability to simulate the impact of long-term glacier retreat on regional stream discharge trends.

4.5.6 Glaciers' potential to further influence hydrological regimes

The "rapid retreat simulation" results relate $\int Q^+$ and Q_{end}/Q_0 values to initial A_{gl_0} and γ_0 conditions (Figure 4.6). $\int Q^+$ values are relative as the highest values represent a high potential for generating further increase in discharge and the lowest values a low potential. $\int Q^+$ values vary from 0 to 18. The lowest values (0 to 1) represent an almost negligible capacity of a glacierized area to generate a significant flow increase even under the extreme retreat rates used in this set of simulations. In contrast, the highest values characterize watersheds where discharge parameters are highly sensitive to changes in glacier retreat path. Q_{end}/Q_0 values vary from 0.1 to 1. The lowest values, obtained for the dry season, represent drastic stream discharge reductions while values above 0.9 will have a low impact on water resources.

The results show the critical role of γ_0 in a glacierized watershed's response to glacial retreat, especially for glacial cover greater than 5.0%. A watershed that has a 25% glacierized area, for example, shows annual $\int Q^+$ values that range from almost 0 to 10, depending on the value of γ_0, and is even more pronounced when only the dry season is considered. The same situation is observed with the Q_{end}/Q_0 ratio where changes in γ_0 can decrease the projected loss in discharge once the glacier is melted by more than 40%.

We estimate the studied watersheds' $\int Q^+$ and Q_{end}/Q_0 values by comparing their characteristics to the rapid retreat scenarios (Figure 4.6). With the lowest $\int Q^+$ values, La Recreta's and Querococha's discharge should not experience a glacierized area loss-related measurable increase in annual or dry-season discharge. Once the glaciers have completely disappeared, the discharge at La Recreta should remain almost unchanged compared to the present level, while Querococha should exhibit a slight dry season decline.

Future glacier influence should be slightly greater for Pachacoto, even if there is a low probability of an increase in melt-related average discharge. The main difference between Querococha and Pachacoto is in their dry-season Q_{end}/Q_0 ratios, which are about 0.8 and 0.6 respectively.

In the long-term, Paron is the watershed that should experience the most drastic glacier retreat impact. Paron glaciers present the highest potential to generate retreat related discharge increases at yearly and dry-season levels, and at complete glaciers disappearance the dry-season discharge could decline to less than 40% of its present level. Yearly discharge averages would also decrease but to about 70% of its present level.

Colcas and Los Cedros have almost the same glacierized area percentage and annual rates of ice area loss. These two watersheds have $\int Q^+$ values that are among the highest although their Q_{end}/Q_0 ratios are close to the average. These characteristics suggest that the potential for an increase in discharge is among the highest, but that the drop in flows after the glaciers have receded will be less drastic than for Chancos or Llanganuco, the latter being predicted to decrease by more than 60 % compared with the actual dry-season regime. Plots of La Balsa $\int Q^+$ values and Q_{end}/Q_0 ratios vary between extremes. When a full year is considered, the potential to further increase discharge due to glacier retreat acceleration is very low. Similarly, the Q_{end}/Q_0 ratio remains high, around 0.9, for

the full year average. The dry-season situation is different as the $\int Q^+$ value for La Balsa is average while the Q_{end}/Q_0 ratio is approximately 0.7. A loss of 30 % of the dry-season discharge at that station would not be without consequences, especially when considering that, on some occasions, the Rio Santa almost dries up before it reaches the Pacific Ocean.

4.6 Conclusion

Glaciers are major components of the hydrological system in many tropical Andean watersheds, making their ongoing retreat a threat to water resources. Predicting the exact consequences of glacial retreat is difficult due to the complexity and scales of the processes involved. Our ASTER-based measurements of recent glacier changes indicate that glacier recession is accelerating in the Rio Santa upper watershed, with the overall glacierized area decreasing annually by 0.81 % between 1990 and 2009.

To assess past and present influences of glaciers on stream discharge, we reanalyzed historical and modern discharge data from the Cordillera Blanca. Using a combination of regression and trend analyses, we found statistically significant indications that these systems have crossed a critical threshold, and now exhibit decreasing annual and dry-season discharge. La Balsa station, which measures discharge from the upper Rio Santa, is undergoing a decline in dry-season flow that probably began during the 1970s. The weak correlation that exists between the discharge parameters and precipitation supports the hypothesis that these trends are driven by the glacier retreat measured during the same period.

The link between glacial retreat and water resources is analyzed by the use of a simple water balance model. It simulates how glacier retreat can influence the annual and dry-season discharge, as well as the annual discharge variability, and reveals four impact phases of the resulting hydrological changes. Examining

historical records and fitting them to these phases suggests a declining contribution of melt water to the studied watershed outflows. At some watersheds, like Querococha, La Recreta, Pachacoto and La Balsa, the decline in discharge is likely not reversible. The decrease in the dry-season discharge should therefore continue for many decades as the watersheds enter an asymptotic decrease phase prior to the glaciers' complete loss of influence on hydrologic regimes. Once the glaciers are completely melted, the discharge will likely be lower than today. In particular, dry-season discharge may decrease more than 60% from present for Paron and Llanganuco. At La Balsa, dry-season average discharge should decline to 70% of current levels.

The model sensitivity analysis confirms that the initial glacierized area is a major driver of glacier influence on hydrology. It also shows that, unlike the total watershed area, annual rate of ice area loss is as important as the initial glacierized area.

Although the upper Rio Santa watershed still has, and should maintain, abundant water resources when annual total discharge is considered, the dry-season situation is clearly different. A decline in dry-season surface water availability has probably already begun and should continue. Considering the vulnerability of the local population to climate change and declining water resources (Bury et al., 2011), our results can represent a future social, ecological and economic concern.

Despite the overall consistency of the results of the present research, it must be recognized that they may possibly be influenced by uncertainty related to data interpolation and glacierized area estimation. The method we used is promising and could potentially be applied to other regions of the world. However, the findings that result from its application to the Cordillera Blanca need to be confirmed by other means. In addition, the method's accuracy should be further tested through future studies.

4.7 Acknowledgments

We are grateful for the historical discharge information provided by Abel Rodriguez and Duke Energy, Peru, and for the funding provided by the National Science Foundation (BCS-0752175), The Ohio State University's Climate, Water and Carbon Program, and McGill University. We thank Robert Carver for his insightful comments.

4.9 Tables

Table 4.1. A description of discharge measurement points, drainage basins, the discharge time series and the made interpolations. The 'Number of years available' is the number of years with recorded data that were screened for quality control. The number in brackets, where shown, is the number of these years of data from the new rehabilitated stations.

Station	Stream	Basin area (km^2)	Period of records	Number of years available	Number of years selected	Number of years with interpolations	Linear interpolation (%)	Polynomial interpolation (%)
Chancos	Marcara	221	1953-2009	48 (1)	40	22	2.0	4.6
Colcas	Colcas	237	1954-1999	46	37	15	1.5	4.2
La Balsa	Rio Santa	4768	1954-2008	55	50	21	1.13	3.2
La Recreta	Rio Santa	297	1952-2009	48 (2)	41	10	0	1.4
Llanganuco	Llanganuco	85	1954-2009	55 (1)	44	31	1.4	7.4
Los Cedros	Los Cedros	114	1952-1999	48	41	16	1.1	3.9
Pachacoto	Pachacoto	194	1953-2009	46 (2)	41	22	0.4	2.4
Paron	Paron	49	1953-2009	43	30	13	1.0	3.2
Querococha	Querococha	62	1953-2009	47 (1)	43	19	0.8	3.0

Table 4.2. Initial parameters for the hydrological model. The "Range" column indicates the parameter range used for the model application to different watersheds. No range means that the parameter is constant regardless of watershed.

Parameter	Description	Unit	Value	Range	Source	Comment
d_{melt}	Portion of yearly ablated ice not sublimated	-	0.82		(Winkler *et al.*, 2009)	After adjustment to dry season definition
d_{melt}'	Portion of dry season ablated ice not sublimated	-	0.74		(Winkler *et al.*, 2009)	After adjustment to dry season definition
et_{ngl}	Non-glacierized area specific evapotranspiration	mm/year	640	300-640	(Kalthoff *et al.*, 2006)	-
ET_{rl}	Evaporation from rivers and lakes	m^3/(day)	5,000	0-50,000	(Baraer *et al.*, 2009a)	Value given for the Querococha lake only
α	Dry season part of the annual ablation	-	0.14		(Kaser and Georges, 1999)	Approximation based on qualitative descriptions
q_{ngl}	Net slow flow dry season specific discharge	mm/year	200	120-200	(Baraer *et al.*, 2009b)	Watershed-dependant
Cv_{melt}	Melt component coefficient of variation	-	0.4		(Baraer *et al.*, 2007)	Calculated from hydrograph separation
Cv_{slow}	Slow flow coefficient of variation	-	0.5		-	Deducted from sensibility analysis realized with Equation (9)
Cv_{fast}	Fast flow coefficient of variation	-	1.3		(Baraer *et al.*, 2009a)	-
Σcov	Sum of covariances	-	0		-	Based on calibration

Table 4.3. Parameter values and formulas used in the sensitivity analysis scenarios. The "Median" scenario (a) represents the reference scenario. Other letters in parenthesis, (b) to (f), refer to the parameter changed for a given scenario.

Parameter	A_{gl0} (%)	A_T (km^2)	γ_0	γ_n with $n \in \{1, 2, \ldots, 200\}$
"Median" scenario (a)	*25*	*200*	*0*	$\gamma_n = \gamma_{n-1} + 3.5.10^{-6} \times n$
Variants	*50 (b)*	*1000 (c)*	*0.005 (d)*	$\gamma_n = \gamma_0 + 0.00024 \times n$ *(e)*
				$\gamma_n = \gamma_0 + \frac{\sin\left(\frac{n}{11} - 0.99\right)}{30}$ *(f)*

Table 4.4. Glacierized percentage of watershed areas. Years in italics are derived from publications (Georges, 2004; Kaser *et al.*, 2003; Mark and Seltzer, 2003). The others (2002 and 2009) were computed using ASTER satellite imagery. The specific acquisition dates for selected ASTER images were August 1, 2001, May 25, 2002, June 17, 2002, July 13, 2003, May 28, 2009, June 11, 2009, July 13, 2009, July 29, 2009, August 7, 2009, and May 29, 2010. The historical values for Querococha are from Hastenrath and Hames (1995) and cover slightly different time periods indicated in parentheses. γ_{period} and $\gamma_{90\text{-}09}$ represent the average rate of ice area loss for the 1930-2009 period and the 1990-2009 period respectively.

Watershed	*1930*	*1970*	*1990*	*1997*	2002	2009	γ_{period}	$\gamma_{90\text{-}09}$
Chancos	*31.1*	*25*	*24*	*22*	22.2	19.5	**0.0059**	**0.0108**
Colcas	*24.4*	*19.3*	*17.5*	*18*	19	17.4	**0.0043**	**0.0003**
La Balsa	*11.7*	*9*	*8.4*	*8*	8.1	7.2	**0.0061**	**0.0081**
La Recreta	*1.6*	*1.5*	*1.4*		1.1	1	**0.0058**	**0.0161**
Llanganuco	*55.5*	*42.6*	*34*		30.8	25.1	**0.01**	**0.0158**
Los Cedros	*25*	*21*	*19*	*18*	19	18.5	**0.0038**	**0.0014**
Pachacoto	*14*	*12*	*10*	*8*	7.1	6.9	**0.0089**	**0.0193**
Paron	*72*	*55*	*47*	*52*	44	38.7	**0.0078**	**0.0064**
Querococha	*4.6(1948)* *4.1(1962)*	*3.9(1973)*	*3.7*	*3*	2.8	2	**0.011**	**0.0248**

Table 4.5. Results of Mann-Kendall trend analysis. The "α" columns describe the level of significance of the reported trends. Statistically significant trends are in bold.

		Linear regression			Quadratic regression				
					Year of min	Sub-Period 1		Sub-Period 2	
	Parameter	Period	Slope	α	(max)	Slope	α	Slope	α
Chancos	Q	1954-1996	0.028		1980	**0.073**	**0.1**	**-0.134**	**0.05**
	Q_d	1954-1996	-0.007		1971	0.025		-0.029	
	Q_{min}	1954-1996	-0.003		1974	0.028		**-0.065**	**0.05**
	Cv	1954-1996	0.002		-				
Colcas	Q	1956-1997	-0.011		1972	-0.003		**-0.073**	**0.05**
	Q_d	1956-1997	-0.004		1977	0.01		-0.032	
	Q_{min}	1956-1997	-0.011		1971	-0.01		**-0.032**	**0.05**
	Cv	1956-1997	0.001		1959	**-0.052**	**0.1**	0.001	
La Balsa	Q	1954-2008	0.007		1975	0.188		0.449	
	Q_d	1954-2008	**-0.065**	**0.1**	1994	**-0.163**	**0.01**	**-0.406**	**0.05**
	Q_{min}	1954-2008	-0.04		1992	**-0.148**	**0.05**	-0.298	
	Cv	1954-2008	**0.003**	**0.05**	1970	-0.013		**0.006**	**0.05**
La Recreta	Q	1954-1995	**-0.028**	**0.1**	-				
	Q_d	1954-1995	**-0.005**	**0.05**	1980	**-0.014**	**0.01**	**-0.014**	**0.01**
	Q_{min}	1954-1995	**-0.004**	**0.01**	1984	**-0.007**	**0.01**	**-0.011**	**0.1**
	Cv	1954-1995	0.001		1976	**0.01**	**0.1**	-0.004	
Llanganuco	Q	1954-2009	0.003		1988	**0.019**	**0.01**	**-0.02**	**0.1**
	Q_d	1954-2009	0		-				
	Q_{min}	1954-2009	0		-				
	Cv	1954-2009	-0.001		-				
Los Cedros	Q	1954-1999	-0.006		1970	0.04		-0.009	
	Q_d	1954-1999	-0.006		1979	-0.017		0.037	
	Q_{min}	1954-1999	**-0.013**	**0.01**	1962	**0.15**	**0.05**	**-0.018**	**0.001**
	Cv	1954-1999	0.001		1956			0.001	
Pachacoto	Q	1954-1996	-0.015		1962	**0.149**	**0.05**	-0.021	
	Q_d	1954-1996	-0.001		1971	0.006		-0.012	
	Q_{min}	1954-1996	0.001		1972	0.018		-0.014	
	Cv	1954-1996	0		1976	-0.01		0.007	
Paron	Q	1954-1983	**0.023**	**0.01**	1962	0.019		**0.046**	**0.001**
	Q_d	1954-1983	**0.025**	**0.001**	1958	0.1		**0.029**	**0.001**
	Q_{min}	1954-1983	**0.024**	**0.001**	1958	0.111		**0.029**	**0.001**
	Cv	1954-1983	**-0.006**	**0.001**					
Querococha	Q	1953-1995	0.002		1975	**0.018**	**0.05**	-0.012	
	Q_d	1953-1995	-0.001		1974	0.006		**-0.009**	**0.01**
	Q_{min}	1953-1995	0		1975	**0.008**	**0.01**	**-0.01**	**0.01**
	Cv	1953-1995	0.001		1972	-0.004		0.003	
Precipitation	Paron	1954-1999	-2.729		1981	**-10.163**	**0.1**	2.800	
	Llanganuco	1954-1999	0.580		1969	19.800		2.187	
	Chancos	1954-1999	**2.386**	**0.1**	-	2.386			
	Huaraz	1954-1999	**6.305**	**0.01**	1990	**7.818**	**0.01**	**30.450**	**0.1**
	Querococha	1954-1999	0.878		1978	**12.226**	**0.05**	**-16.392**	**0.05**
	Pachacoto	1954-1999	-1.066		1988	-0.495		-9.529	

Table 4.6. Coefficient of determination (R^2) and statistical significance (p-value) calculated for the seven precipitation time series. R^2 values appear below the oblique line, p-values above. R^2 values equal to or over 0.2 associated with a p-value under 0.1 are in bold.

R^2 \ p-value	**Paron**	**Llanganuco**	**Chancos**	**Huaraz**	**Querococha**	**Pachacoto**	**La Recreta**
Paron		0.0163	0.0438	0.0142	0.0434	0.0001	0.0001
Llanganuco	0.13		0.0001	0.0019	0.0013	0.0001	0.0001
Chancos	0.09	**0.30**		0.0001	0	0.0001	0.0001
Huaraz	0.13	**0.20**	**0.29**		0	0	0
Querococha	0.09	**0.22**	**0.38**	**0.51**		0	0.0001
Pachacoto	**0.31**	**0.30**	**0.31**	**0.35**	**0.40**		0
La Recreta	**0.30**	**0.29**	**0.32**	**0.37**	**0.29**	**0.54**	

Table 4.7. Coefficient of determination (R^2) and their associated statistical significance (p-value) calculated between the precipitation records from the three closest measurement points and the discharge parameters of each gauging station. R^2 values equal to or over 0.2 associated to a p-value above 0.1 are in bold.

	precipitation	**Q**		**Q_d**		**Q_{min}**		**Cv**	
	measurement point	R^2	p-value	R^2	p-value	R^2	p-value	R^2	p-value
Chancos	Llanganuco	0.00	0.9491	0.01	0.661	0.01	0.5929	0.06	0.1417
	Chancos	0.10	0.0589	0.00	0.9826	0.00	0.8997	0.07	0.1199
	Huaraz	0.15	0.0183	0.00	0.8897	0.02	0.3476	0.17	0.0106
Colcas	Paron	0.02	0.4537	0.04	0.2788	0.03	0.2895	**0.22**	**0.005**
	Llanganuco	0.00	0.751	0.01	0.4965	0.04	0.2447	0.19	0.0082
	Chancos	0.06	0.1547	0.04	0.2678	0.00	0.8953	0.00	0.9736
La Balsa	Chancos	**0.24**	**0.001**	0.01	0.6441	0.00	0.7952	0.18	0.0068
	Huaraz	**0.32**	**2E-04**	0.00	0.9639	0.00	0.9126	**0.33**	**1E-04**
	Querococha	0.09	0.0584	0.00	0.7185	0.01	0.5549	0.08	0.0748
La Recreta	Querococha	**0.39**	**0**	0.13	0.0261	0.02	0.347	0.17	0.0091
	Pachacoto	**0.61**	**0**	**0.39**	**0**	0.13	0.0263	0.15	0.0131
	La Recreta	**0.67**	**0**	**0.37**	**0**	0.13	0.0219	0.05	0.1547
Llanganuco	Paron	0.05	0.2007	0.03	0.3251	0.01	0.5263	0.13	0.0238
	Llanganuco	0.01	0.4672	0.03	0.3265	0.08	0.0871	**0.33**	**2E-04**
	Chancos	0.11	0.0397	0.01	0.5515	0.00	0.7421	0.11	0.0414
Los Cedros	Paron	0.03	0.2572	0.00	0.7115	0.00	0.8282	0.07	0.0967
	Llanganuco	**0.33**	**1E-04**	0.07	0.0981	0.02	0.341	**0.23**	**0.002**
	Chancos	0.19	0.005	0.05	0.1857	0.00	0.9562	**0.45**	**0**
Pachacoto	Querococha	**0.32**	**2E-04**	0.02	0.4479	0.01	0.5795	0.10	0.0528
	Pachacoto	**0.51**	**0**	0.02	0.346	0.03	0.3189	**0.23**	**0.002**
	La Recreta	**0.55**	**0**	0.03	0.3048	0.03	0.2737	0.16	0.0131
Paron	Paron	0.17	0.0287	0.16	0.0378	0.19	0.0216	0.10	0.1018
	Llanganuco	0.04	0.3303	0.12	0.0738	0.13	0.0592	0.17	0.0272
	Chancos	0.10	0.1051	0.05	0.2697	0.04	0.3013	0.03	0.3557
Querococha	Huaraz	**0.40**	**0**	0.04	0.2344	0.17	0.0075	0.13	0.0217
	Querococha	**0.68**	**0**	0.04	0.2301	0.13	0.0199	**0.26**	**7E-04**
	Pachacoto	**0.49**	**0**	0.02	0.3719	0.00	0.7775	**0.23**	**0.002**

Table 4.8. Model performance evaluation. The "Linear trends" and "Quad. trends" columns provide a comparison of the number of observed (Obs.) significant trends in the time series and the number of matching trends in the modeled results (Mod.) for linear and quadratic regressions respectively. The "Q_n/Q_0" column shows the error calculation components for the Q_n/Q_0 ratios.

Station	Linear trends		Quad. trends		Q_n/Q_0		
	Obs.	Mod.	Obs.	Mod.	Obs.	Mod.	Error
Chancos	0		3	3	1.22	0.97	-0.25
Colcas	0		3	3	0.88	0.89	0.01
La Balsa	2	2	4	4	1.06	0.93	-0.13
La Recreta	3	3	5	5	0.66	1.00	0.34
Llanganuco	0		2	2	1.05	0.91	-0.14
Los Cedros	1	1	2	2	0.94	0.99	0.05
Pachacoto	0		1	1	0.84	1.01	0.17
Paron	4	3*	3	3	1.42	1.05	-0.38
Querococha	0		4	4	1.06	1.01	-0.05
	match=90%		match=100%		MAE**		0.17
	match overall=97%						

* The linear negative trend in the coefficient of variability of discharge for the Paron dataset was incorrectly replicated.

** Mean absolute error.

Table 4.9. Trends associated with the "typical" glacier retreat model compared to measured trends. The symbols used for trend description are "+" for an increase, "-" for a decrease, "+,-" for an increase followed by a decrease, and "-,0" for a decrease followed by parameter stabilization. The "Phases" lines summarize phase definitions. Reproduced watershed data are indicated for statistically significant trends only (Table 4.5). In case of trends that were split by quadratic regression, the year separating the two sub-periods is given into brackets. Trends excluded from the phase allocation due to possible precipitation influence are in grey. The cause of rejection is presented in the "possible precipitation influence" column. The watershed names are followed by the year to which the interpretation statement applies.

(Table at following page for readability)

Parameter		Q	Q_d	Q_{min}	Cv	Possible precipitation influence	Phases #
Phases	1	+	+	+	-		
	2	+	+,-	+,-	+		
	3	-	-	-	+		
	4	-,0	-,0	-,0	+,0		
Chancos (1996)	linear						**2** until 1980 then phase **3**
	quad.1	+ (1980)					
	quad.2	- (1980)		- (1974)			
Colcas (1996)	linear						**1** until 1959 and **3** from 1972
	quad.1				- (1959)		
	quad.2	- (1972)		- (1971)			
La Balsa (2008)	linear		-		+	*Cv* / Huaraz	**3** from 1970
	quad.1		- (1994)	- (1992)			
	quad.2		- (1994)		+ (1970)		
La Recreta (1995)	linear	-	-	-		Q_d / La Recreta	**3** and possibly **4** from 1982
	quad.1		- (1980)	- (1984)	+ (1976)		
	quad.2		- (1980)	- (1984)			
Llanganuco (2009)	linear						**2** until 1988 then **3**
	quad.1	+ (1988)					
	quad.2	- (1988)					
Los Cedros (1999)	linear			-			**3** since 1962
	quad.1			+ (1962)			
	quad.2			- (1962)			
Pachacoto (2009)	linear						Possibly **3** since 1962
	quad.1	+ (1962)					
	quad.2						
Paron (1983)	linear	+	+	+	-		1
	quad.1						
	quad.2	+ (1962)	+ (1958)	+ (1958)			
Querococha (2009)	linear						**2** until 1976 then **3**
	quad.1	+ (1975)		+ (1975)		Q / Querococha	
	quad.2		- (1976)	- (1976)			

4.10 Figures

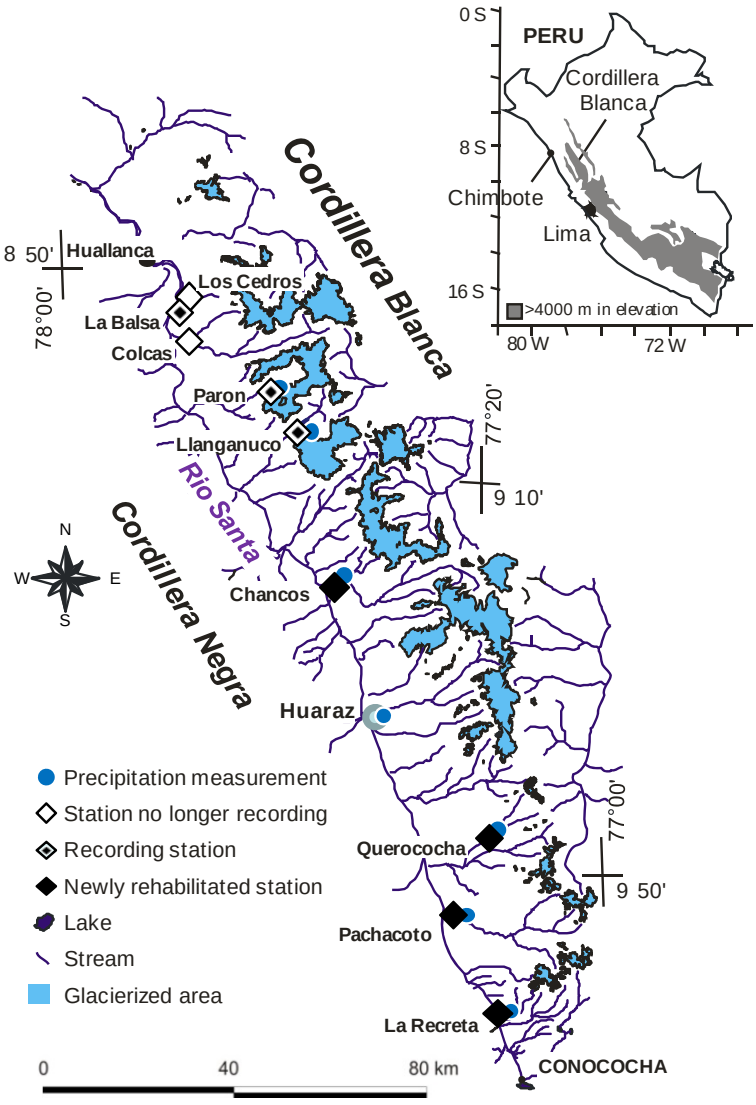

Figure 4.1. The Cordillera Blanca and locations of the precipitation measurement stations (circles) and discharge measurement stations (squares) considered for the study.

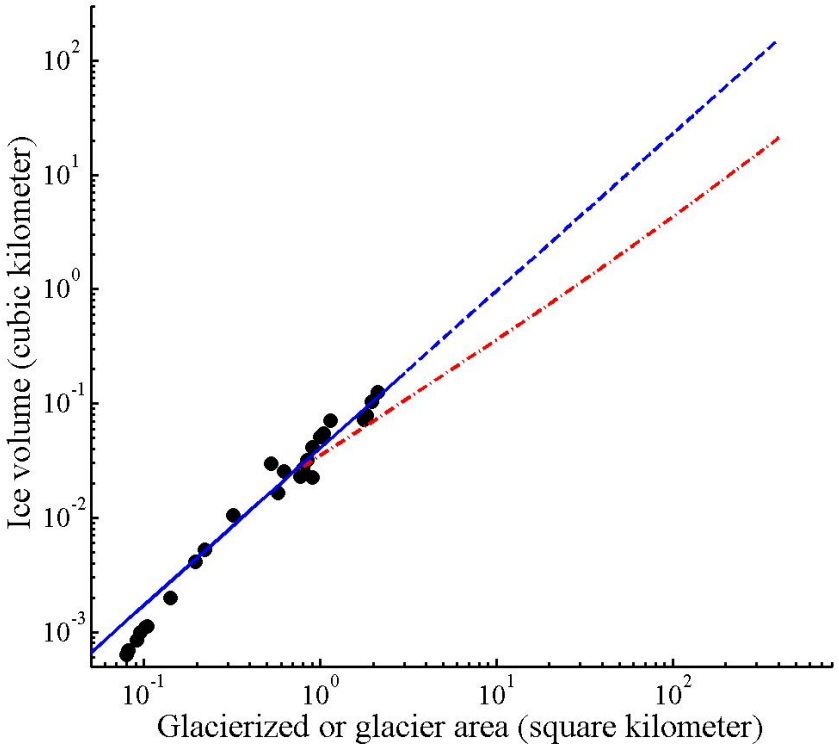

Figure 4.2. Ice volume versus glacier area for tropical glaciers of the Andes. Black dots represent measured values from Ramirez et al. (2001), Rabatel et al. (2006), Soruco et al. (2009), Hastenrath et al. (1995) and Ames and Hastenrath (1996). The blue line plots the Bahr et al. (1997) equation which slope is adjusted to fit the measured values. The dashed portion of the blue line corresponds to the projection of the trend outside the regression range. The red curve represents the ice volume evaluated for the glacierized area of a watershed.

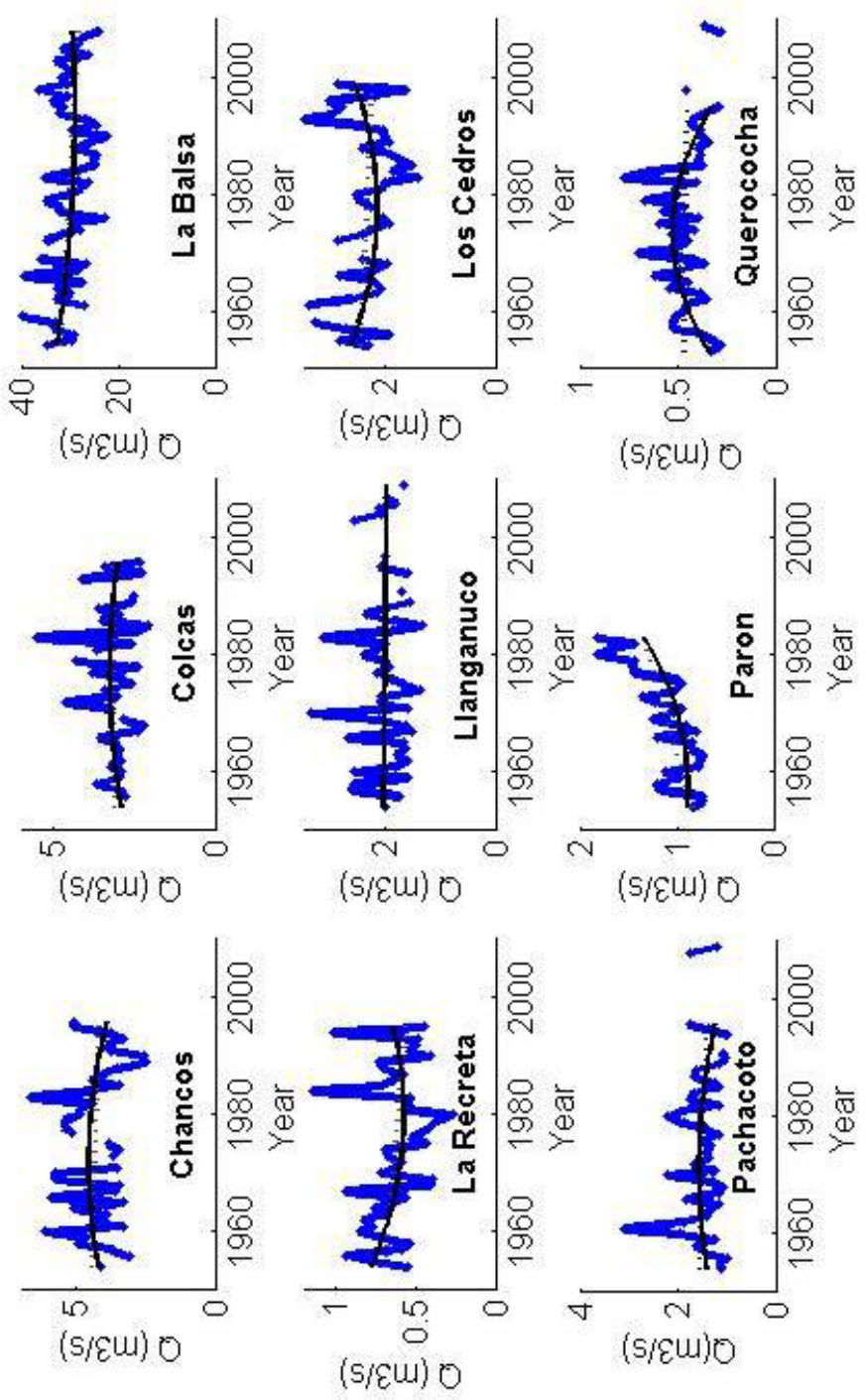

Figure 4.3. Dry-season average discharge calculated from daily data (full blue line). Linear and quadratic regressions lines (curves) calculated from datasets are drawn in black dashed lines and full black curves respectively.

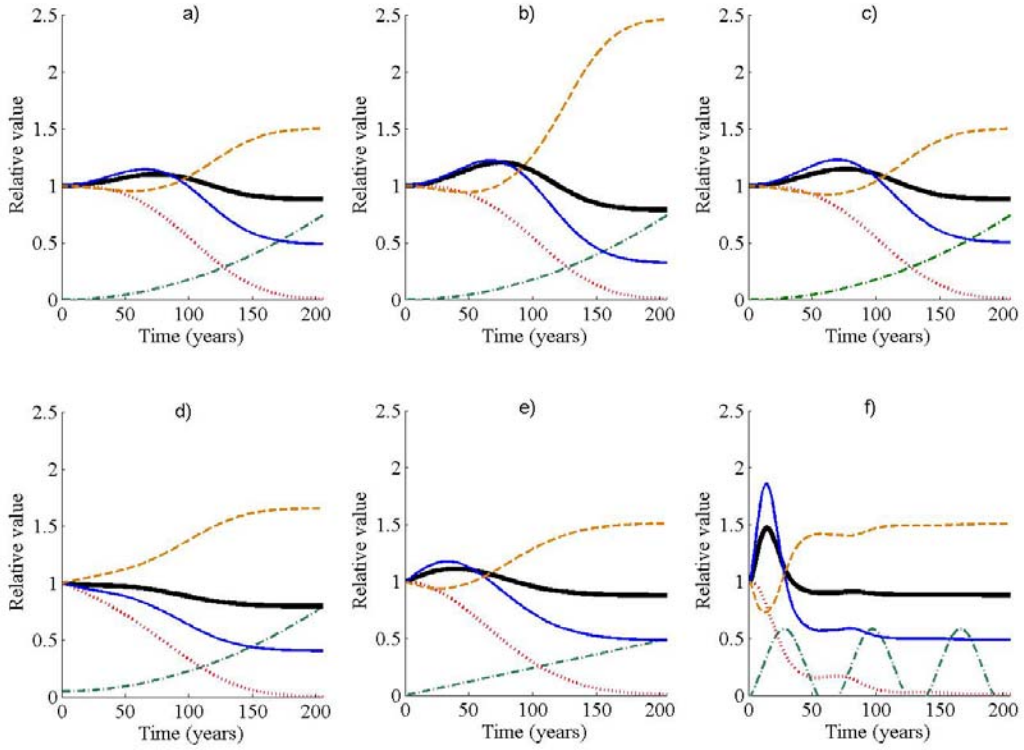

Figure 4.4. Results of sensitivity analysis simulation. The thick black lines and the blue lines are the mean annual and dry-season discharge respectively, the yellow dashed line is the annual discharge coefficient of variation, the red dotted line is the glacierized area and the green dash dotted line is the applied annual rate of glacier area loss. All parameters are given relative to year zero values. Graph (a) presents the "Median" scenario output, while the five others are variants described in Table 4.3: b) A_{gl0} increase; (c) A_T increase; (d) γ_0 increase; (e) linear γ_n increase and (f) oscillating γ_n.

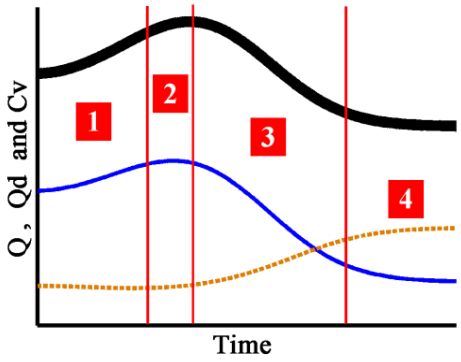

Figure 4.5. “Typical” glacier retreat hydrological impact phases (delimited and labelled in red). The thick black line and the blue line represent the mean annual and dry-season discharge respectively and the yellow dashed line corresponds to the annual discharge coefficient of variation. As the phases are conceptual, axes are kept unit-free.

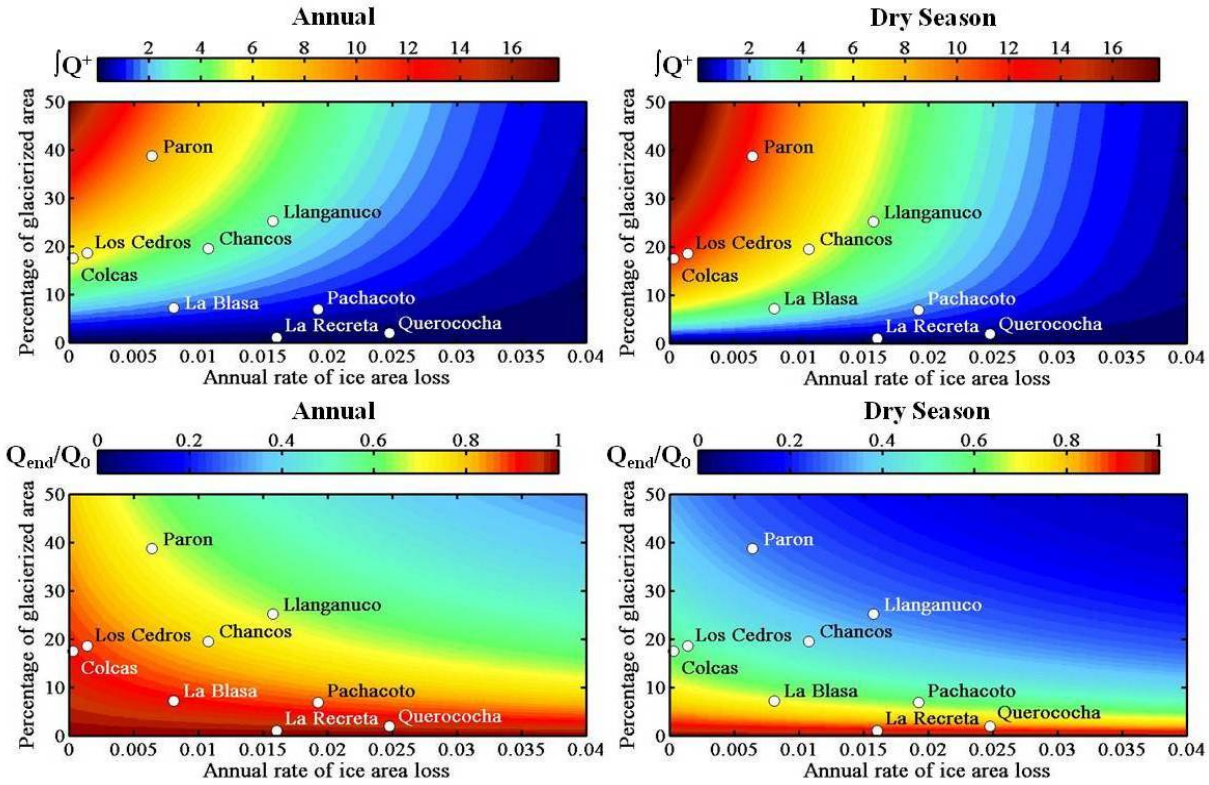

Figure 4.6. Variations of $\int Q^+$ (top graphs) and Q_{end}/Q_0 (bottom graphs) for the "rapid retreat simulations", as a function of percentage of glacierized area and the annual rate of ice area loss. Colors represent values of $\int Q^+$ (indicator of the glaciers capacity to further increase the watershed flows) and of Q_{end}/Q_0 (starting and ending simulated discharge ratio). Full year simulations appear on the left and dry-season ones are reported at the right. All parameters are dimensionless.

5. Summary, Conclusion and Direction for Future Research

In a context of potential future water scarcity for millions of people, making reliable predictions about discharge evolution is of major importance. Previously, stream discharge modeling in the Rio Santa watershed considered the groundwater contribution to stream discharge in a very simplified way, and relied on assumptions for parameterisation. The lack of a comprehensive study on groundwater contribution to surface water in the Cordillera Blanca was identified as a major reason for this limitation.

Bridging this gap in knowledge, the present thesis shows that:

- Groundwater is a major component of the surface water that flows out of the glacierized valleys of the Cordillera Blanca during the dry season. In July 2008, watersheds with less than 8% glacier cover were dominated by groundwater as opposed to melt water, indicating that groundwater components in the region's water resource models need to be rigorously constrained.
- Groundwater contribution is highly variable in time. This variability is likely due to limited storage capacity, estimated to be four years maximum at the Querococha watershed. This characteristic makes groundwater recharge sensitive to cyclic climatic phenomena such as the El-Nino Southern Oscillation (ENSO).
- Differences exist in groundwater relative contribution to surface water from glacierized valley to glacierized valley but these differences are constrained, at least partly, by the valleys' glacierized surface. Despite their differences in attributes (location, geology, glacial cover, etc.) all of the valleys we studied were able to capture water in their soil at a certain times of the year, store it, then release it during the dry season.

- Valley talus plays a key role these systems. It collects water running off from higher elevations and releases it at lower elevations. It also transfers part of the collected water to different layers of deposits that lie beneath the Pampa surfaces which are made of very low permeability material.
- Most of the springs are precipitation-fed but at least one melt water-fed spring was identified. There is a possibility that this type of spring will run dry during the dry season when the small amount of ice that currently feeds them is gone.
- Integrating groundwater discharge values into the hydrological model to study the impact of glacier retreat on stream discharge leads to conclusions that slightly differ from previous modeling experiments. The augmentation of the seasonality pattern in stream flows is confirmed by the present study but, with a decrease of up to 30% of the actual level, the decrease in annual discharge appears much more pronounced that in preceding predictions.
- Peak water in the Cordillera Blanca is not coming for most of the studied watersheds; it has passed and in some cases it happened several decades ago. The glacier-related decrease in flows is unlikely reversible, meaning that the dry-season and annual discharge should continue to decrease as the glaciers retreat.

These findings have numerous consequences for water resources management. Further decreases in surface water availability, especially during the dry season, are anticipated. In a context of increasing demand, this negative trend could have heavy consequences. With most of the studied glacierized valleys of the Cordillera Blanca having passed peak water related to glacier retreat, there is no time left before flow decreases. According to the hydrological model presented in chapter four, the evolution of the stream flows is in a phase that is characterised by a steepening in the downward slope. As a demonstrated contributor to surface waters during the dry season, groundwater can be seen as a resource to be protected. Unlike glaciers, this source of water can sustain dry-season flows under warming conditions but, like glaciers, it can also be affected by human activities.

In addition to hydrological-related findings, the present thesis introduces new or adapted methods that could be used in other contexts. Of these, HBCM is particularly useful. Based on common tracer conservation equations, its cell-based spatial coverage allows the estimation of the watershed-wide groundwater contribution. In addition, its lake component derives absolute end-member contributions from hydrochemical and isotopic signatures only. The hydrological model presented in chapter four represents another original application. Because its use allows situating watersheds on glacier retreat-related stream discharge evolution curves, it represents a potential water resource assessment tool wherever glacier retreat impact on water resources is a concern. Still, these two methods lack extended use, and applicability to other regions needs to be verified.

By answering questions on the hydrology of the Cordillera Blanca, this thesis raises others. The conceptual model proposed in chapter three, for example, depicts talus and other valley side deposits as key hydrological features but does not explain the mechanisms that drive their hydrological processes. How do these debris accumulations, whose surface layers exhibit high permeability, retain water long enough to release it all year long? Are fracture flows hidden by these features? Are less conductive materials buried under permeable layers, making the top part of the talus not representative of its entire mass?

In addition, key recharge mechanisms require a better understanding too. Large amounts of water flow out of non-glacierized areas, and a large part of chapter four is implicitly based on the hypothesis that groundwater is rain-fed. On the other hand, chapter three characterises one of the sampled springs as being melt water-fed. How much of the groundwater is fed by melt water from glaciers and how the related aquifers might evolve with retreating glaciers are other questions that remain unexplored.

The present thesis shows that the dry-season flows of the Rio Santa will likely keep decreasing, losing up to 30% in discharge compared to today once glaciers

lose their hydrological influence. Adapting water resources management in anticipation of this change is a way to avoid or mitigate the potential human, ecological and economical consequences of a water shortage. This requires reliable and precise projections of the future of flows in streams like the Rio Santa. Scientists therefore need to produce better-performing predictive models. It is by strengthening our knowledge of the regional hydrology in general and answering questions such as the ones cited above that we will move toward this objective.

6. References

Anderson, SP. 2005. Glaciers show direct linkage between erosion rate and chemical weathering fluxes. *Geomorphology*, **67**(1-2): 147-157.

Alford D and Armstrong R. 2010. The role of glaciers in stream flow from the Nepal Himalaya. *Cryosphere Discussions* **4**(2): 469-494.

Ames A and Hastenrath S. 1996. Diagnosing the imbalance of Glaciar Santa Rosa, Cordillera Raura, Peru. *Journal of Glaciology* **42**(141): 212-218.

Bahr DB. 1997. Global distributions of glacier properties: A stochastic scaling paradigm. *Water Resources Research* **33**(7): 1669-1679.

Bahr DB, Meier MF and Peckham SD. 1997. The physical basis of glacier volume-area scaling. *Journal of Geophysical Research B: Solid Earth* **102**(B9): 20355-20362.

Ballantyne CK. 2002. Paraglacial geomorphology. *Quaternary Science Reviews* **21**(18-19): 1935-2017.

Baraer M, Mark BG, McKenzie JM, Condom T, Bury J, Huh K, Portocarrero C, Gomez J and Rathay S. 2012. Glacier recession and water resources in Peru's Cordillera Blanca. *Journal of Glaciology* **58**(207): 134-150.

Baraer M, McKenzie JM, Mark BG and Knox S. 2009a. Nature and variability of water resources in the Rio Santa upper watershed, Peru. In *AGU -CGU joint assembly,* AGU ed.: Toronto.

Baraer M, McKenzie JM, Mark BG, Bury J and Palmer S. 2009b. Characterizing contributions of glacier melt and groundwater during the dry season in a poorly gauged catchment of the Cordillera Blanca (Peru). *Advances in Geosciences* **22**: 41-49.

Baraer M, McKenzie JM, Mark BG and Palmer S. 2007. An Integrated approach to modeling runoff from glacier-fed basins, Cordillera Blanca, Peru In *Glaciers in Watershed and Global Hydrology,* Workshop, Obergurgl, Austria.

Barbieri M, Boschetti T, Petitta M and Tallini M. 2005. Stable isotope (2H, 18O and 87Sr/ 86Sr) and hydrochemistry monitoring for groundwater

hydrodynamics analysis in a karst aquifer (Gran Sasso, Central Italy). *Applied Geochemistry* **20**(11): 2063-2081.

Barnett TP, Adam JC and Lettenmaier DP. 2005. Potential impacts of a warming climate on water availability in snow-dominated regions. *Nature* **438**(7066): 303-309.

Barry, RG. 2006. The status of research on glaciers and global glacier recession: a review. *Progress in Physical Geography*, **30**(3): 285-306.

Birsan MV, Molnar P, Burlando P and Pfaundler M. 2005. Streamflow trends in Switzerland. *Journal of Hydrology* **314**(1-4): 312-329.

Bradley RS, Vuille M, Diaz HF and Vergara W. 2006. Threats to water supplies in the tropical Andes. *Science* **312**(5781): 1755-1756.

Braun LN, Weber M and Schulz M. 2000. Consequences of climate change for runoof from Alpine regions. *Annals of Glaciology* **31**: 19-25.

Brown LE, Milner AM and Hannah DM. 2010. Predicting river ecosystem response to glacial meltwater dynamics: a case study of quantitative water sourcing and glaciality index approaches. *Aquatic Sciences* **72**(3): 325-334.

Brown, LE., Hannah, DM, Milner AM,, Soulsby C, Hodson JA. and Brewer J. 2006. Water source dynamics in a glacierized alpine river basin (Taillon-Gabietous, French Pyrenees). *Water Resources Research*, **42**(8), W08404, doi:10.1029/2005WR004268.

Bury J, Mark B, McKenzie J, French A, Baraer M, Huh K, Zapata Luyo M and Gómez López R. 2011. Glacier recession and human vulnerability in the Yanamarey watershed of the Cordillera Blanca, Peru. *Climatic Change* **105**(1): 179-206.

Buytaert W, Deckers J and Wyseure G. 2006. Description and classification of nonallophanic Andosols in south Ecuadorian alpine grasslands (pÃ¡ramo). *Geomorphology* **73**(3-4): 207-221.

Caballero Y, Jomelli V, Chevallier P and Ribstein P. 2002. Hydrological characteristics of slope deposits in high tropical mountains (Cordillera Real, Bolivia). *Catena* **47**(2): 101-116.

Carey, M. 2010. In the shadow of melting glaciers. Climate change and Andean society. Oxford University Press.

Casassa G, Haeberli W, Jones G, Kaser G, Ribstein P, Rivera A and Schneider C. 2007. Current status of Andean glaciers. *Global and Planetary Change* **59** (1-4): 1-9.

Cerling TE, Pederson BL and Vondamm KL. 1989. Sodium-calcium ion-exchange in the weathering of shales - implications for global weathering budgets. *Geology* **17**(6): 552-554.

Chevallier P, Pouyaud B, Suarez W and Condom T. 2010. Climate change threats to environment in the tropical Andes: Glaciers and water resources. *Regional Environmental Change* **11**(1-9): 179-187.

Chevallier P, Pouyaud B and Suarez W. 2004. Climate Change impact on the water resources from the mountains in Peru. *Global Forum on Sustainable Development: Development and Climate Change*. OECD: Paris.

Christophersen N, Neal C, Hooper R, Vogt R and Andersen S. 1990. Modeling streamwater chemistry as a mixture of soilwater end-members. A step towards 2nd generation acidification models. *Journal of Hydrology* **116**(1-4): 307-320.

Collins DN. 2008. Climatic warming, glacier recession and runoff from Alpine basins after the Little Ice Age maximum. *Annals of Glaciology* **48**: 119-124.

Collins DN and Taylor D. 1990. Variability of runoff from partialy glacierised alpine basins. *Hydrology in Mountainous Regions*. IAHS: Lausanne, CH;365-372.

Condom T, Escobar M, Purkey D, Pouget JC, Suarez W, Ramos C, Apaestegui J, Zapata M, Gomez J and Vergara W. 2010. Modelling the hydrologic role of glaciers within a Water Evaluation and Planning System (WEAP): A case study in the Rio Santa watershed (Peru). *Hydrology and Earth System Sciences Discussions* **8**: 869-916.

Cooper RJ, Wadham JL, Tranter M, Hodgkins R and Peters NE. 2002. Groundwater hydrochemistry in the active layer of the proglacial zone, Finsterwalderbreen, Svalbard. *Journal of Hydrology* **269**(3-4): 208-223.

Coudrain A, Francou B and Kundzewicz ZW. 2005. Glacier shrinkage in the Andes and consequences for water resources. *Hydrological Sciences Journal-Journal Des Sciences Hydrologiques* **50**(6): 925-932.

Crossman J, Bradley C, Boomer I and Milner A. 2011. Water flow dynamics of groundwater-fed streams and their ecological significance in a glacierized catchment. *Arctic, Antarctic, and Alpine Research* **43**(3): 364-379.

Delclaux F, Coudrain A and Condom T. 2007. Evaporation estimation on Lake Titicaca: a synthesis review and modelling. *Hydrological Processes* **21**(13): 1664-1677.

Dingman SL. 2002. Physical Hydrology. Prentice-Hall, Inc.;646.

Drever. 2005. *Surface and Ground Water, Weathering, and Soils*. Eslevier-Pergamon Oxford.

Favier V, Coudrain A, Cadier E, Francou B, Ayabaca E, Maisincho L, Praderio E, Villacis M and Wagnon P. 2008. Evidence of groundwater flow on Antizana ice-covered volcano, Ecuador. *Hydrological Sciences Journal-Journal Des Sciences Hydrologiques* **53**(1): 278-291.

Fleming S and Clarke G. 2005. Attenuation of High-Frequency Interannual Streamflow Variability by Watershed Glacial Cover. *Journal of Hydraulic Engineering,* **131**(7): 615–618.

Fortner SK, Mark BG, McKenzie JM, Bury J, Trierweiler A, Baraer M, Burns PJ and Munk L. 2011. Elevated stream trace and minor element concentrations in the foreland of receding tropical glaciers. *Applied Geochemistry* **26**(11): 1792-1801.

Fountain AG and Tangborn, WV. 1985. The effect of glaciers on streamflow variations. *Water Resources Research* **21**(4): 579-586.

Gat JG. 2010. *Isotope Hydrology, a study of the water cycle*. Imperial College Press: London; 189.

Georges C. 2004. 20th-century glacier fluctuations in the tropical Cordillera Blanca, Peru. *Arctic Antarctic and Alpine Research* **36**(1): 100-107.

Girard S. 2005. Paramos, strategic spaces for managing water resources in the northern Andes: The RÃo Ambato basin (Ecuador). *Mappemonde* **78**.

Goldthwait RP and Matsch CL. 1989. Genetic classification of glacigenic deposits. A. A. Balkema: Rotterdam, Nederland.

Gonfiantini R, Roche M-A, Olivry J-C, Fontes J-C and Zuppi GM. 2001. The altitude effect on the isotopic composition of tropical rains. *Chemical Geology* **181**(1-4): 147-167.

Hagg W and Braun L. 2005. The influence of Glacier retreat on Water Yield from High Mountain Areas: Comparison of Alps and Central Asia. *Climate and Hydrology in Mountain Areas*. John Wiley & Sons: Chichester, England; 315.

Hannah DM, Sadler JP and Wood PJ. 2007. Hydroecology and ecohydrology: a potential route forward? *Hydrological Processes* **21**(24): 3385-3390.

Hastenrath S and Ames A. 1995. Diagnosing the imbalance of Yanamarey Glacier in the Cordillera Blanca of Peru. *Journal of Geophysical Research* **100**(D3): 5105-5112.

Hirsch RM and Slack JR. 1984. A nonparametric trend test for seasonal data with serial dependence. *Water Resources Research* **20**(6): 727-732.

Hofer M, Molg T, Marzeion B and Kaser G. 2010. Empirical-statistical downscaling of reanalysis data to high-resolution air temperature and specific humidity above a glacier surface (Cordillera Blanca, Peru). *Journal of Geophysical Research-Atmospheres* **115**(12), D12120.

Hood J, Roy J and Hayashi M. 2006. Importance of groundwater in the water balance of an alpine headwater lake. *Geophysical Research Letters*, **33**(13): L13405, doi:10.1029/2006GL026611.

Huss M, Jouvet G, Farinotti D and Bauder A. 2010. Future high-mountain hydrology: a new parameterization of\ glacier retreat. *Hydrology and Earth System Sciences* **14**(5): 815-829.

Huss M, Farinotti D, Bauder A and Funk M. 2008. Modelling runoff from highly glacierized alpine drainage basins in a changing climate. *Hydrological Processes* **22**(19): 3888-3902.

IPCC, 2007. Climate Change 2007: Impacts, Adaptation and Vulnerability. 976 pp, IPCC (Intergovernmental Panel on Climate Change), Cambridge.

Jansson P, Hock R and Schneider T. 2003. The concept of glacier storage: A review. *Journal of Hydrology* **282**(1-4): 116-129.

Jeelani G, Bhat NA and Shivanna K. 2010. Use of Oxygen eighteen tracer to identify stream and spring origins of a mountainous catchment: A case study from Liddar watershed, Western Himalaya, India. *Journal of Hydrology* **393**(3-4): 257-264.

Juen I, Kaser G and Georges C. 2007. Modelling observed and future runoff from a glacierized tropical catchment (Cordillera Blanca, Peru). *Global and Planetary Change* **59**(1-4): 37-48.

Kalthoff N, Fiebig-Wittmaack M, Meissner C, Kohler M, Uriarte M, Bischoff-Gauss I and Gonzales E. 2006. The energy balance, evapo-transpiration and nocturnal dew deposition of an arid valley in the Andes. *Journal of Arid Environments* **65**(3): 420-443.

Kappenberger G. 2007. Climate changes and mountains. *Developments in Earth Surface Processes*. **10:** 133-142.

Kaser G, Grosshauser M and Marzeion B. 2010. Contribution potential of glaciers to water availability in different climate regimes. *Proceeding of the National Academy of Sciences of the United Statesof America* **107**(47): 20223-20227.

Kaser G, Cogley J, Dyurgerov M, Meier M and Ohmura A. 2006. Mass balance of glaciers and ice caps: Consensus estimates for 1961-2004, *Geophysical Research Letters* **33**(19): L19501**,** doi:10.1029/2006GL027511.

Kaser G, Juen I, Georges C, Gomez J and Tamayo W. 2003. The impact of glaciers on the runoff and the reconstruction of mass balance history from hydrological data in the tropical Cordillera Blanca, Peru. *Journal of Hydrology* **282**(1-4): 130-144.

Kaser G and Ostmaston H. 2002. *Tropical Glaciers*. Cambridge University press.

Kaser G and Georges C. 1999. On the mass balance of low latitude glaciers with particular consideration of the Peruvian Cordillera Blanca. *Geografiska Annaler Series a-Physical Geography* **81A**(4): 643-651.

Kistin EJ, Fogarty J, Pokrasso RS, McCally M and McCornick PG. 2010. Climate change, water resources and child health. *Archives of Disease in Childhood* **95**(7): 545-549.

Knutsson G. 2008. Hydrogeology in the Nordic countries. *Episodes* **31**: 148-154.

Koboltschnig GR and Schoner W. 2010. The relevance of glacier melt in the water cycle of the Alps: An example from Austria. *Hydrology and Earth System Sciences Discussions* **7**(3): 2897-2913.

Kohfahl C, Sprenger C, Herrera JB, Meyer H, Chacon FF and Pekdeger A. 2008. Recharge sources and hydrogeochemical evolution of groundwater in semiarid and karstic environments: A field study in the Granada Basin (Southern Spain). *Applied Geochemistry* **23**: 846-862.

Kundzewicz ZW, Graczyk D, Maurer T, Pinskwar I, Radziejewski M, Svensson C and Szwed M. 2005. Trend detection in river flow series: 1. Annual maximum flow. *Hydrological Sciences Journal-Journal Des Sciences Hydrologiques* **50**(5): 797-810.

Lambrecht A and Mayer C. 2009. Temporal variability of the non-steady contribution from glaciers to water discharge in western Austria. *Journal of Hydrology* **376**(3-4): 353-361.

Langmuir D. 1997. *Aqueous Environmental Geochemistry*. Prentice-Hall: Upper Saddle River, NJ, USA.

Langston G, Bentley LR, Hayashi M, McClymont A and Pidlisecky A. 2011. Internal structure and hydrological functions of an alpine proglacial moraine. *Hydrological Processes* **25**(19): 2967-2982.

Love DA, Clark H and Glover J. 2004. The lithologic, stratigraphic, and structural setting of the giant antamina copper-zinc skarn deposit, Ancash, Peru, *Economic Geology and the Bulletin of the Society of Economic Geologists* **99**(5): 887-916.

Maidment DR. 2002. Arc Hydro: GIS for Water Resources. ESRI Press: Redlands, CA, USA.

Mann HB. 1945. Non-parametric tests against trend. *Econometrica* **13**: 245-259.

Marengo JA. 1995. Variations and change in South-American streamflow. *Climatic Change* **31**(1): 99-117.

Mark BG, Bury J, McKenzie JM, French A and Baraer M. 2010. Climate change and tropical Andean Glacier recession: Evaluating hydrologic changes and livelihood vulnerability in the Cordillera Blanca, Peru. *Annals of the Association of American Geographers* **100**(4): 794-805.

Mark BG and McKenzie JM. 2007. Tracing increasing tropical Andean glacier melt with stable isotopes in water. *Environmental Science & Technology* **41**(20): 6955-6960.

Mark BG, McKenzie JM and Gomez J. 2005. Hydrochemical evaluation of changing glacier meltwater contribution to stream discharge: Callejon de Huaylas, Peru. *Hydrological Sciences Journal-Journal Des Sciences Hydrologiques* **50**(6): 975-987.

Mark BG and Seltzer GO. 2003. Tropical glacier meltwater contribution to stream discharge: a case study in the Cordillera Blanca, Peru. *Journal of Glaciology* **49**(165): 271-281.

McClymont AF, Roy JW, Hayashi M, Bentley LR, Maurer H and Langston G. 2011. Investigating groundwater flow paths within proglacial moraine using multiple geophysical methods. *Journal of Hydrology* **399**(1-2): 57-69.

McKenzie JM, Mark BG, Thompson LG, Schotterer U and Lin PN. 2010. A hydrogeochemical survey of Kilimanjaro (Tanzania): Implications for water sources and ages. *Hydrogeology Journal* **18**(4): 985-995.

McKenzie JM, Siegel DI, Patterson W and McKenzie DJ. 2001. A geochemical survey of spring water from the main Ethiopian rift valley, southern Ethiopia: Implications for well-head protection. *Hydrogeology Journal* **9**(3): 265-272.

McNulty BA, Farber DL, Wallace GS, Lopez R and Palacios O. 1998. Role of plate kinematics and plate-slip-vector partitioning in continental magmatic arcs: Evidence from the Cordillera Blanca, Peru. *Geology* **26**(9): 827-830.

Menzies J. 2002. *Modern and Past glacial Environment*. Butterworth - Heinemann.

Meriano M and Eyles N. 2003. Groundwater flow through Pleistocene glacial deposits in the rapidly urbanizing Rouge River-Highland Creek watershed, City of Scarborough, southern Ontario, Canada. *Hydrogeology Journal* **11**(2): 288-303.

Milner AM, Brown LE and Hannah DM. 2009. Hydroecological response of river systems to shrinking glaciers. *Hydrological Processes* **23**(1): 62-77.

Moore RD, Fleming SW, Menounos B, Wheate R, Fountain A, Stahl K, Holm K and Jakob M. 2009. Glacier change in western North America: Influences on hydrology, geomorphic hazards and water quality. *Hydrological Processes* **23**(25): 3650-3650.

Muir DL, Hayashi M and McClymont AF. 2011. Hydrological storage and transmission characteristics of an alpine talus. *Hydrological Processes* **25**(19): 2954-2966.

Myers JS. 1975. Vertical crustal movements of Andes in Peru. *Nature* **254**(5502): 672-674.

Nogues-Bravo D, Araujo MB, Errea MP and Martinez-Rica J. 2007. Exposure of global mountain systems to climate warming during the 21st Century. *Global Environmental Change-Human and Policy Dimensions* **17**(3-4): 420-428.

Nolin AW, Phillippe J, Jefferson A and Lewis SL. 2010. Present-day and future contributions of glacier runoff to summertime flows in a Pacific Northwest watershed: Implications for water resources. *Water Resources Research* **46**(12): W12509.

Ohmura A. 2001. Physical basis for the temperature-based melt-index method. *Journal of Applied Meteorology* **40**(4): 753-761.

Painter, J. 2007. Deglaciation in the Andean Region. *Human Development Report 2007/2008*, 21 pp., UNDP, Human Development Report Office.

Parriaux A and Nicoud G. 1993. Glacial deposits and groundwater. An example with a north-western alpine context. *Les formations glaciaires et l'eau souterraine. Exemple du contexte Nord alpin occidental* **4**(2-3): 61-67.

Petford N and Atherton MP. 1992. Granitoid emplacement and emplacement and deformation along a major crustal lineament - The Cordillera Blanca, Peru. *Tectonophysics* **205**(1-3): 171-185.

Pouyaud B, Zapata M, Yerren J, Gomez J, Rosas G, Suarez W and Ribstein P. 2005. On the future of the water resources from glacier melting in the Cordillera Blanca, Peru. *Hydrological Sciences Journal-Journal Des Sciences Hydrologiques* **50**(6): 999-1022.

Pouyaud B. 2004. Impact of climate change on water resources: the Rio Santa Basin (White Cordillera - Peru) In *CONAM*. Bonn.

Pouyaud B, Vignon F, Yerren J, Suarez W, Vegas F, Zapata M, Gomez J, Tamayo W and Rodriguez A. 2003. Glaciers et ressources en eau dans le bassin du rio Santa. IRD-SENAMHI-INRENA.

Rabatel A, Machaca A, Francou B and Jomelli V. 2006. Glacier recession on Cerro Charquini (16°S), Bolivia, since the maximum of the Little Ice Age (17th century). *Journal of Glaciology* **52**(176): 110-118.

Racoviteanu. 2005. GLIMS Glacier Database. National Snow and Ice Data Center/World Data Center for Glaciology.

Racoviteanu AE, Arnaud Y, Williams MW and Ordonez J. 2008. Decadal changes in glacier parameters in the Cordillera Blanca, Peru, derived from remote sensing. *Journal of Glaciology* **54**(186): 499-510.

Racoviteanu AE, Paul F, Raup B, Khalsa SJS and Armstrong R. 2009. Challenges and recommendations in mapping of glacier parameters from space: Results of the 2008 global land ice measurements from space (GLIMS) workshop, Boulder, Colorado, USA. *Annals of Glaciology* **50**(53): 53-69.

Ramirez E, Francou B, Ribstein P, Descloitres M, Guerin R, Mendoza J, Gallaire R, Pouyaud B and Jordan E. 2001. Small glaciers disappearing in the tropical Andes: A case-study in Bolivia: Glaciar Chacaltaya (16°S). *Journal of Glaciology* **47**(157): 187-194.

Raup BH, Khalsa SJS, Armstrong R, Helm C and Dyurgerov M. 2008. GLIMS: Progress in mapping the world's glaciers. *International Geoscience and Remote Sensing Symposium (IGARSS)*.3991-3993.

Risi C, Bony S and Vimeux F. 2008. Influence of convective processes on the isotopic composition ($\delta^{18}O$ and δD) of precipitation and water vapor in the tropics 2. Physical interpretation of the amount effect. *Journal of Geophysical Research D: Atmospheres* **113**(19): D19306.

Robinson ZP, Fairchild IJ and Russell AJ. 2008. Hydrogeological implications of glacial landscape evolution at Skeioararsandur, SE Iceland. *Geomorphology* **97**(1-2): 218-236.

Rodbell DT. 1993. Subdivision of late pleistocene moraines in the cordillera blanca, peru, based on rock-weathering features, soils, and radiocarbon-dates.. *Quaternary Research* **39**(2): 133-143.

Roy JW and Hayashi M. 2009a. Groundwater flow patterns of glacial moraine features in an alpine environment In *IAHS-AISH Publication*.126-132.

Roy JW and Hayashi M. 2009b. Multiple, distinct groundwater flow systems of a single moraine-talus feature in an alpine watershed. *Journal of Hydrology* **373(**1-2): 139-150.

Ryu JS, Lee KS and Chang HW. 2007. Hydrochemistry and isotope geochemistry of Song Stream, a headwater tributary of the South Han River, South Korea. *Geosciences Journal* **11**(2): 157-164.

Selveradjou S-K, Montanarella L, Spaargaren O and Dent D. 2005. European Digital Archive of Soil Maps (EuDASM). Office of the Official Publications of the European Communities: Luxembourg.

Shrestha RR and Simonovic SP. 2010. Fuzzy set theory based methodology for the analysis of measurement uncertainties in river discharge and stage. *Canadian Journal of Civil Engineering* **37**(3): 429-439.

Sidle WC. 1998. Environmental isotopes for resolution of hydrology problems. *Environmental Monitoring and Assessment* **52**(3): 389-410.

Singh P and Bengtsson L. 2005. Impact of warmer climate on melt and evaporation for the rainfed, snowfed and glacierfed basins in the Himalayan region. *Journal of Hydrology* **300**(1-4): 140-154.

Smith JA, Seltzer GO, Farber DL, Rodbell DT and Finkel RC. 2005. Early local last glacial maximum in the tropical Andes. *Science* **308**(5722): 678-681.

Soruco A, Vincent C, Francou B, Ribstein P, Berger T, Sicart JE, Wagnon P, Arnaud Y, Favier V and Lejeune Y. 2009. Mass balance of Glaciar Zongo, Bolivia, between 1956 and 2006, using glaciological, hydrological and geodetic methods. *Annals of Glaciology* **50**(50): 1-8.

Soulsby C, Brewer MJ, Dunn SM, Ott B and Malcolm I. 2003. Identifying and assessing uncertainty in hydrological pathways: a novel approach to end member mixing in a Scottish agricultural catchment. *Journal of Hydrology*, **274**(1-4): 109-128.

Stahl K and Moore RD. 2006. Influence of watershed glacier coverage on summer streamflow in British Columbia, Canada. *Water Resources Research* **42**(6): W06201.

Strauch G, Oyarzun J, Fiebig-Wittmaack M, Gonzalez E and Weise S. 2006. Contributions of the different water sources to the Elqui river runoff (northern Chile) evaluated by H/O isotopes. *Isotopes in Environmental and Health Studies* **42**(3): 303-322.

Suarez W, Chevallier P, Pouyaud B and Lopez P. 2008. Modelling the water balance in the glacierized Paron Lake basin (White Cordillera, Peru). *Hydrological Sciences Journal-Journal Des Sciences Hydrologiques* **53**(1): 266-277.

Uehlinger U, Robinson CT, Hieber M and Zah R. 2010. The physico-chemical habitat template for periphyton in alpine glacial streams under a changing climate. *Hydrobiologia* **657**(1): 107-121.

Urrutia R and Vuille M. 2009. Climate change projections for the tropical Andes using a regional climate model: Temperature and precipitation simulations for the end of the 21st century. *Journal of Geophysical Research-Atmospheres* **114**(2): D02108.

Van de Griend AA, Seyhan E, Engelen GB and Geirnaert W. 1986. Hydrological characteristics of an Alpine glacial valley in the North Italian Dolomites. *Journal of Hydrology* **88**(3-4): 275-299.

Vergara W, Deeb AM, Valencia AM, Bradley RS, Francou B, Zarzar A, Grunwald A and Haeussling SM. 2007. Economic impact of rapid glacier retreat in the Andes. *EOS, Transactions, American Geophysical Union* **88**(25): 261-264.

Vimeux F, Gallaire R, Bony S, Hoffmann G and Chiang JCH. 2005. What are the climate controls on δD in precipitation in the Zongo Valley (Bolivia)? Implications for the Illimani ice core interpretation. *Earth and Planetary Science Letters* **240**(2): 205-220.

Viviroli D, Archer DR, Buytaert W, Fowler HJ, Greenwood GB, Hamlet AF, Huang Y, Koboltschnig G, Litaor MI, Lopez-Moreno JI, Lorentz S, Schadler B, Schwaiger K, Vuille M and Woods R. 2010. The role of glaciers in stream flow from the Nepal Himalaya: Overview and recommendations for research, management and politics. *Hydrology and Earth System Sciences Discussions* **7**(3): 2829-2895.

Vuille M, Francou B, Wagnon P, Juen I, Kaser G, Mark BG and Bradley RS. 2008a. Climate change and tropical Andean glaciers: Past, present and future. *Earth-Science Reviews* **89**(3-4): 79-96.

Vuille M, Kaser G and Juen I. 2008b. Glacier mass balance variability in the Cordillera Blanca, Peru and its relationship with climate and the large-scale circulation. *Global and Planetary Change* **62**(1-2): 14-28.

Wagnon P, Ribstein P, Schuler T and Francou B. 1998. Flow separation on Zongo Glacier, Cordillera Real, Bolivia. *Hydrological Processes* **12**(12): 1911-1926.

Winkler M, Juen I, Molg T, Wagnon P, Gomez J and Kaser G. 2009. Measured and modelled sublimation on the tropical Glaciar Artesonraju, Peru. *Cryosphere* **3**(1): 21-30.

Xu ZX, Liu ZF, Fu GB and Chen YN. 2010. Trends of major hydroclimatic variables in the Tarim River basin during the past 50 years. *Journal of Arid Environments* **74**(2): 256-267.

Yamanaka M, Nakano T and Tase N. 2005. Hydrogeochemical evolution of confined groundwater in northeastern Osaka Basin, Japan: estimation of confined groundwater flux based on a cation exchange mass balance method. *Applied Geochemistry* **20**(2): 295-316.

Yang J, Ding Y and Chen R. 2007. Climatic causes of ecological and environmental variations in the source regions of the Yangtze and Yellow Rivers of China. *Environmental Geology* **53**(1): 113-121.

Yang Q, Xiao H, Zhao L, Yang Y, Li C and Yin L. 2011. Hydrological and isotopic characterization of river water, groundwater, and groundwater recharge in the Heihe River basin, northwestern China. *Hydrological Processes* **25**(8): 1271-1283.

Yue S and Pilon P. 2004. A comparison of the power of the t test, Mann-Kendall and bootstrap tests for trend detection. *Hydrological Sciences Journal-Journal Des Sciences Hydrologiques* **49**(1): 21-37.